CHARGED-PARTICLE DISTRIBUTIONS & TWO PARTICLES BOSE-EINSTEIN CORRELATIONS AT 0.9 – 13 TeV WITH THE ATLAS DETECTOR

YURI KULCHITSKY, PAVEL TSIARESHKA

INSTITUTE OF PHYSICS, NATIONAL ACADEMY OF SCIENCES OF BELARUS, MINSK, BELARUS

JINR, DUBNA, RUSSIA

ON BEHALF OF ATLAS COLLABORATION

WORKSHOP
"LHC DAYS IN BELARUS",
INSTITUTE FOR NUCLEAR PROBLEMS
OF BELARUSIAN STATE UNIVERSITY,
MINSK, BELARUS,
17 – 18 JANUARY 2017

CHARGED-PARTICLE DISTRIBUTIONS IN PP-INTERACTIONS

Understanding of soft-QCD interactions has direct impact on

1. **precision measurements**
2. **searches for new physics**

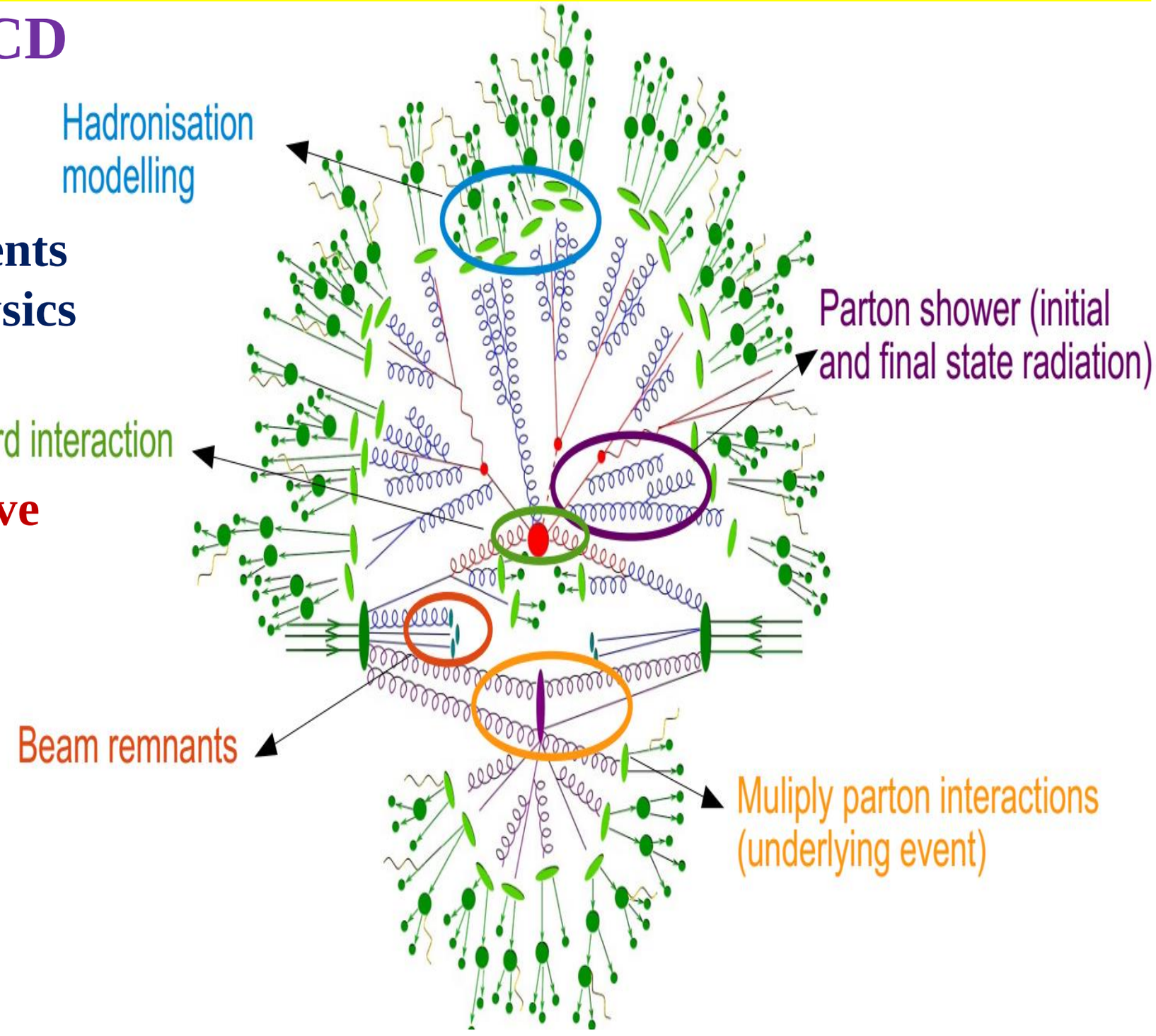

Provides insight into strong interactions in non-perturbative QCD regime:

- **Soft QCD results used in Monte-Carlo generators tuning**
- **Low energy QCD description essential for simulating multiple pp interactions**

Publication: *Charged-particle distributions in √s=13 TeV pp interactions measured with the ATLAS detector at the LHC;* ***PL B758 (2016) 67–88.*** Charged-particle distributions at low transverse momentum in √s = 13 TeV *pp* interactions measured with the ATLAS detector at the LHC ***Eur. Phys. J. C 76 (2016) 502***

A TOROIDAL LHC APPARATUS

The focus of ATLAS is high-p_T physics, and also provides a window onto important softer QCD processes. Selected topics, *often 13 TeV first results*.

►Charged-particles distributions ►Bose Einstein Correlations.

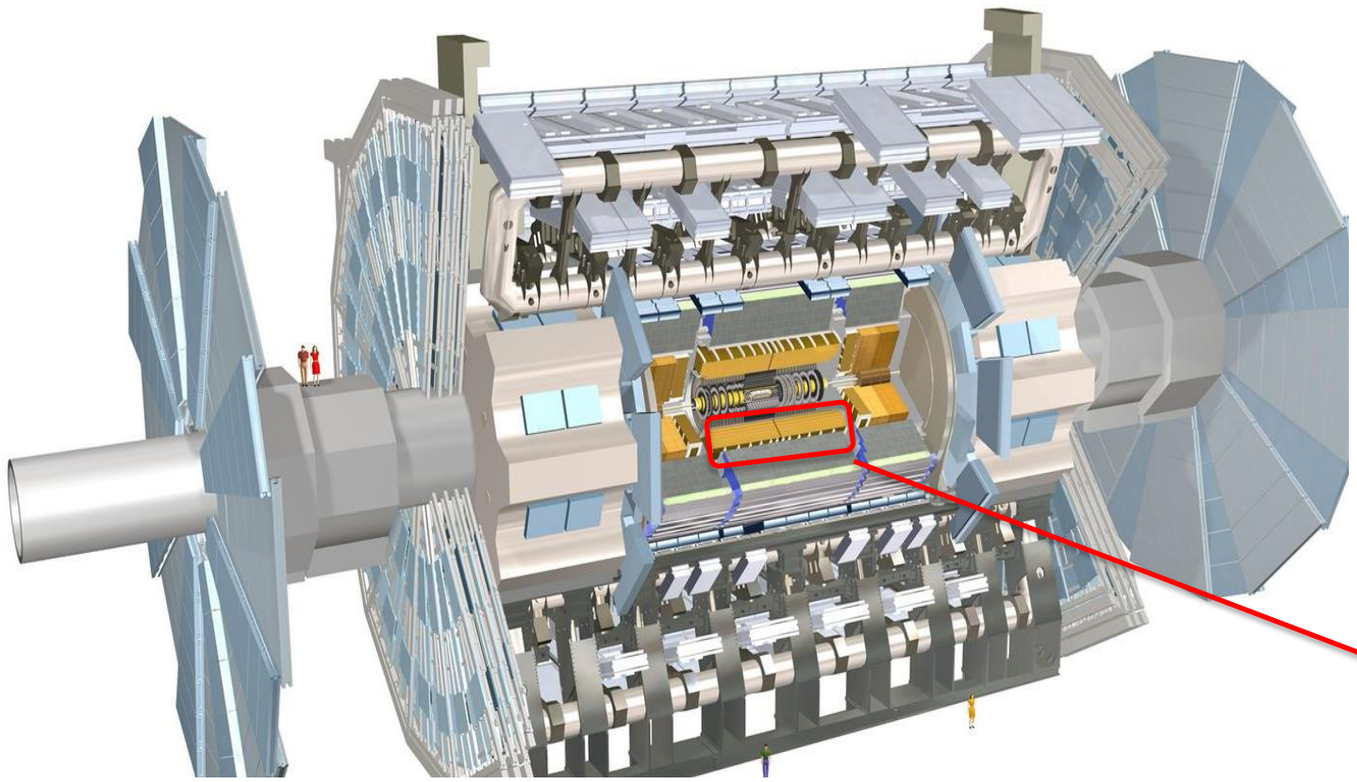

ATLAS Inner Detector:
main tracking device (Run 2)

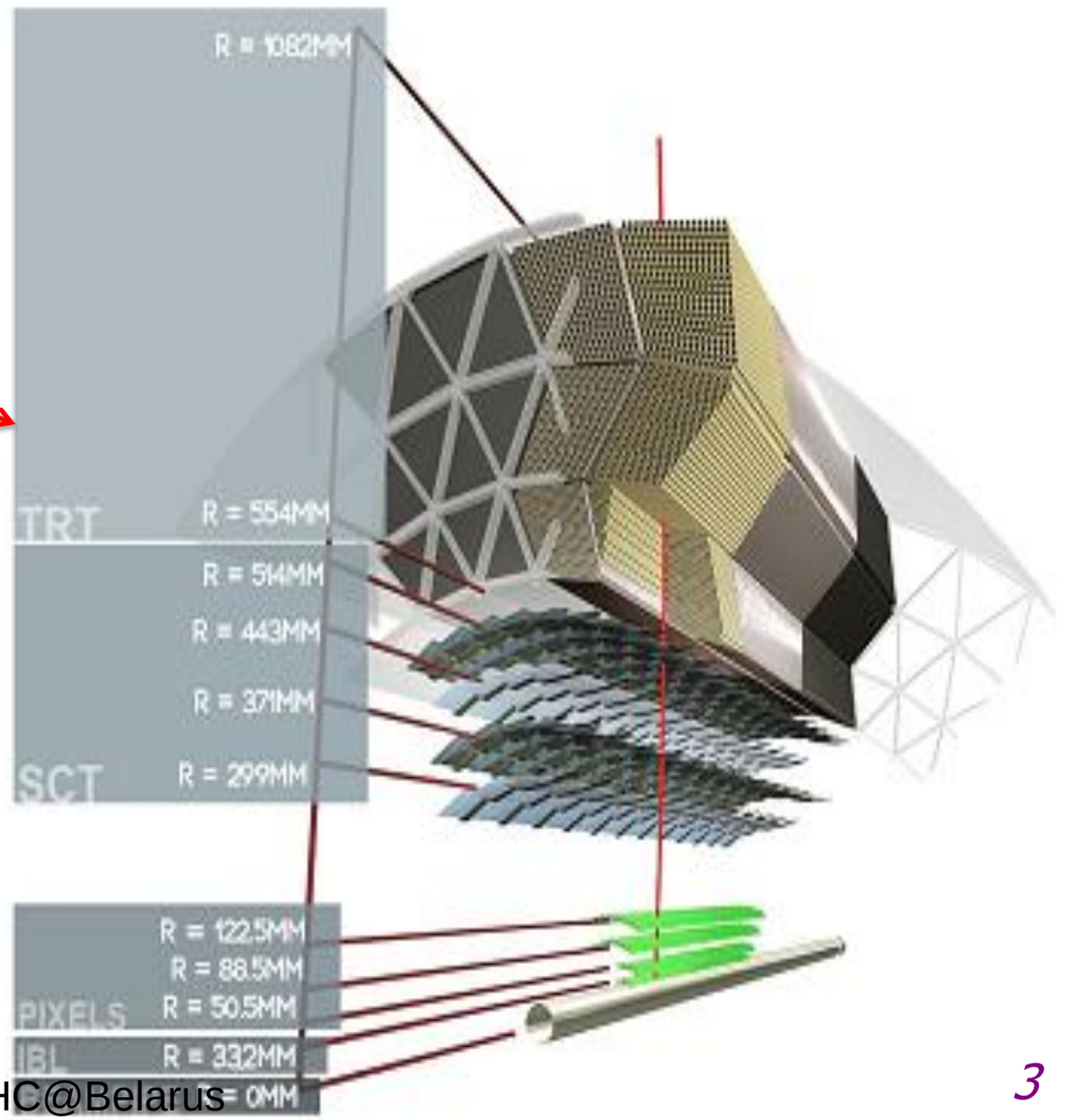

Inner Detector ($|\eta|<2.5$, $p_T>100$ MeV**):**
Tracking; ***2T*** Solenoid Magnet

- Silicon Pixels *50 x 400 μm²*
- Silicon Strips (SCT) *40 μm* rad stereo strips
- Transition Radiation Tracker (TRT) up to *36* points/track

New: *Insertable B-Layer* (IBL) in the Pixel

MINIMUM BIAS TRIGGER SCINTILLATOR (MBTS)

32 independent wedge-shaped plastic scintillators (16 per side) read out by PMTs, $2.09<|\eta|<3.84$*

* Pseudorapidity is defined as $\eta = -\frac{1}{2} \ln(\tan(\theta/2))$, θ is the polar angle with respect to the beam.

Run 1

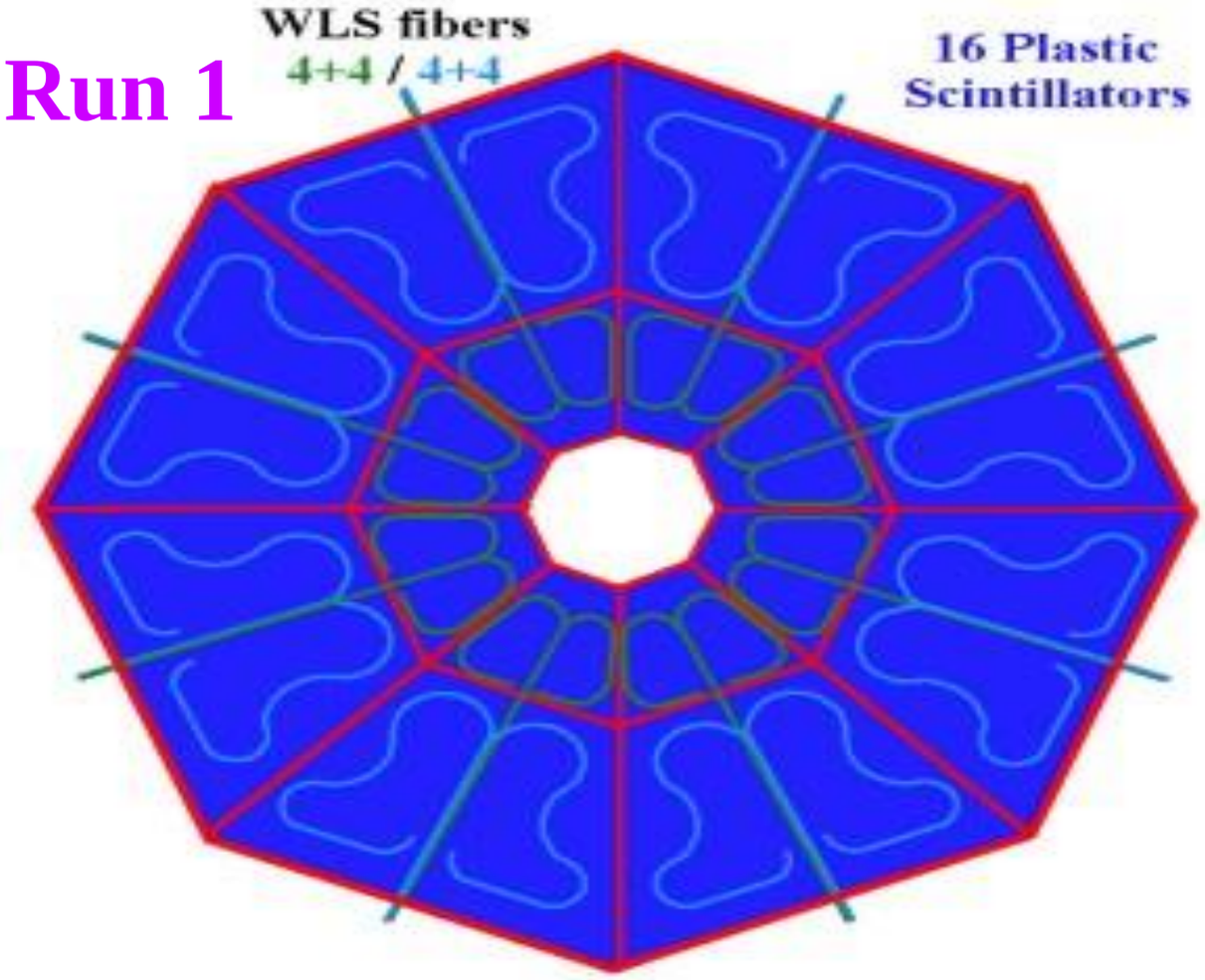

- Designed for triggering on min bias events, >99% efficiency
- MBTS timing used to veto halo and beam gas events
- Also being used as gap trigger for various diffractive subjects

MINIMUM-BIAS EVENT SELECTION CRITERIA

Events pass the data quality criteria **("Good events":** *1) all ID sub-systems nominal cond., 2) stable beam, 3) defined beam spot*)

- Accept on signal-arm Minimum Bias Trigger Scintillator
- **Primary vertex** (*2 tracks* with p_T*>100 MeV*),
- **Veto** to any additional vertices with ≥4 tracks.
- **At least 2 tracks with** p_T*>100 MeV,* $|\eta|$*<2.5*
- **At least 1 first Pixel layer hit & 2, 4, or 6 SCT hits** for p_T*>100, 200, 300 MeV* respectively.
- Cuts on the **transverse impact parameter**: $|d_0^{BL}|$*<1.5 mm*
- Cuts on the **longitudinal impact parameter**: $|\Delta z_0 sin\Theta|$*<1.5 mm* (Δz_0 is difference between tracks z_0 and vertex z position)
- Track fit χ^2 **probability > 0.01** for tracks with p_T*>10 GeV*

Charged-particle distributions at 13 TeV

PL B758 (2016) 67–88, Eur.Phys.J. C 76 (2016) 502

The composition of inelastic p-p collisions: **Statistics: 9 million inelastic interactions**

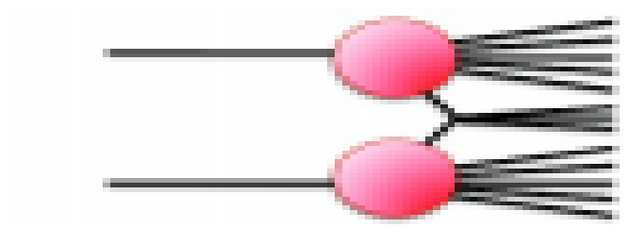

Non-diffractive

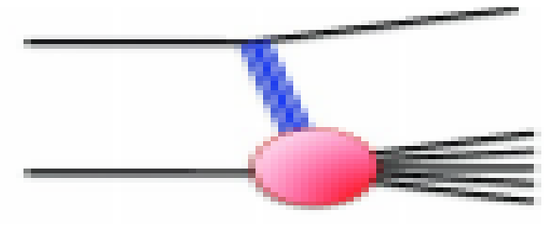

Single-diffractive

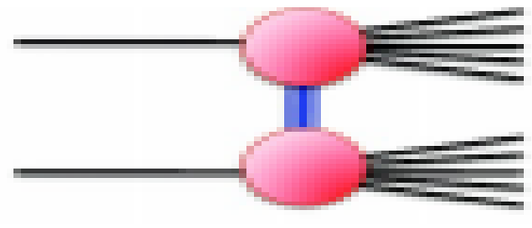

Double-diffractive

Perturbative QCD describes only the hard-scattered partons, all the rest is predicted with **phenomenological models.**

ND: QCD motivated models with many parameters; **Background** when >1 interactions per bunch crossing; **SD+DD** not well constrained by models.

Strange baryons with $30 < \tau < 300$ ps are excluded.

Task: measure spectra of primary charged particles corrected to hadron level.

Multiplicity vs.η;

$$\frac{1}{N_{ch}}\cdot\frac{dN_{ch}}{d\eta},$$

Multiplicity vs. p_T;

$$\frac{1}{N_{ev}}\cdot\frac{1}{2\pi p_T}\cdot\frac{d^2N_{ch}}{d\eta dp_T},$$

Multiplicity distributions

$$\frac{1}{N_{ev}}\cdot\frac{dN_{ev}}{dn_{ch}},$$

$$\langle p_T\rangle \text{ vs. } n_{ch}$$

Measurement – do not apply model dependent corrections and allow to tune models to data measured in well defined kinematic range.

MC MODELS

Different settings of model parameters optimised to reproduce the existing experimental data have been used in the simulation. These settings are referred to as tunes.

For **PYTHIA 8** two tunes are used (A2 and MONASH), for **EPOS** the LHC tunes are respectively used. **QGSJET-II** uses the default tune from the generator.

Each tune incorporates 7 TeV underlying event and/or minimum-bias data. Each tune is summarised in Table 1, together with the version of each generator used to produce the samples. The **A2 PYTHIA 8** (with MSTW2008LO PDF) sample is used to derive the detector corrections for these measurements.

Generator	Version	Tune	PDF
PYTHIA 8	8.185	A2	MSTW2008LO
PYTHIA 8	8.186	MONASH	NNPDF2.3LO
EPOS	LHCv3400	LHC	N/A
QGSJET-II	II-04	default	N/A

All the events are processed through the ATLAS detector simulation program, which is based on GEANT4. They are then reconstructed and analysed by the same program chain used for the data.

Charged-particle multiplicities vs p_T and multiplicity

PL B758 (2016) 67–88

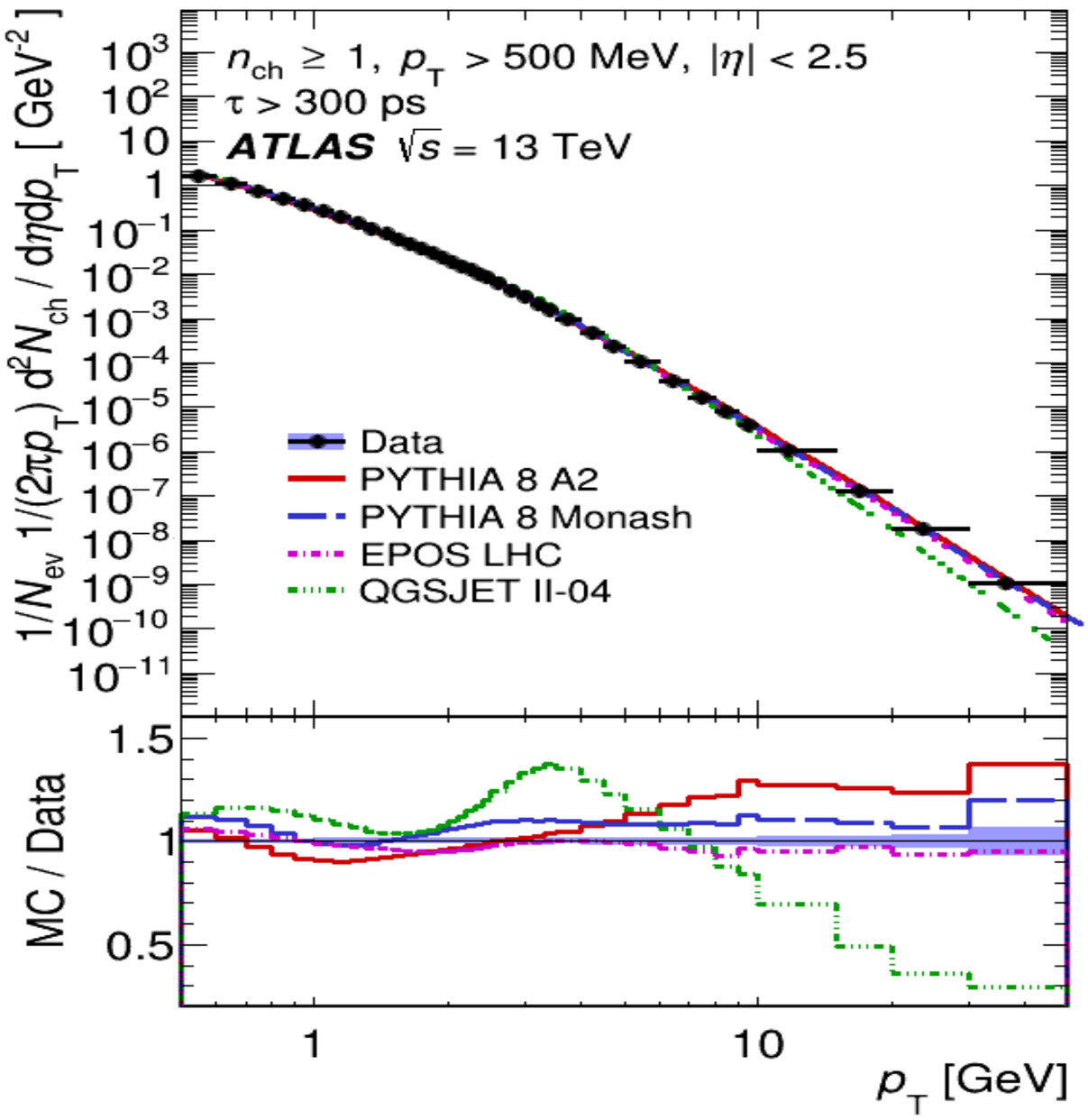

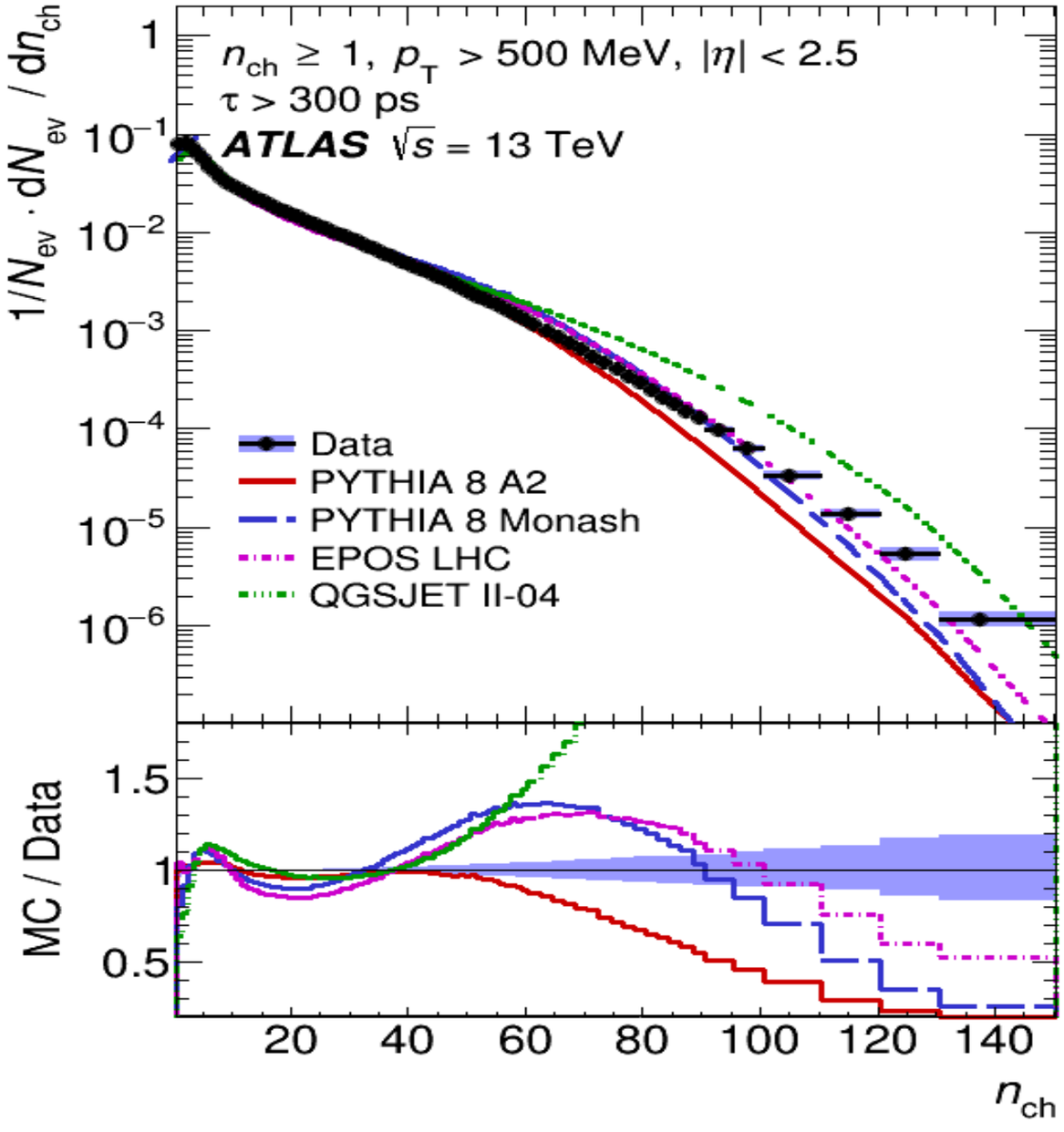

Measurement spans 10 orders of magnitude. **EPOS** and **Pythia 8 Monash** give remarkably good predictions.

Low n_{ch} not well modelled by any MC; because of large contribution from diffraction.

Average transverse momentum distribution

PL B758 (2016) 67–88

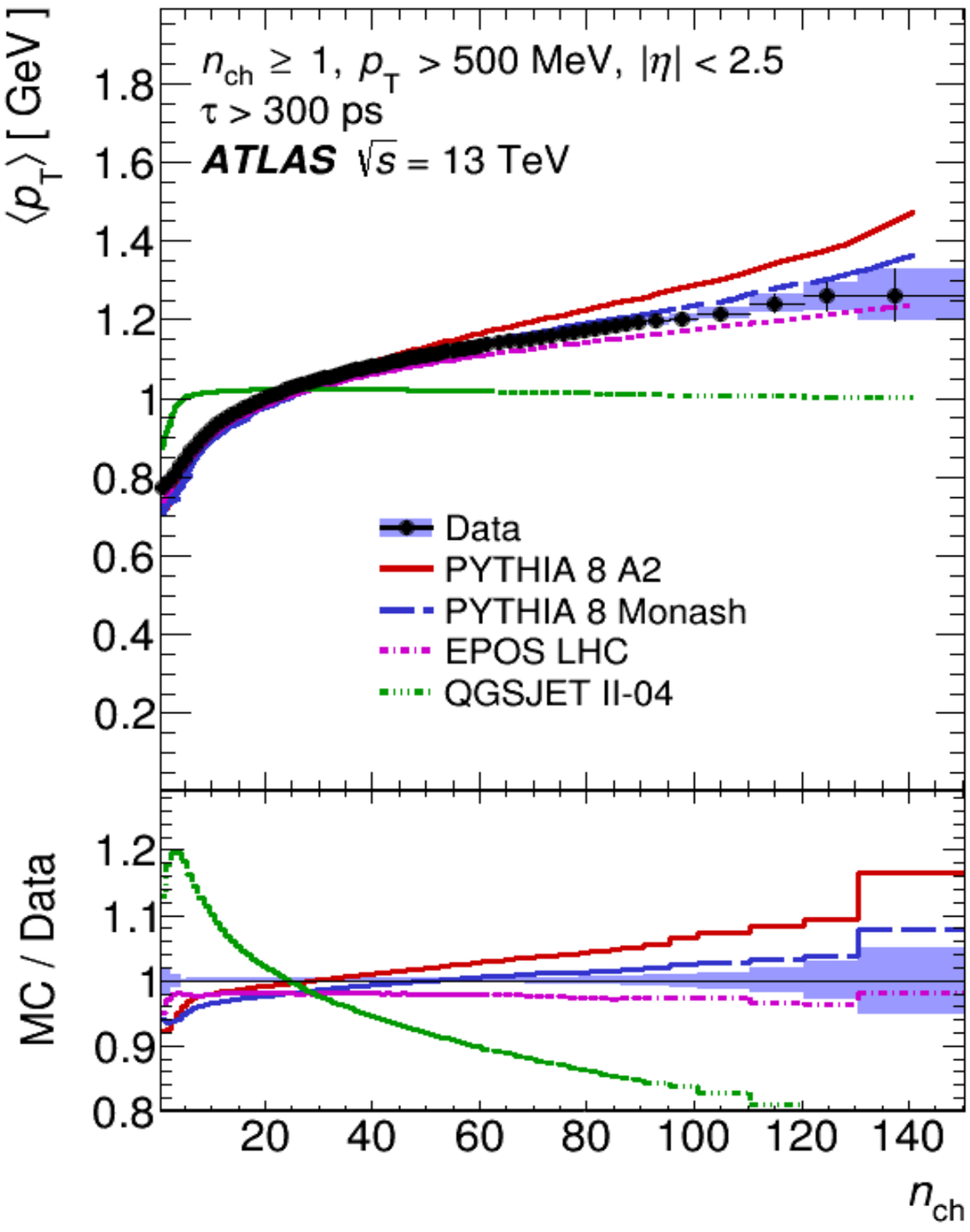

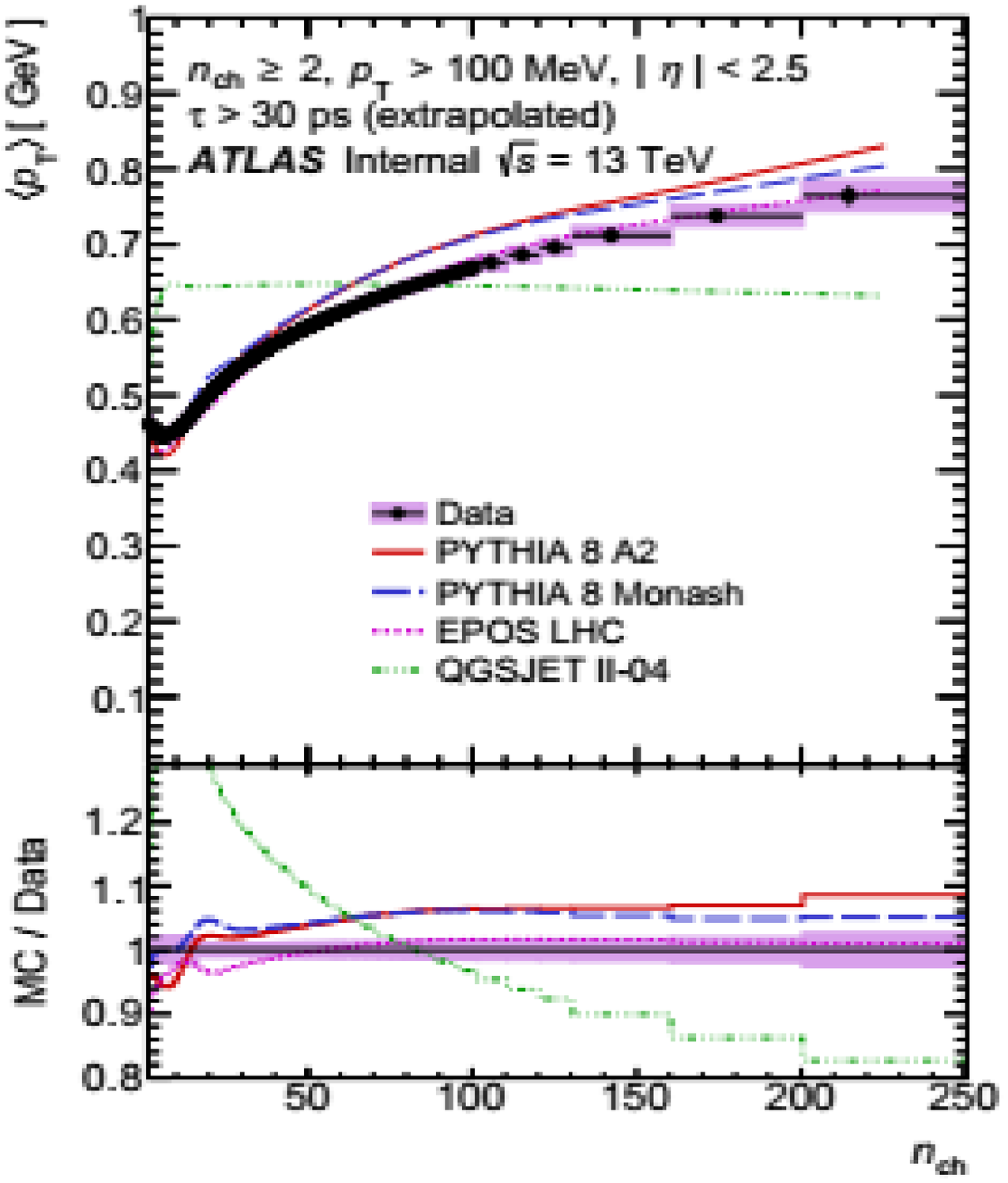

Models without colour reconnection, **QGSJET,** fail to model scaling with n_{ch} very well.

Charged-particle multiplicities vs η and energy

PL B758 (2016) 67–88

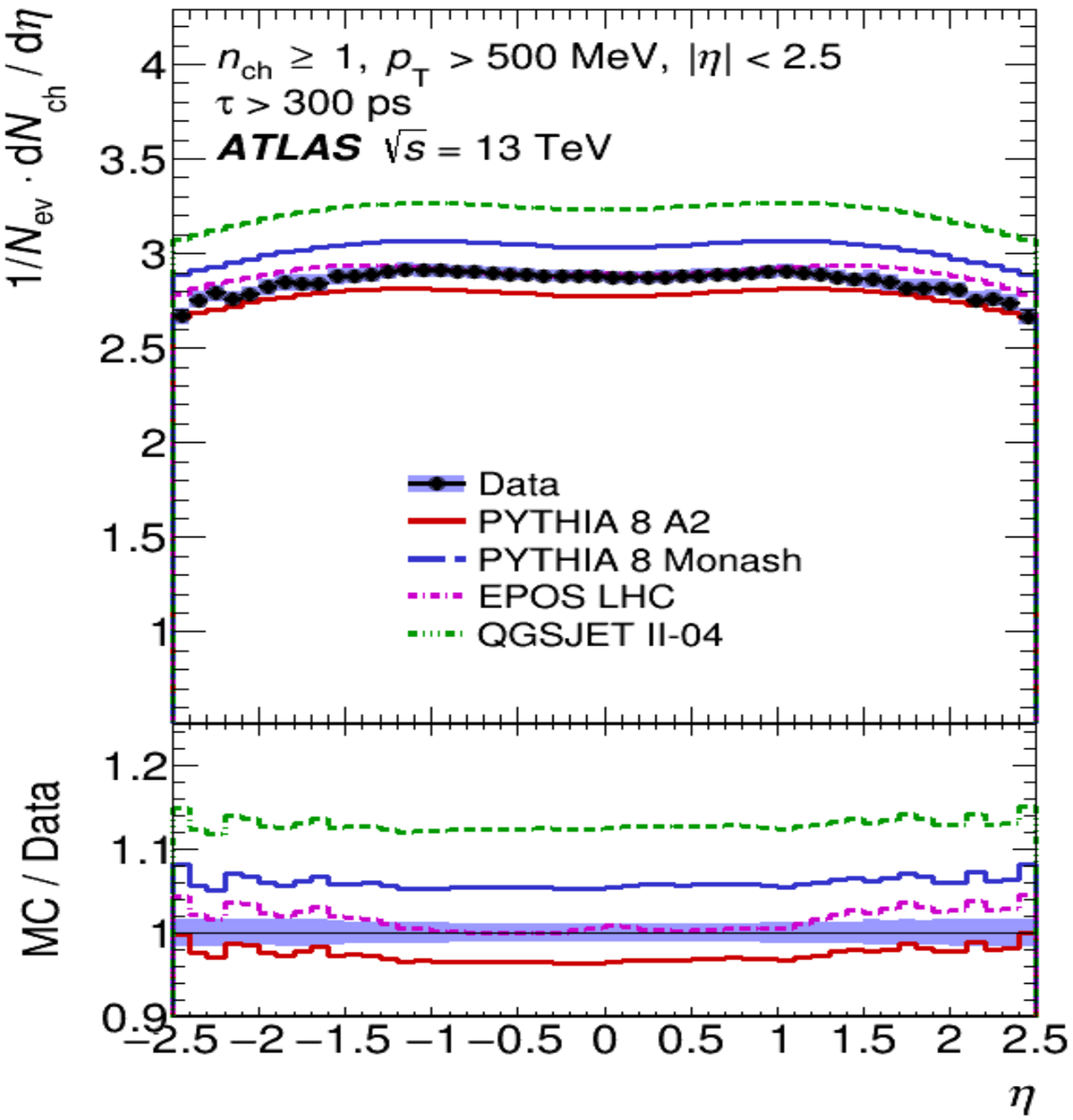

The same shape in Models but different normalisation. Except **HERWIG** which is tuned entirely on ***UE***. **EPOS** and **Pythia 8 A2** give remarkably <u>good predictions</u>

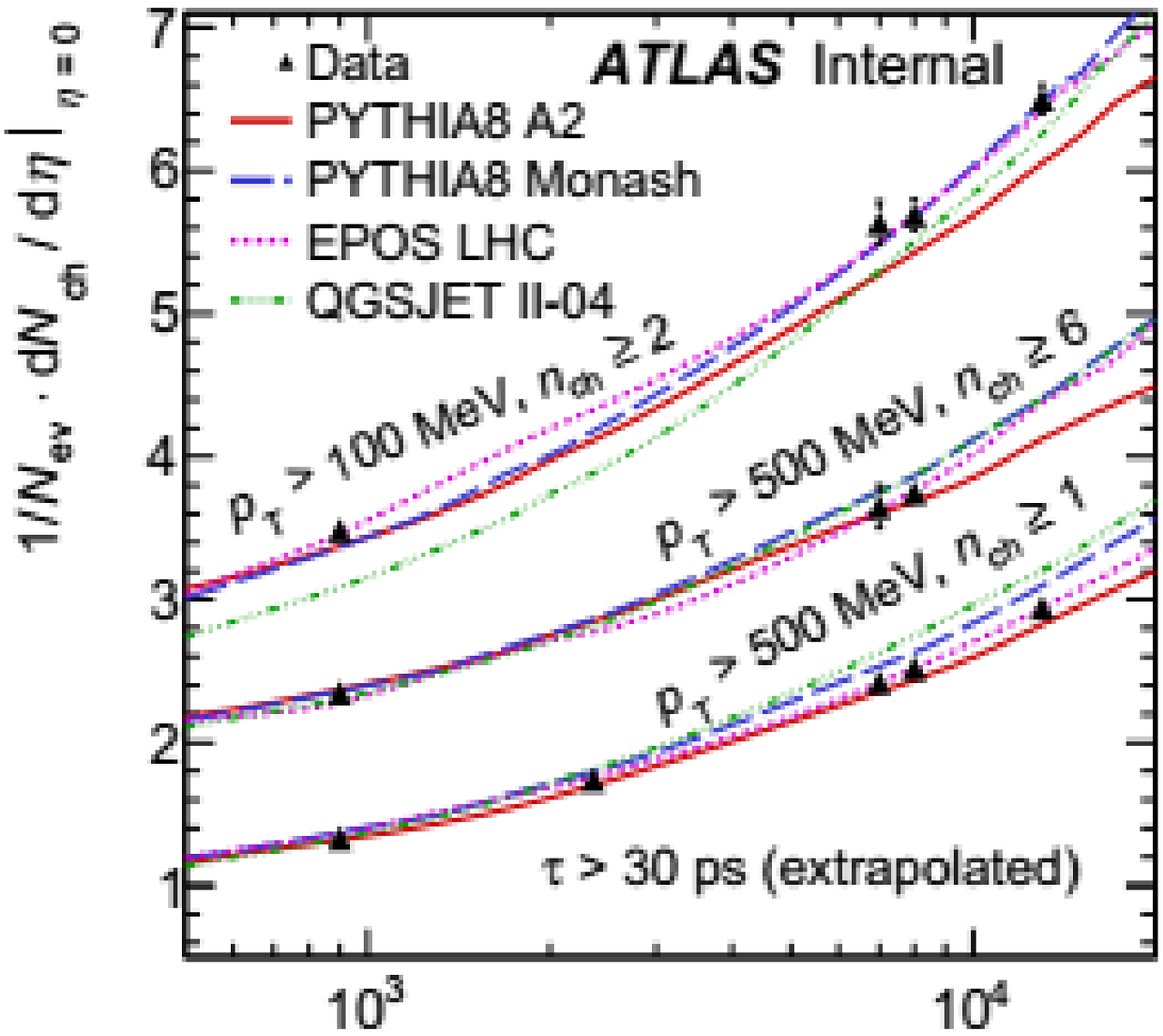

The mean number of primary charged particles increases by a factor of **2.2** when $\sqrt{s}$ increases by a factor of about **14** from **0.9 TeV to 13 TeV**. EPOS and Pythia 8 A2 describe the dependence on $\sqrt{s}$ very well, while Pythia 8 Monash and QGSJET-ii predict a steeper rise in multiplicity with $\sqrt{s}$.

MOTIVATION FOR BOSE-EINSTEIN CORRELATIONS

- Bose-Einstein correlations (BEC) represent a unique probe of the *space-time geometry* of the *hadronization region* and allow the *determination the size and shape of the source* from which particles are *emitted*.

- Studies of the dependence of BEC on *particle multiplicity* and *transverse momentum* are of special interest. They help in the understanding of multiparticle production mechanisms.

- High-multiplicity data in proton interactions can serve as a reference for studies in nucleus-nucleus collisions. The effect is reproduced in both hydrodynamical/hydrokinetic and Pomeron-based approaches for hadronic interactions where high multiplicities play a crucial role.

BOSE-EINSTEIN CORRELATIONS

Correlations in phase space **between two identical bosons** from symmetry of wave functions.

- ► Enhances likelihood of two particles close in phase space
- ► Allows one to 'probe' the source of the bosons in size and shape
- ► Dependence on particle multiplicity and transverse momentum probes the production mechanism

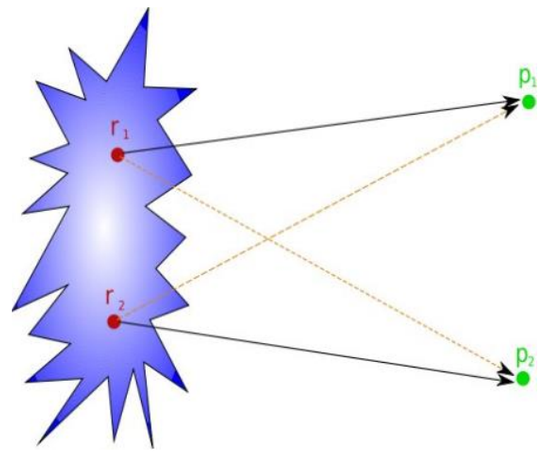

Correlation function $C_2(Q)$ a ratio of probabilities:

$$C_2(Q) = \frac{\rho(p_1, p_2)}{\rho_0(p_1, p_2)} = C_0\left(1 + \Omega(\lambda, RQ)\right)\cdot\left(1 + Q\varepsilon\right), \qquad Q^2 = -(p_1 - p_2)^2$$

$$\Omega^G(\lambda, RQ) = \lambda e^{-R^2Q^2}$$

$$\Omega^E(\lambda, RQ) = \lambda e^{-RQ}$$

$\mathbf{C_0}$ is a normalisation, $\boldsymbol{\varepsilon}$ accounts for long range effects, **R** is the effective radius parameter of the source, $\boldsymbol{\lambda}$ is the strength of the effect parameter, 0/1 for coherent/chaotic source. Two possible parameterisation: Gaussian and Exponential.

$$C_2(Q) = \frac{N(p_1^{\pm}, p_2^{\pm})(Q)}{N^{ref}(p_1, p_2)(Q)}$$

N^{ref} without BEC effect from: unlike-charge particles (UCP), opposite hemispheres, event mixing. **Basic Reference**: distribution of UCP pairs of non-identical particle taken from the same event.

$$R_2(Q) = \frac{C_2^{Data}(Q)}{C_2^{MC}(Q)} = \frac{\rho^{Data}(p_1^{\pm}, p_2^{\pm}) \,/\, \rho_0^{Data}(p_1^{\pm}, p_2^{\mp})}{\rho^{MC}(p_1^{\pm}, p_2^{\pm}) \,/\, \rho_0^{MC}(p_1^{\pm}, p_2^{\mp})}$$

The studies are carried out using the **double ratio correlation function**. The **$R_2(Q)$** eliminates problems with energy-momentum conservation, topology, resonances etc. **MC without BEC.**

PARAMETRIZATION MODELS

- **GSSg model.** ***The Goldhaber spherical source model.***

$$\Omega^{(G)} = C_0\left(1+\lambda \mathrm{e}^{-R^2Q^2}\right)\cdot\left(1+Q\varepsilon\right)$$

- **GSSe model.** ***Empirical model. Used since it represents well the shape of the correlation.***

$$\Omega^{(G)} = C_0\left(1+\lambda \mathrm{e}^{-RQ}\right)\cdot\left(1+Q\varepsilon\right)$$

R is the source radius

λ is the *incoherence factor (0, 1)* introduced empirically.

- **QOg model.** ***Quantum Optics model.***

$$\Omega^{(GO)} = C_0\left(1+2\mathrm{p}(1-p)\mathrm{e}^{-R^2Q^2} + p^2\mathrm{e}^{-2\mathrm{R}^2Q^2}\right)\cdot\left(1+Q\varepsilon\right)$$

- **QOe model.** ***Empirical but inspired to the Quantum Optics model.***

$$\Omega^{(EO)} = C_0\left(1+2\mathrm{p}(1-p)\mathrm{e}^{-RQ} + p^2\mathrm{e}^{-2\mathrm{RQ}}\right)\cdot\left(1+Q\varepsilon\right)$$

***p* is the chaoticity: =0 (=1) for purely coherent (chaotic) sources.**

DATA AND MC SAMPLES

- Statistics *for **0.9 TeV** 357,523 events with 4,532,663 tracks* and for ***7 TeV** 10,066,072 events with 209,809,430 tracks* passed selection criteria.
- Integrated luminosities: ***9 μb^{-1} at 0.9 TeV and 190 μb^{-1} at 7 TeV.***
- Track and event selection criteria as in the Min Bias 2.0 analysis.
- The tracking and event efficiencies, unfolding – follow this study.
- In addition the High Multiplicity (HM) dataset at 7 TeV is studied, for the first time in BEC analyses. Statistic *for **7 TeV (HM)** 17784 events with 2,719,536 tracks* were selected with
  - Integrated luminosities: ***12.4 nb^{-1} at 7 TeV HM.***
- Closure tests show good agreement between the reconstructed unfolded and truth MC spectra.
- Study based on the Min Bias 2.0 datasets and MC samples: Pythia MC09 (main), Perugia0, Phojet, and EPOS.

MONTE-CARLO MODELS

Four recent versions of MC event generators were used to provide calculation of R_2 correlation functions and for systematic studies.

➢ **The MC models do not contain BEC effects.**

Generator	Version	Tune	PDF	Focus of Tune	Statistic
PYTHIA 6	6.421	MC09	MRST LO	MB/UE	1.1×10^7 at 0.9 TeV 2.7×10^7 at 7 TeV MBT 1.8×10^6 at 7 TeV HMT
PYTHIA 6	6.421	Perugia0	CTEQ 5L	MB	
PHOJET	1.12.1.35	No tune	MRST LO	MB/UE	
EPOS	1.99 v2965	LHC	CTEQ6.6 LO	MB	for HMT only

➢ Large MC samples of minimum-bias and high-multiplicity events were generated with **PYTHIA 6.421 ATLAS MC09** set of optimised parameters with non-diffractive, single-diffractive and double-diffractive processes included in proportion to the cross sections predicted by the model.

For the study of systematic effects, additional MC samples were produced using the **PHOJET 1.12.1.35, PYTHIA with the Perugia0** tune, and the **EPOS 1.99 v2965** for the HM analysis.

❑ The **PHOJET** program uses the Dual Parton Model for low-p_T physics and is interfaced to PYTHIA for the fragmentation of partons.

❑ The **EPOS** generator is based on an implementation of the QCD inspired Gribov-Regge field theory describing soft and hard scattering simultaneously, and relies on the same parton distribution functions as used in PYTHIA.

TRACK RECONSTRUCTION CORRECTIONS

Performed corrections on:

- *The reconstruction track efficiency* – $\varepsilon\,(p_T,\eta)$,
- *The fraction of secondaries particles* – $f_{sec}(p_T,\eta)$,
- *The fraction of selected tracks for which the corresponding primary particles are outside the kinematic range* – $f_{okr}(p_T,\eta)$,
- *The fake tracks* – $f_{fake}(p_T,\eta)$,

We use the formula:

$$w_i(p_T,\eta)=\frac{\left(1-f_{\sec}(p_T,\eta)\right)\cdot\left(1-f_{okr}(p_T,\eta)\right)\cdot\left(1-f_{fake}(p_T,\eta)\right)}{\varepsilon(p_T,\eta)}$$

- The effect of events lost due to the trigger and vertex reconstruction corrected using even-by-event weights applied to a pair of particles
- The resolution of Q obtained to be better than 5 MeV so to exclude track fake reconstruction the Q-threshold taken 20 MeV

COULOMB CORRECTION

The measured ***N(Q) distribution*** for the like or unlike signed particle (track) pairs in presence of the Coulomb interaction is given by:

$$N_{meas}(Q) = G(Q)N(Q)$$

where $N_{meas}(Q)$ is the measured distribution, $N(Q)$ is the distribution free of Coulomb correlations.

Gamov penetration factor

$$G(Q) = \frac{2\pi\eta}{e^{2\pi\eta} - 1}$$

Sommerfeld parameter

$$\eta = \frac{\pm\alpha_m}{|Q|}$$

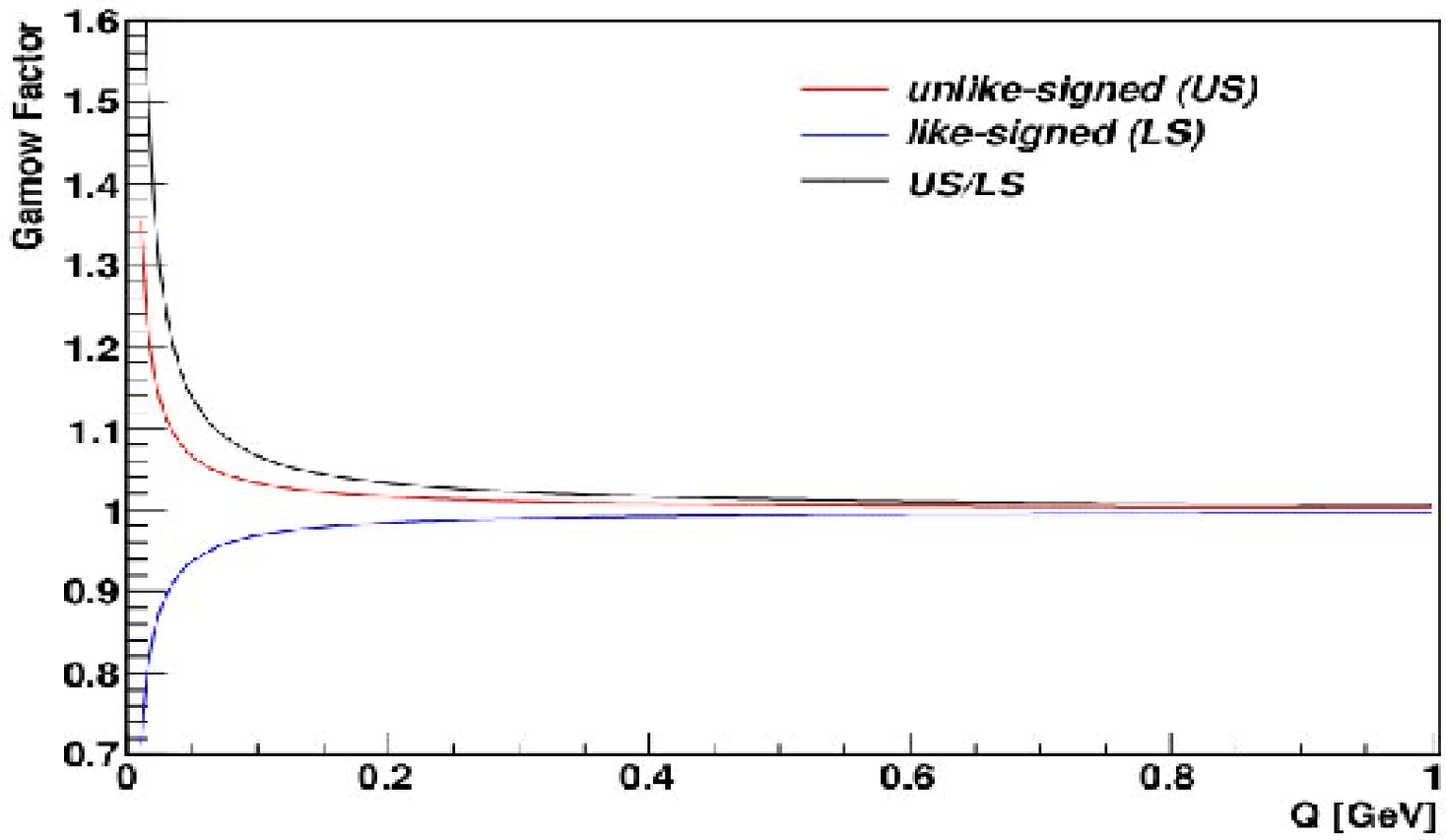

Distribution of Gamma factor for unlike-signed particle pairs, like-signed particle pairs and ratio of unlike-signed to like-signed.

THE RESONANCES STUDY

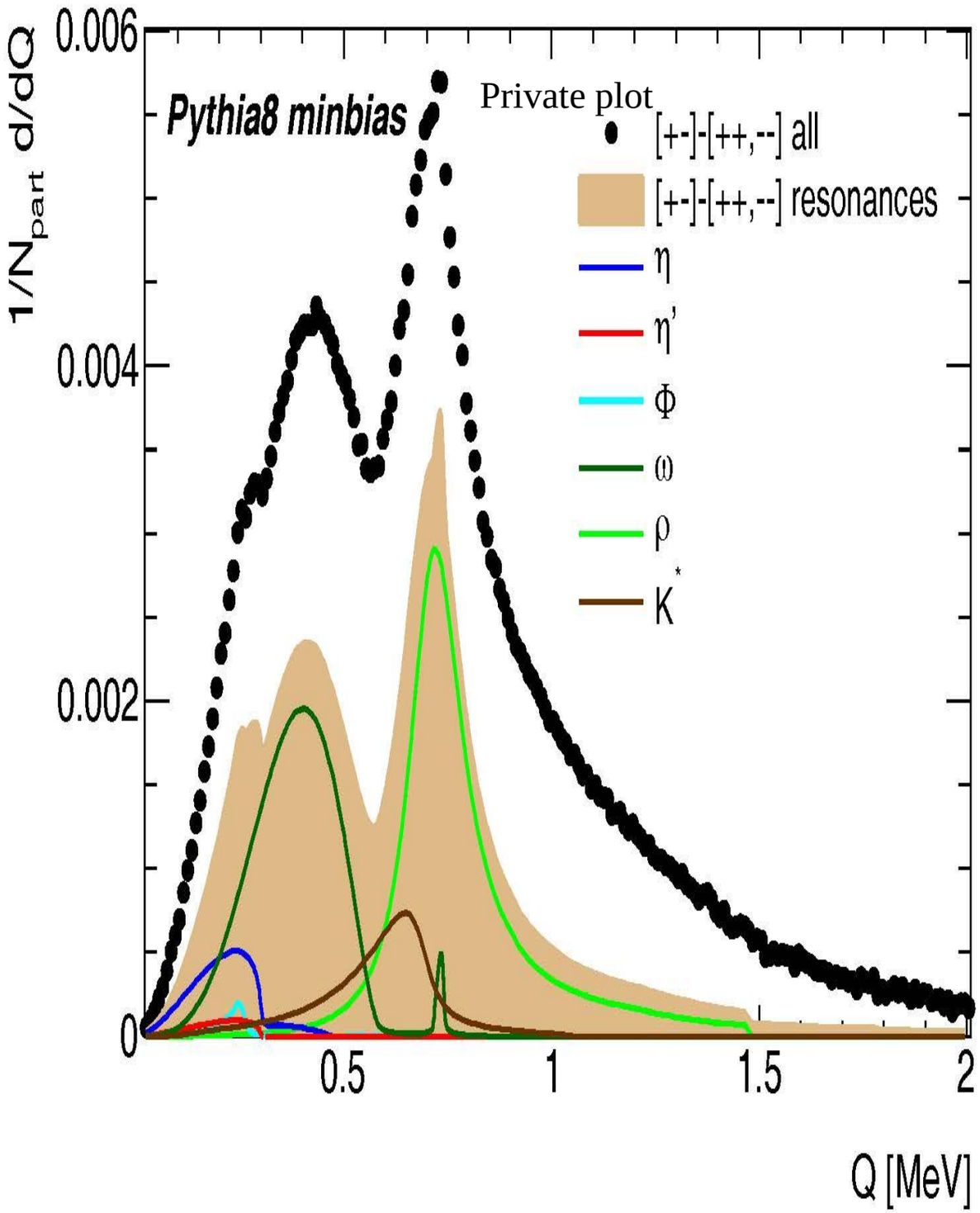

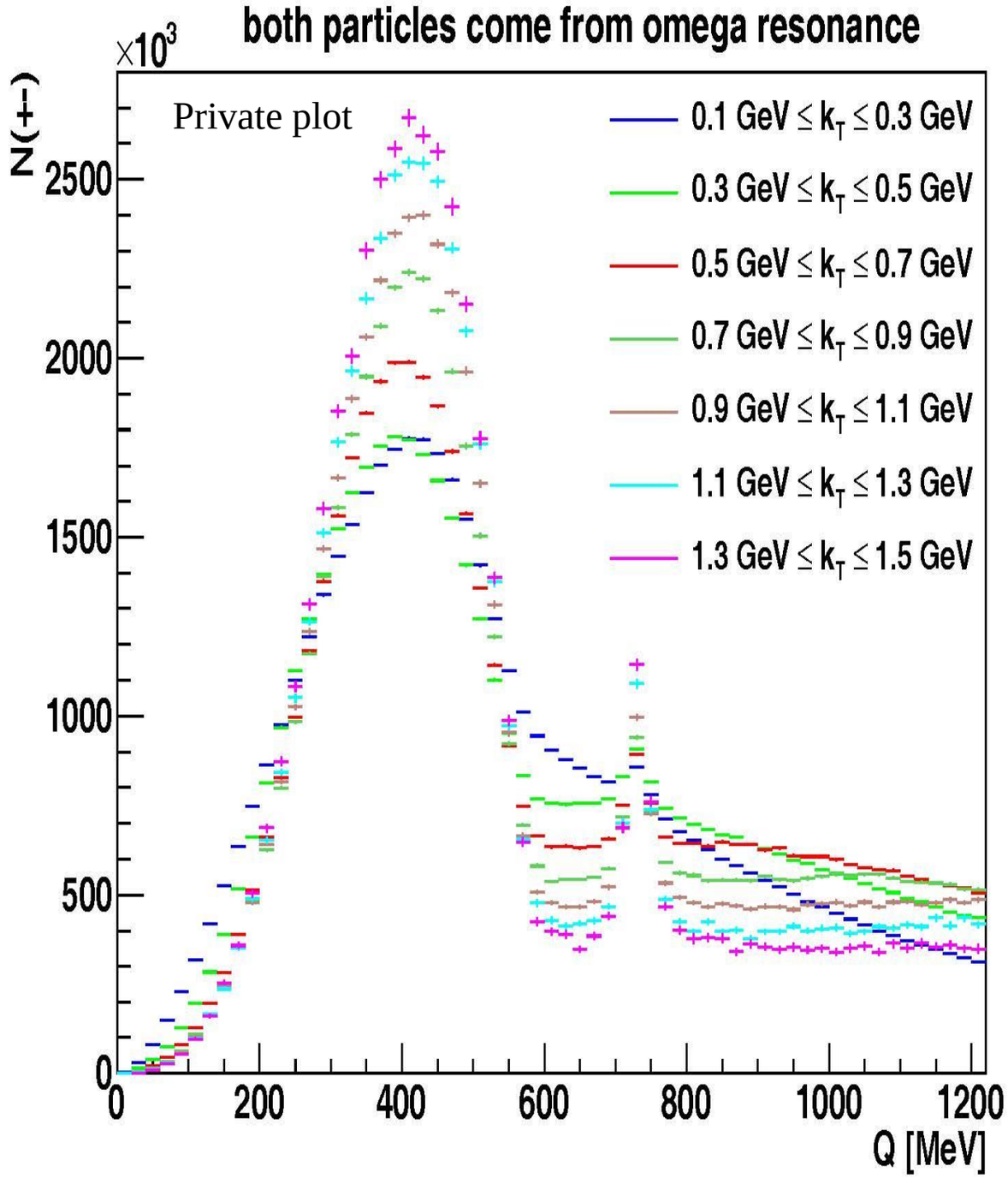

The ΔQ spectrum generated by Pythia8 and the decomposition of its resonant part into leading contributions at 7 TeV. The normalised ω-meson peak is increasing with k_T increase.

OHP (MIX) AND UCP REFERENCE SAMPLES: K_T

The two-particle correlation function C_2 (Q) at 7 TeV for different k_T intervals using the opposite-hemisphere reference sample for data (red) and MC (blue)

Artificial peak in C_2 in BEC region

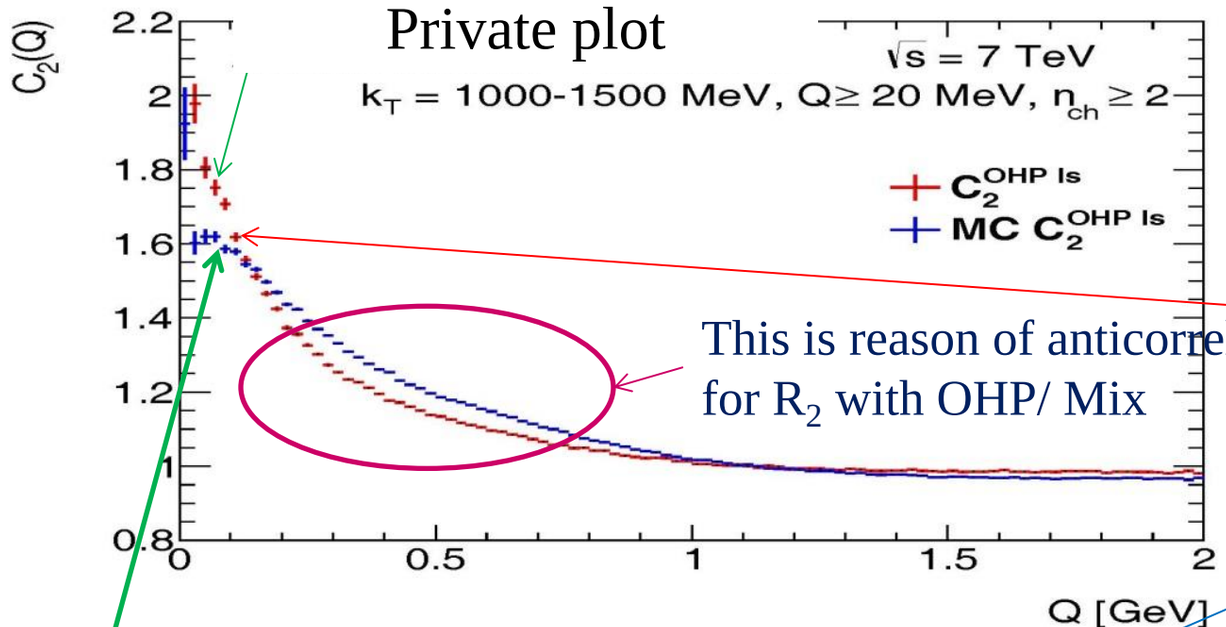

This is reason of anticorrelation for R_2 with OHP/ Mix

Small BEC peak for R_2 OHP

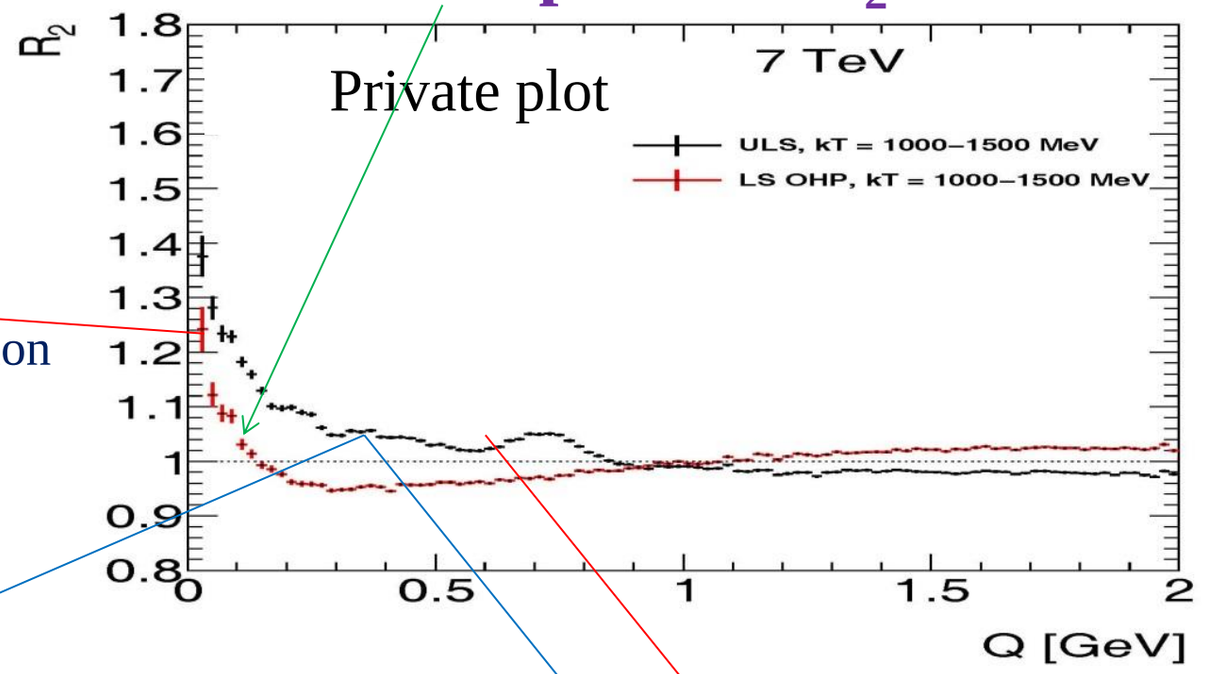

Reflection of resonances in C_2 UCP

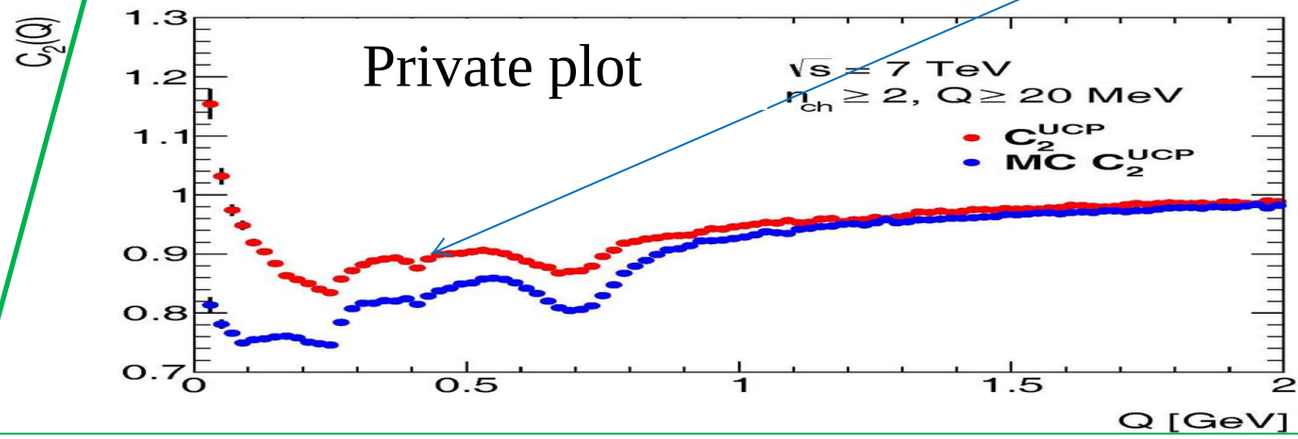

k_T dependences for parameter R for R_2 with different reference samples

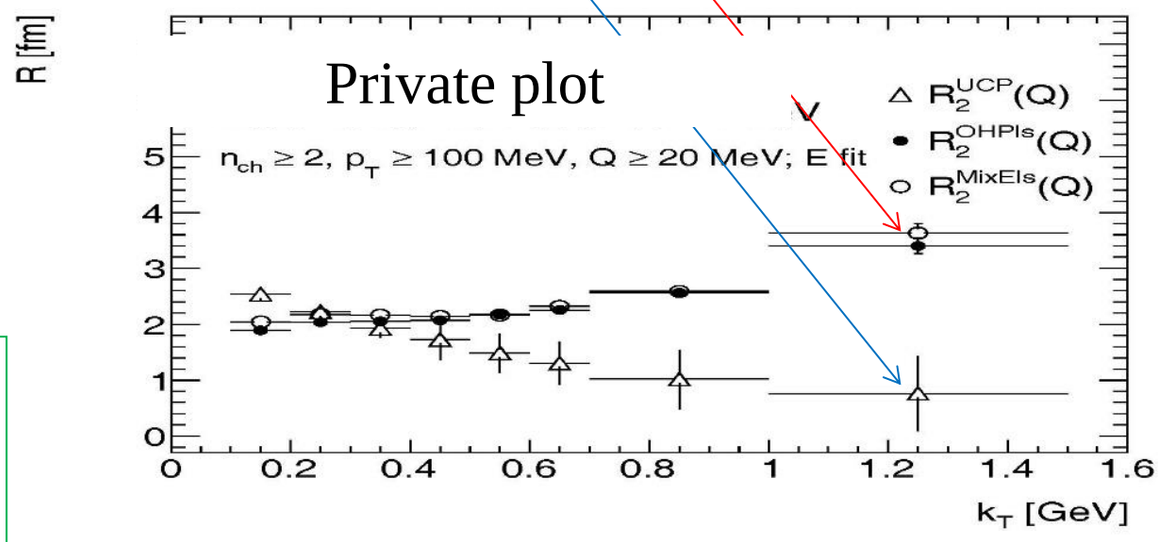

To note is that the slope in the MC can be explained by the fact that MC is tuned to the data and so reflects different dynamical constraints, but MC has no possibility to reproduce a peak at small Q as in the data but shows a broad enhancement.. The additional correlations in large multiplicity intervals seem to be due to multi-jet events in MC where the correlations between particles within the same jet can contribute to the region of low-Qs. In this case, the single-ratio C_2(Q) correlation function numerator contains contributions from multi-jets, while the denominator does not have this effect as no correlations are expected in randomly paired particles.

Disadvantage for OHP/MIX: violation of energy-momentum constraint, event topology, destroying other features such as non-BEC etc.

INCLUSIVE DOUBLE RATIO CORRELATION FUNCTIONS

EPJC 75 (2015) 466

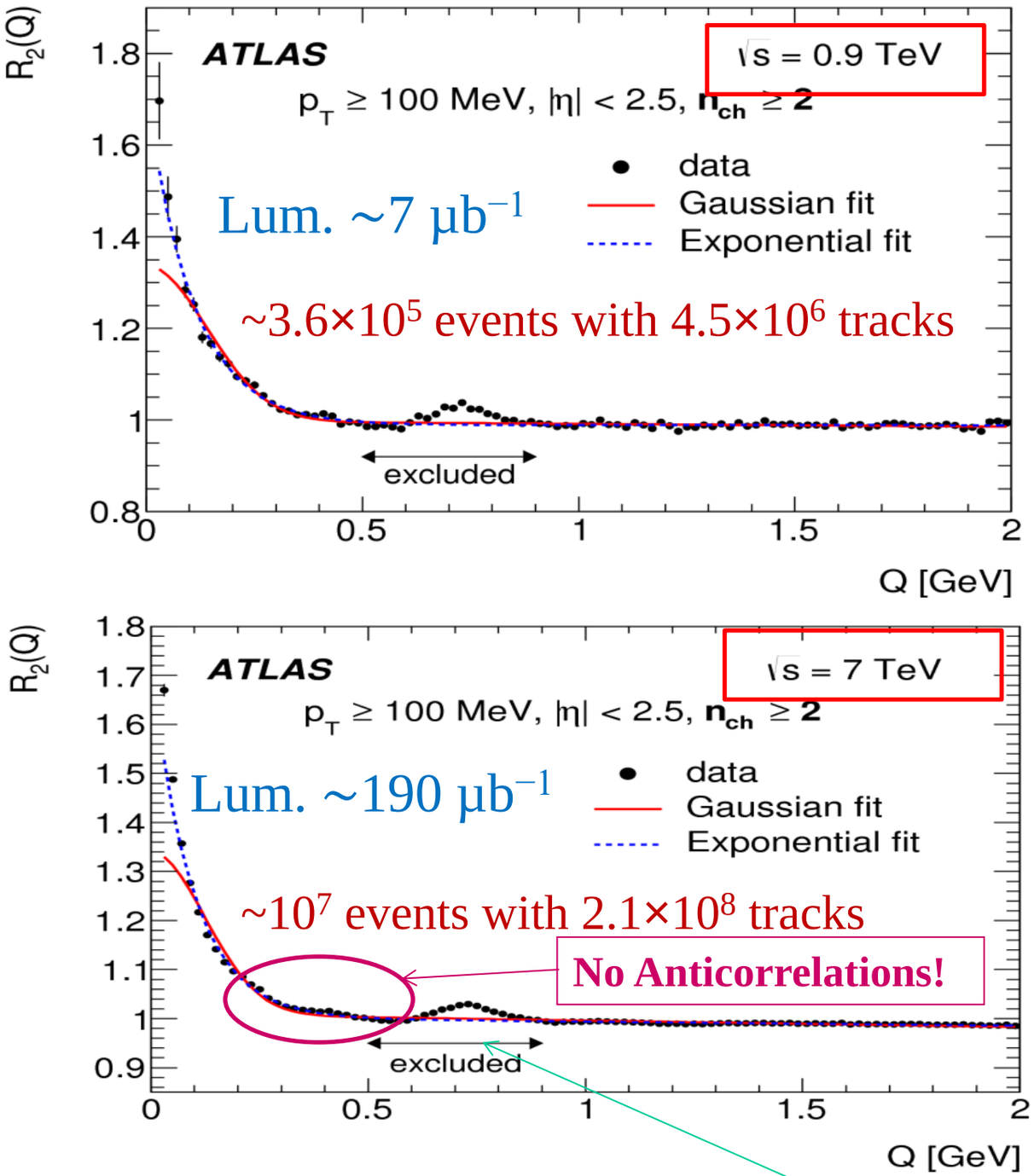

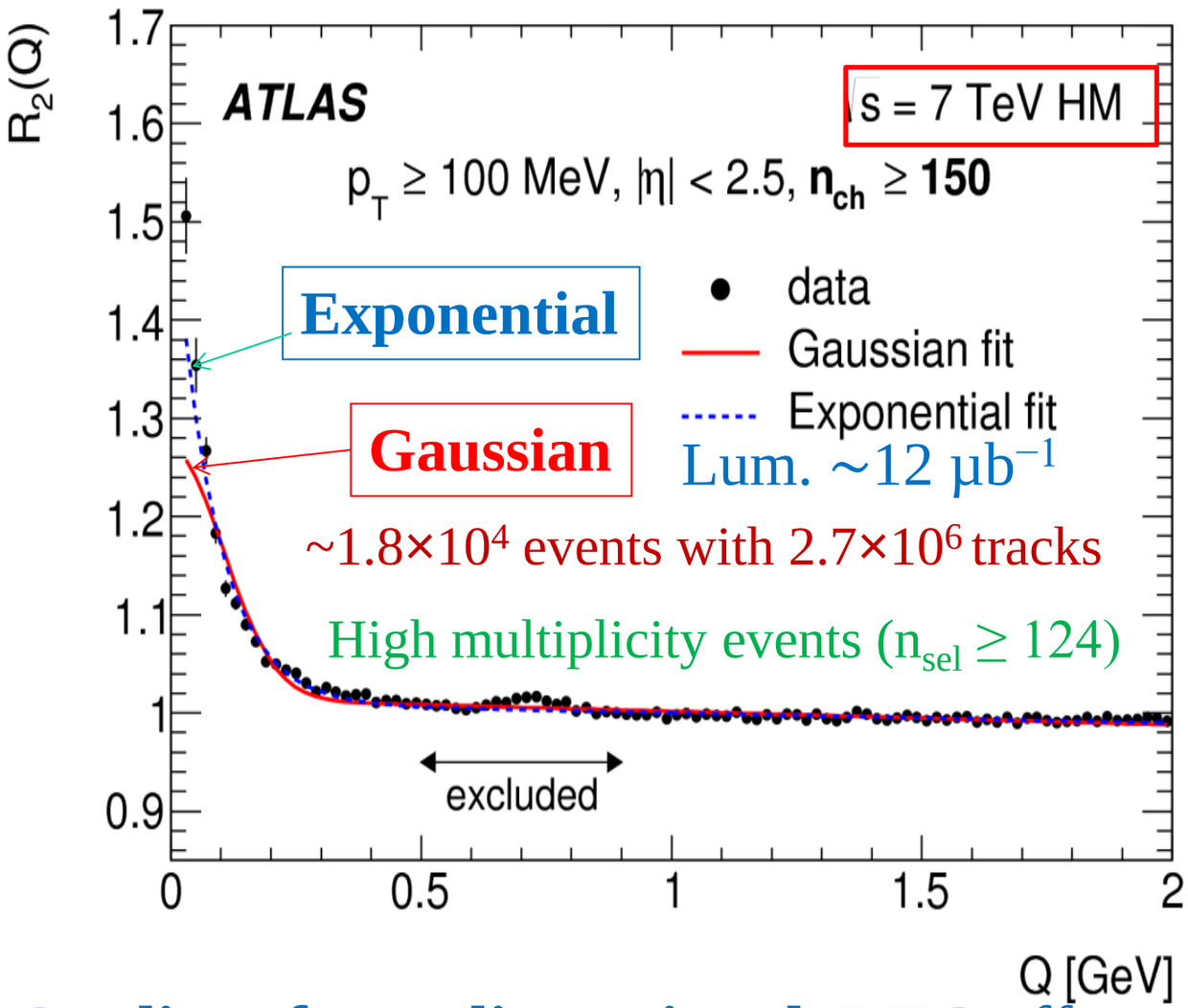

Studies of one-dimensional BEC effects in **pp** collisions for $p_T > 100$ *MeV* **and** $|\eta| < 2.5$ at centre-of-mass energies of **0.9 and 7 TeV**.

Fit to extract strength and source size. **Goldhaber** spherical shape with a **Gaussian** distribution of the source. **Exponential**, radial Lorentzian distribution of the source -> **much better at low Q.**

Bump in ρ-meson region because **MC overestimates ρ→ππ**, therefore **region 0.5 – 0.9 GeV excluded** from the fit. **Q region is from 0.02 to 2 GeV.**

SYSTEMATIC UNCERTAINTIES FOR BEC

EPJC 75 (2015) 466

- The systematic uncertainties of the inclusive Bose-Einstein correlation parameters, **R** (the effective radius parameter of the source) and **λ** (the strength of the effect parameter), of the *fit of $R_2(Q)$ correlation functions with exponential model* are summarized in the Table.
- The systematic uncertainties are combined by adding them in quadrature and the resulting values are given in the bottom row.
- The same sources of uncertainty are considered for the differential measurements in n_{ch} and the average transverse momentum k_T of a pair, and their impact on the fit parameters is found to be similar in size.

	0.9 TeV		7 TeV		7 TeV (HM)	
Source	λ	R	λ	R	λ	R
Track reconstruction efficiency	0.6%	0.7%	0.3%	0.2%	1.3%	0.3%
Track splitting and merging	negligible		negligible		negligible	
Monte Carlo samples	14.5%	12.9%	7.6%	10.4%	5.1%	8.4%
Coulomb correction	2.6%	0.1%	5.5%	0.1%	3.7%	0.5%
Fitted range of Q	1.0%	1.6%	1.6%	2.2%	5.5%	6.0%
Starting value of Q	0.4%	0.3%	0.9%	0.6%	0.5%	0.3%
Bin size	0.2%	0.2%	0.9%	0.5%	4.1%	3.4%
Exclusion interval	0.2%	0.2%	1%	0.6%	0.7%	1.1%
Total	14.8%	13.0%	9.6%	10.7%	9.4%	10.9%

Comparison with other experiments

The results of BEC parameters for
Exponential fits of R_2 used total uncertainties
Statistical uncertainties are below 2–4 %

Energy [GeV]	n_{ch}	λ	$R^{(E)}$ [fm]
0.9	≥2	0.74 ± 0.10	1.83 ± 0.25
7	≥2	0.71 ± 0.07	2.06 ± 0.22
7 (HM)	≥150	0.74 ± 0.06	2.36 ± 0.30
13	≥2	0.90±0.02	2.85±0.04

Comparison with results of previous experiments

$$R^{(G)} = R^{(E)} / \sqrt{\pi}$$

Energy [GeV]	n_{ch}	$R^{(G)}$ [fm]
0.9	≥2	1.03 ± 0.14
7	≥2	1.16 ± 0.12
7 (HM)	≥150	1.33 ± 0.17
13	≥2	1.58±0.02

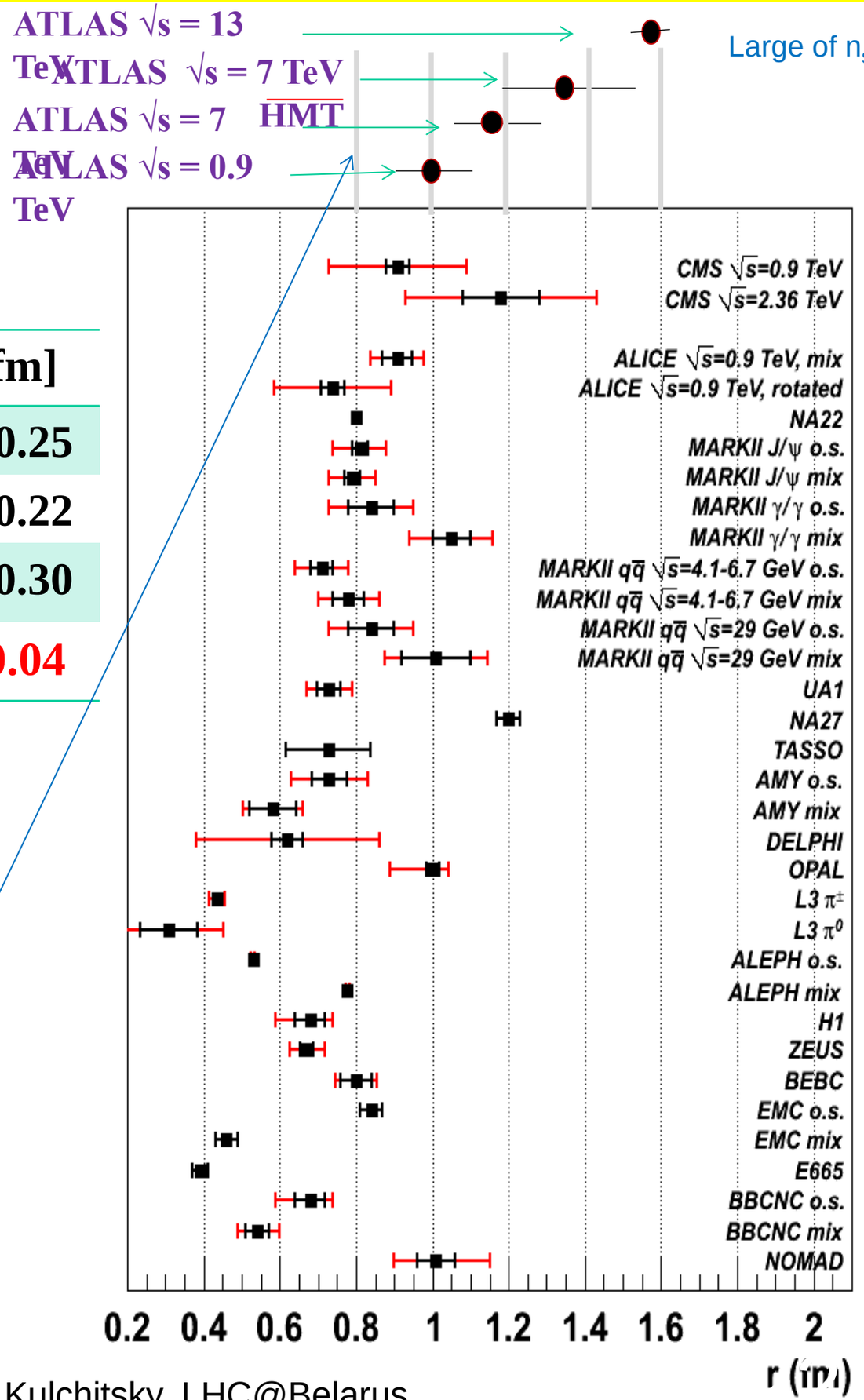

MULTIPLICITY DEPENDENCE OF λ AND R BEC PARAMETERS

EPJC 75 (2015) 466

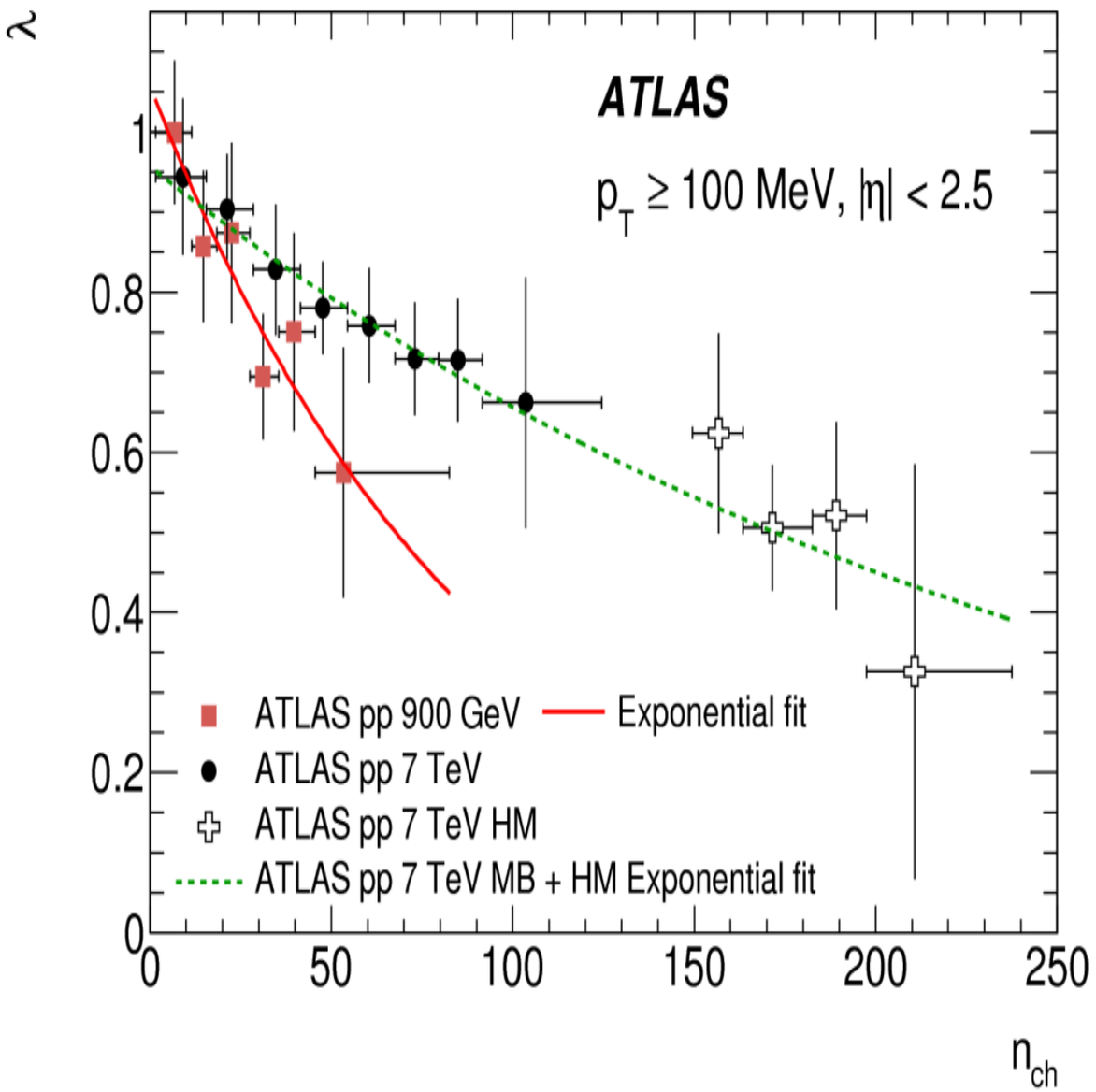

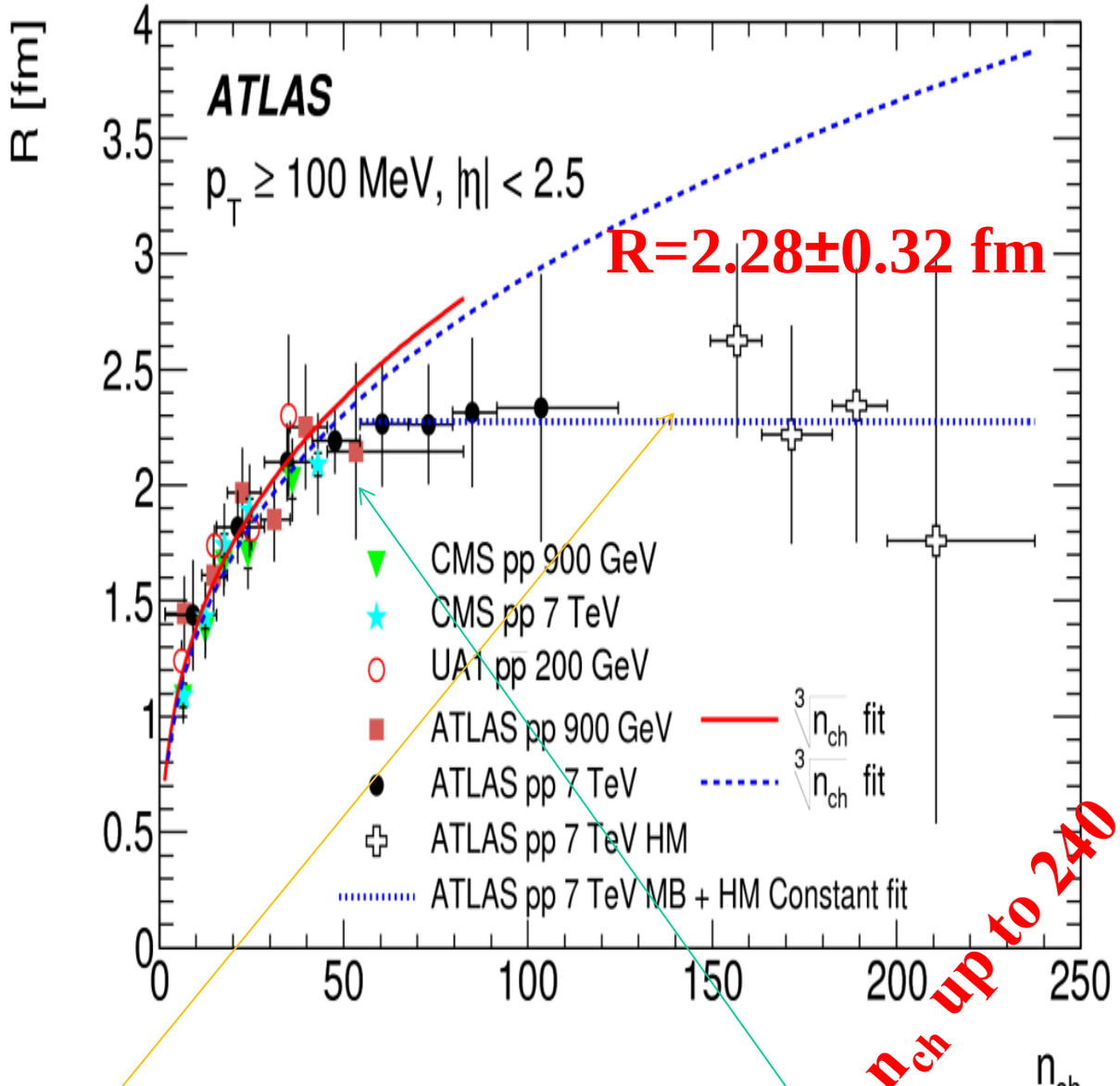

- **λ and R are energy independent within the uncertainties**
- **λ exponentially decrease with multiplicity**

Good Agreement with CMS & UA1

- R of the $\alpha \cdot n_{ch}^{1/3}$ fit for $n_{ch} \leq 55$: *0.9 TeV is $\alpha = 0.64 \pm 0.07$ fm, 7 TeV is $\alpha = 0.63 \pm 0.05$ fm*
- **R** is a ***Constant*** for $n_{ch} > 55$ at 7 TeV ***R = 2.28±0.32 fm*** **observed for the first time**

THEORY PREDICTION

V.A. Shegelsky, et al, Phys Letter B703 (2011) 288; Nucl Phys B219 (2011) 10

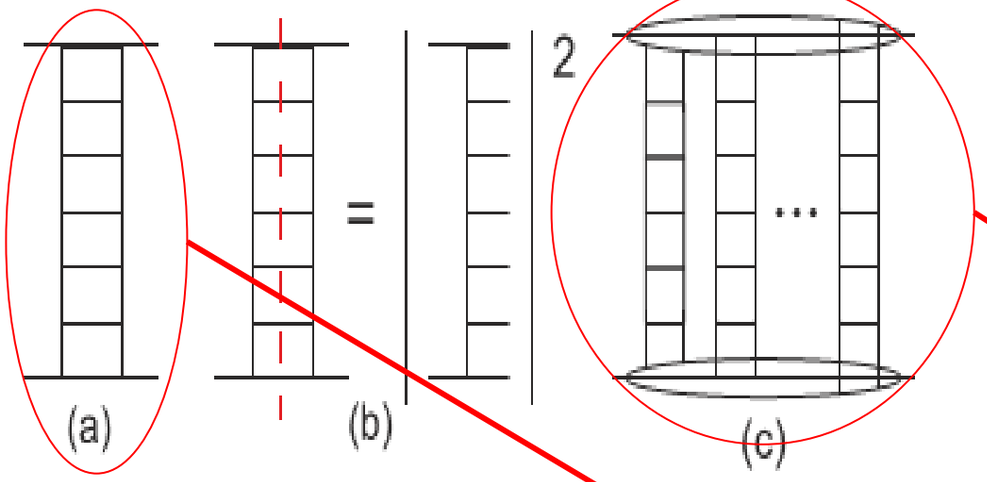

Fig. 1. (a) The ladder diagram for one-Pomeron exchange; (b) cutting one-Pomeron exchange leads to the multiperipheral chain of final state particles; (c) a multi-Pomeron exchange diagram.

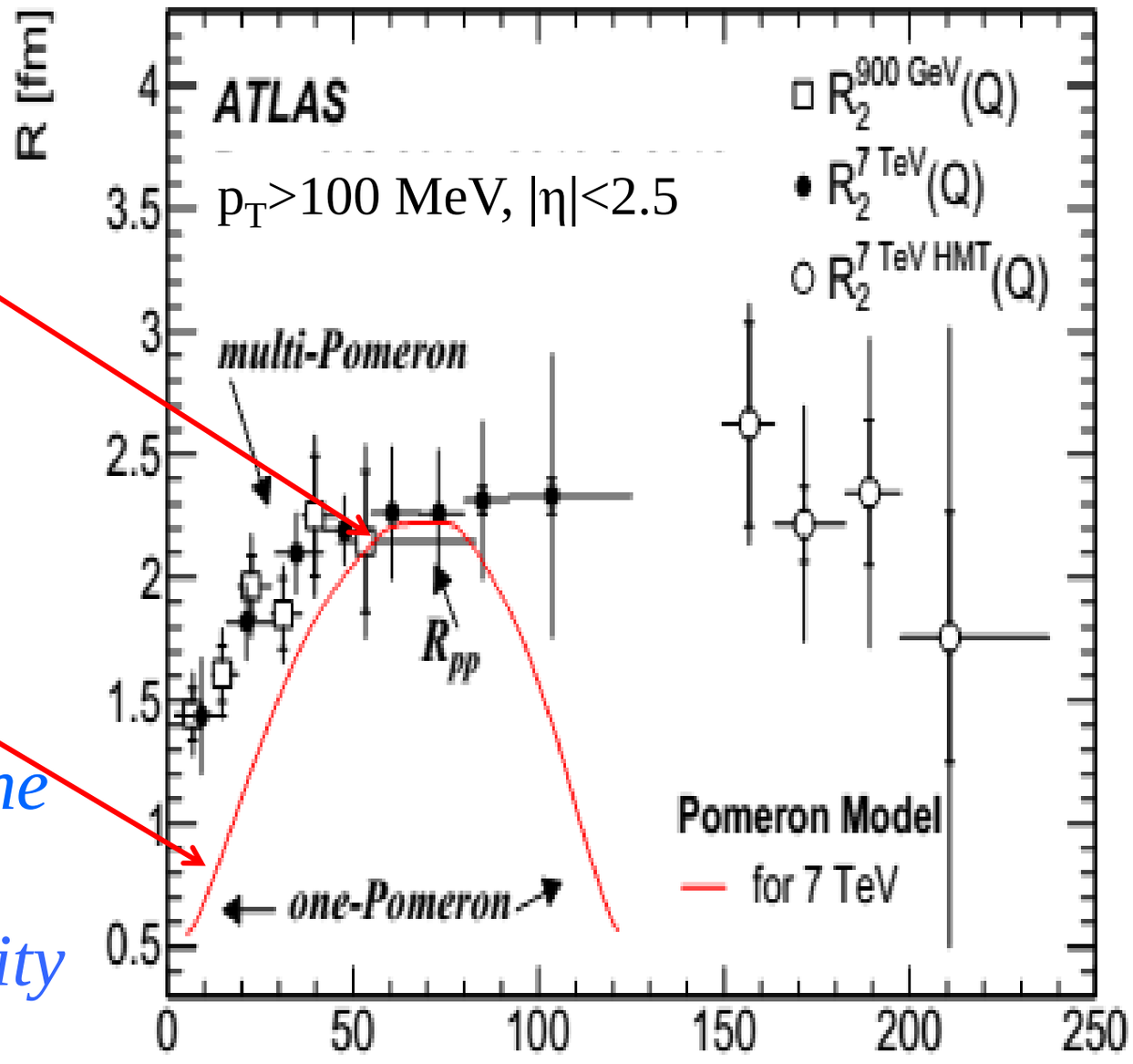

Interpretation: *The BEC radius for* ***one parton-parton interaction*** *(underline events, cut Pomeron) is* ***~1 fm****, like for smallest multiplicity. For high multiplicity events* we see BEC signal from **some** *parton-parton interactions*. **The radius** for high multiplicity can be interpret as an *average distance between separate parton-parton interactions is* ***~2 fm****.*

The prediction of **Pomeron model** for **R_{max}=2.2 fm** is in agreement with our saturated radius **R=2.3 fm**. There is not principal agreement with data for n>80

K_T DEPENDENCE OF λ AND R PARAMETERS

EPJC 75 (2015) 466

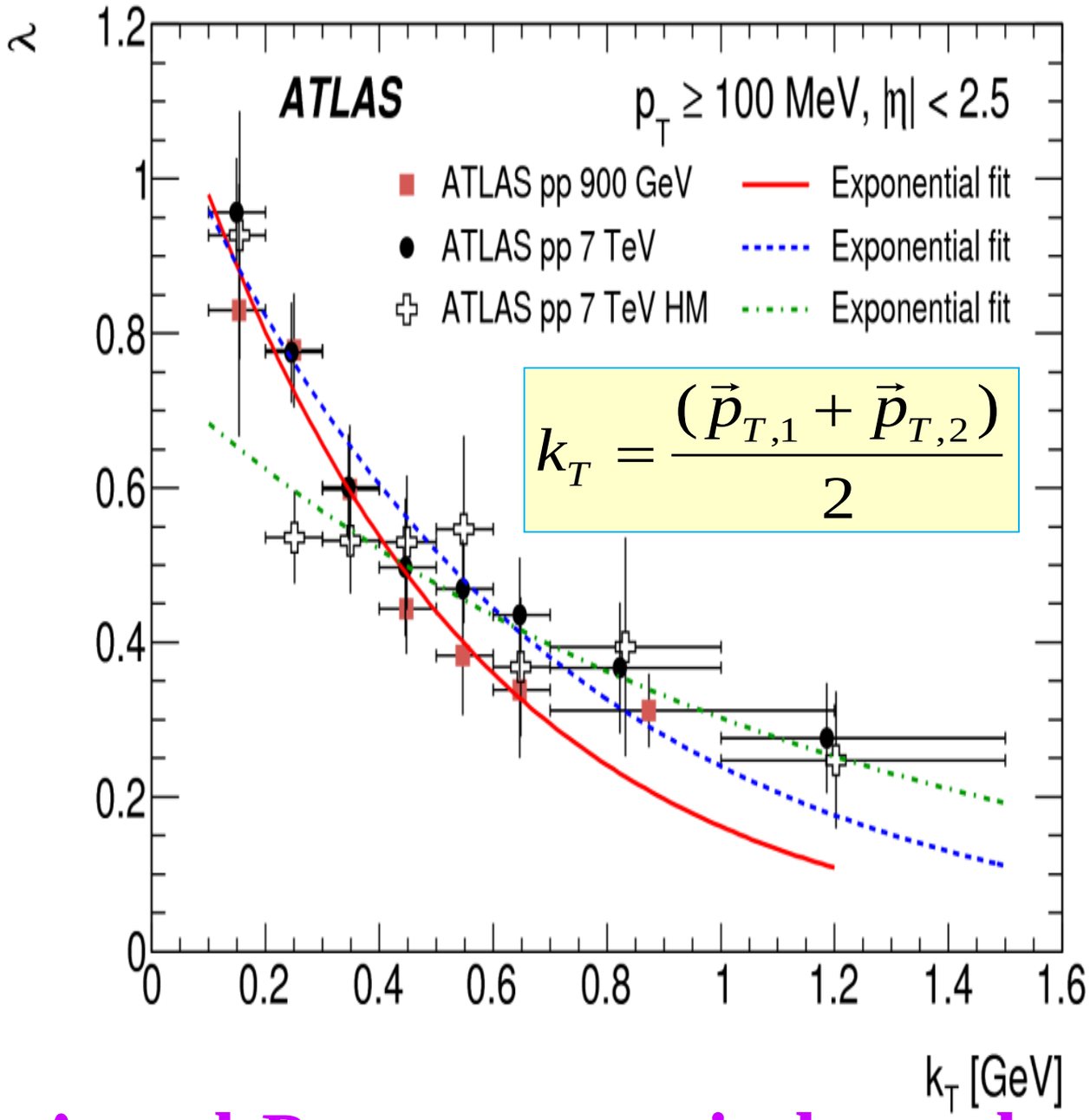

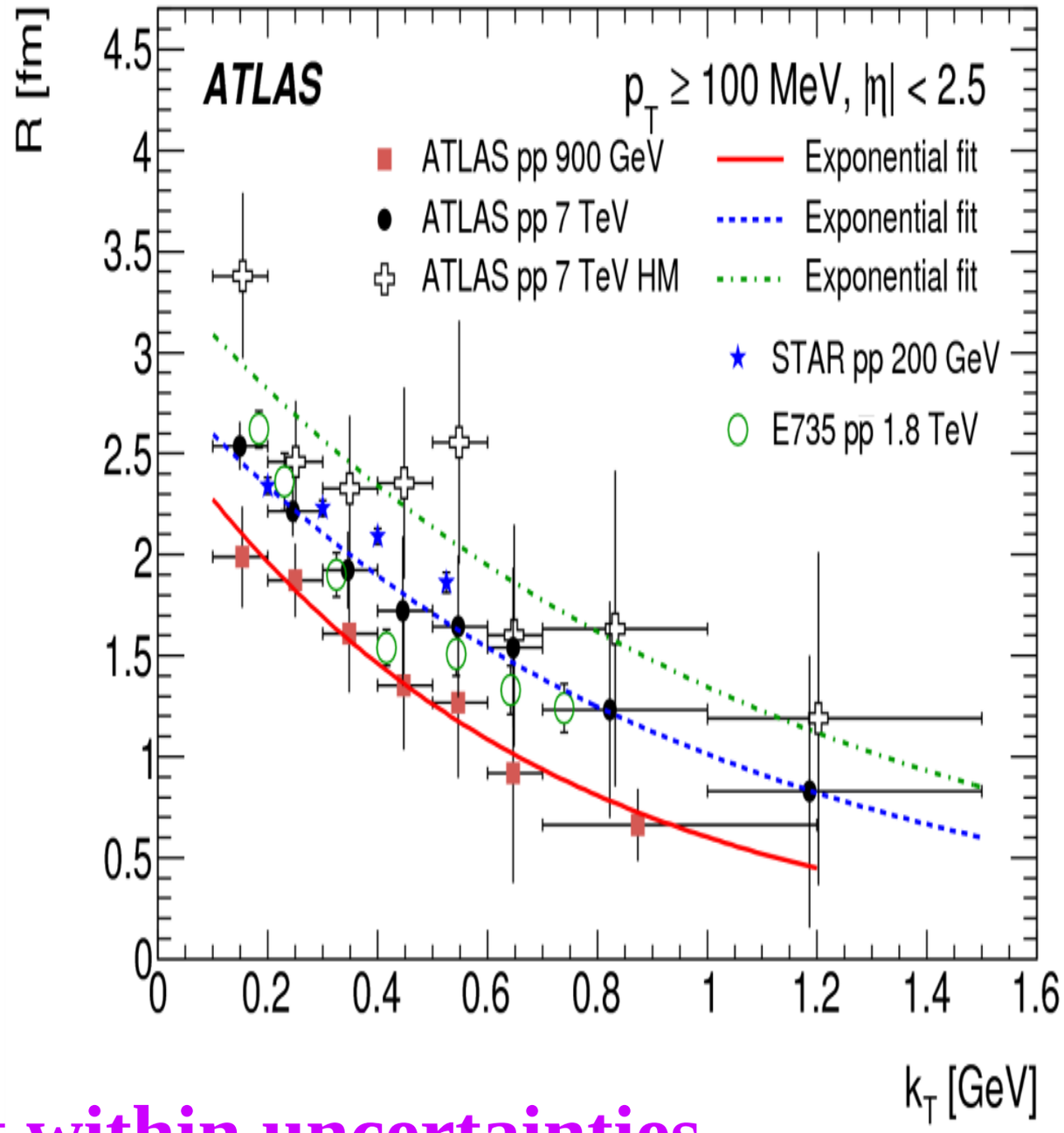

- **λ and *R* are energy-independent within uncertainties**
- **λ and R decrease exponentially with k_T**
- **Good agreement with earlier (non-LHC) measurements**

K_T DEPENDENCE OF λ AND R PARAMETERS

EPJC 75 (2015) 466

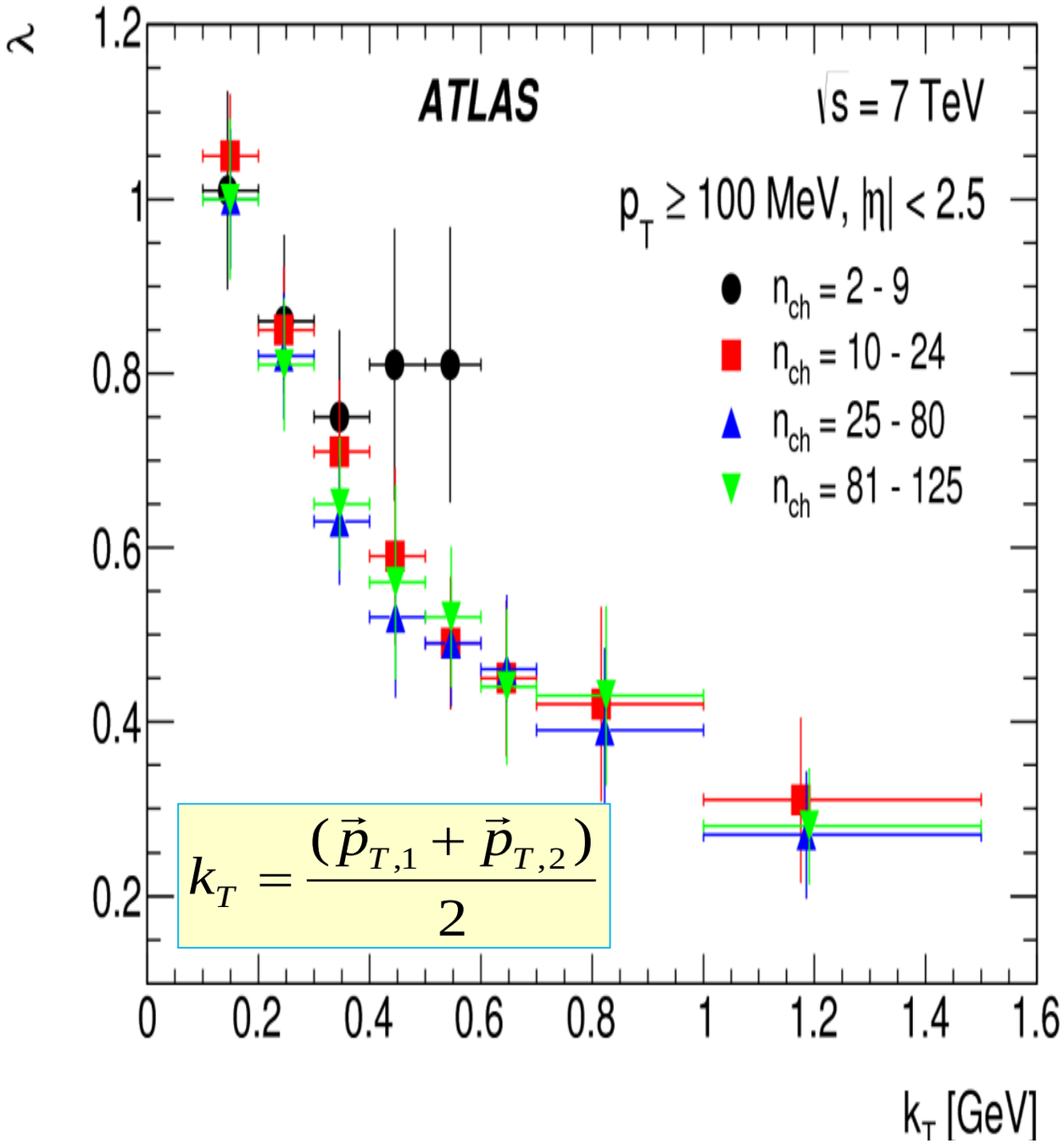

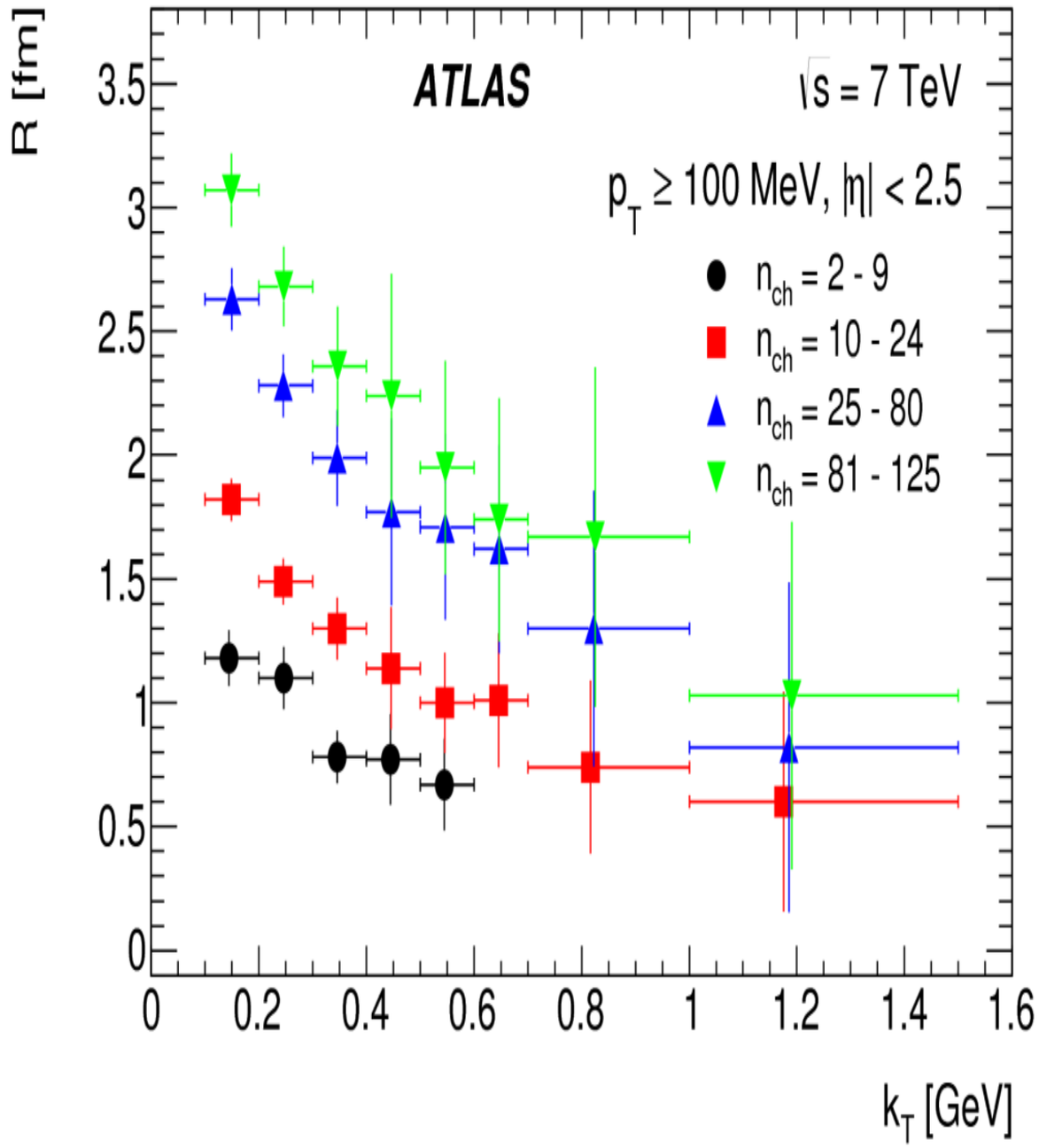

- **No k_T –dependence of λ for different multiplicity intervals**
- k_T–dependence of R shows R increasing with multiplicity interv.

MULTIPLICITY DISTRIBUTIONS FOR DATA AND MC SAMPLES

Data √s = 13 TeV MB & HMT

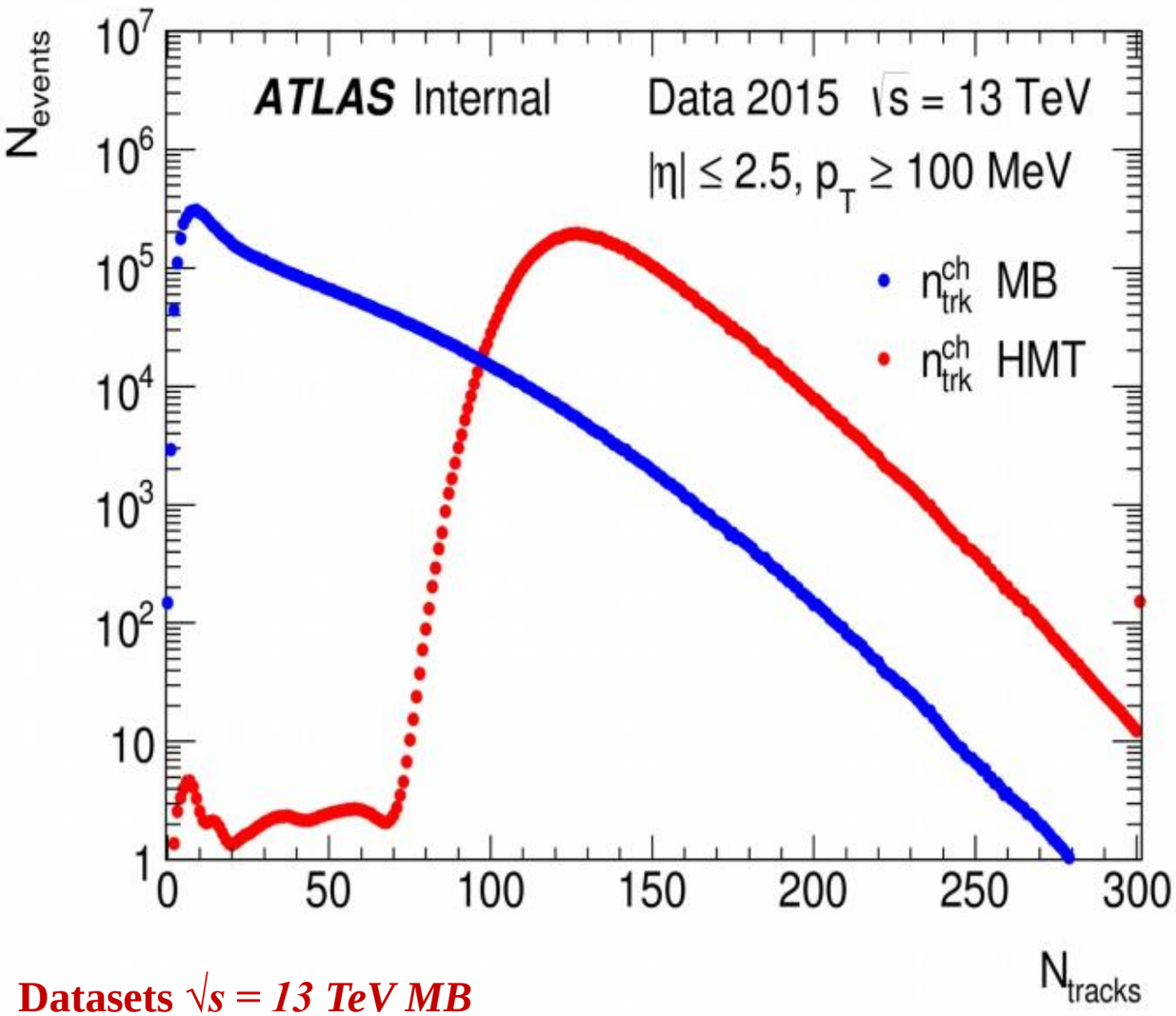

MC √s = 13 TeV

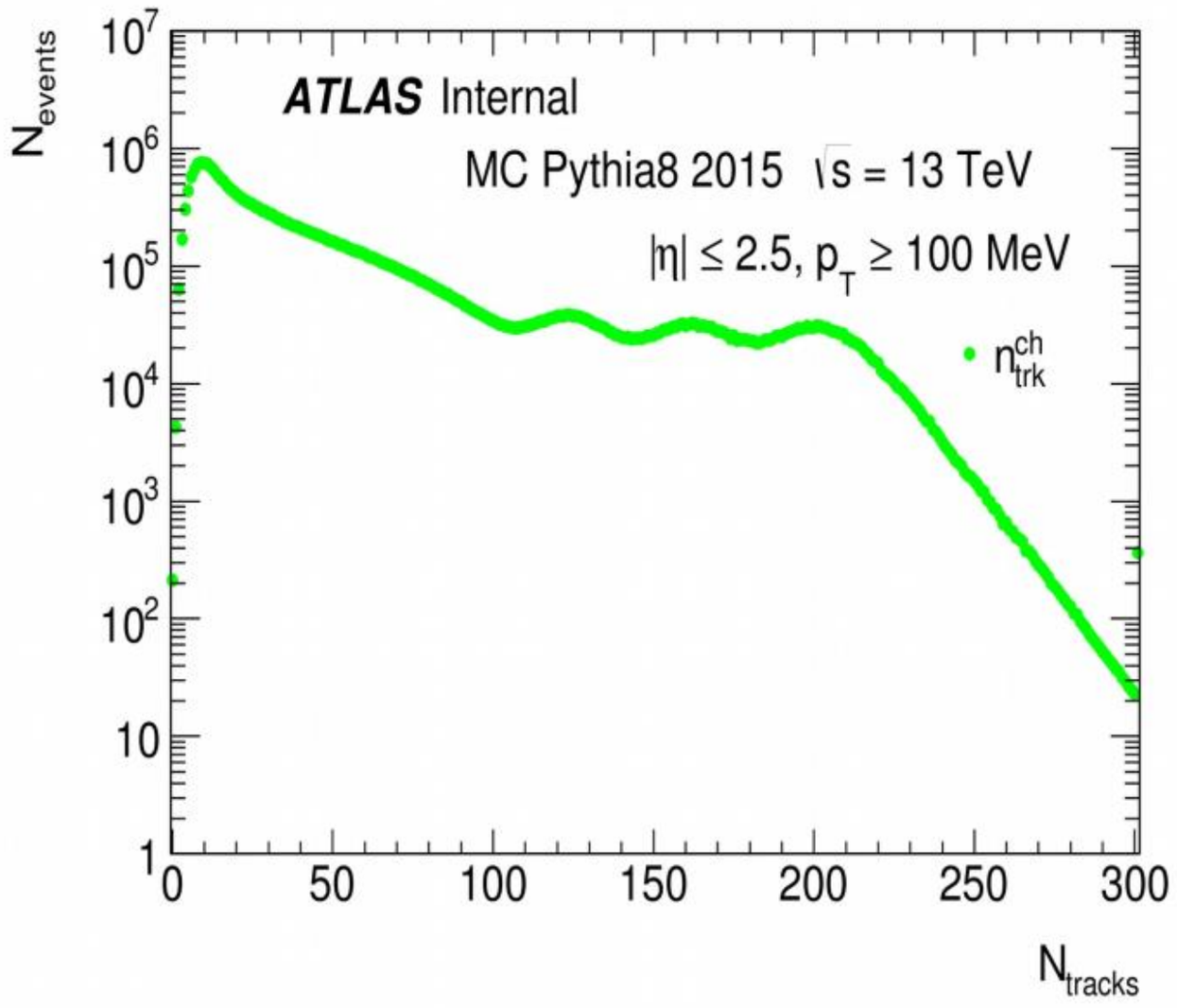

Datasets *√s = 13 TeV MB*

data15_13TeV:data15_13TeV.00267358.physics_MinBias.merge.AOD.r6945_p2410/

data15_13TeV:data15_13TeV.00267359.physics_MinBias.merge.AOD.r6945_p2410/

9 318 378 selected events, 237 960 365 selected tracks

Datasets *√s = 13 TeV HMT*

data15_13TeV:data15_13TeV.00267360.physics_MinBias.merge.AOD.r6945_p2410/

data15_13TeV:data15_13TeV.00267367.physics_MinBias.merge.AOD.r6945_p2410/

data15_13TeV:data15_13TeV.00267385.physics_MinBias.merge.AOD.r6945_p2410/

data15_13TeV:data15_13TeV.00267599.physics_MinBias.merge.AOD.r6945_p2410/

9 126 240 selected events, 977 657 200 selected tracks

$R_2(Q)$ EXAMPLES OF DIFFERENT SLICES AT 13 TEV

MB

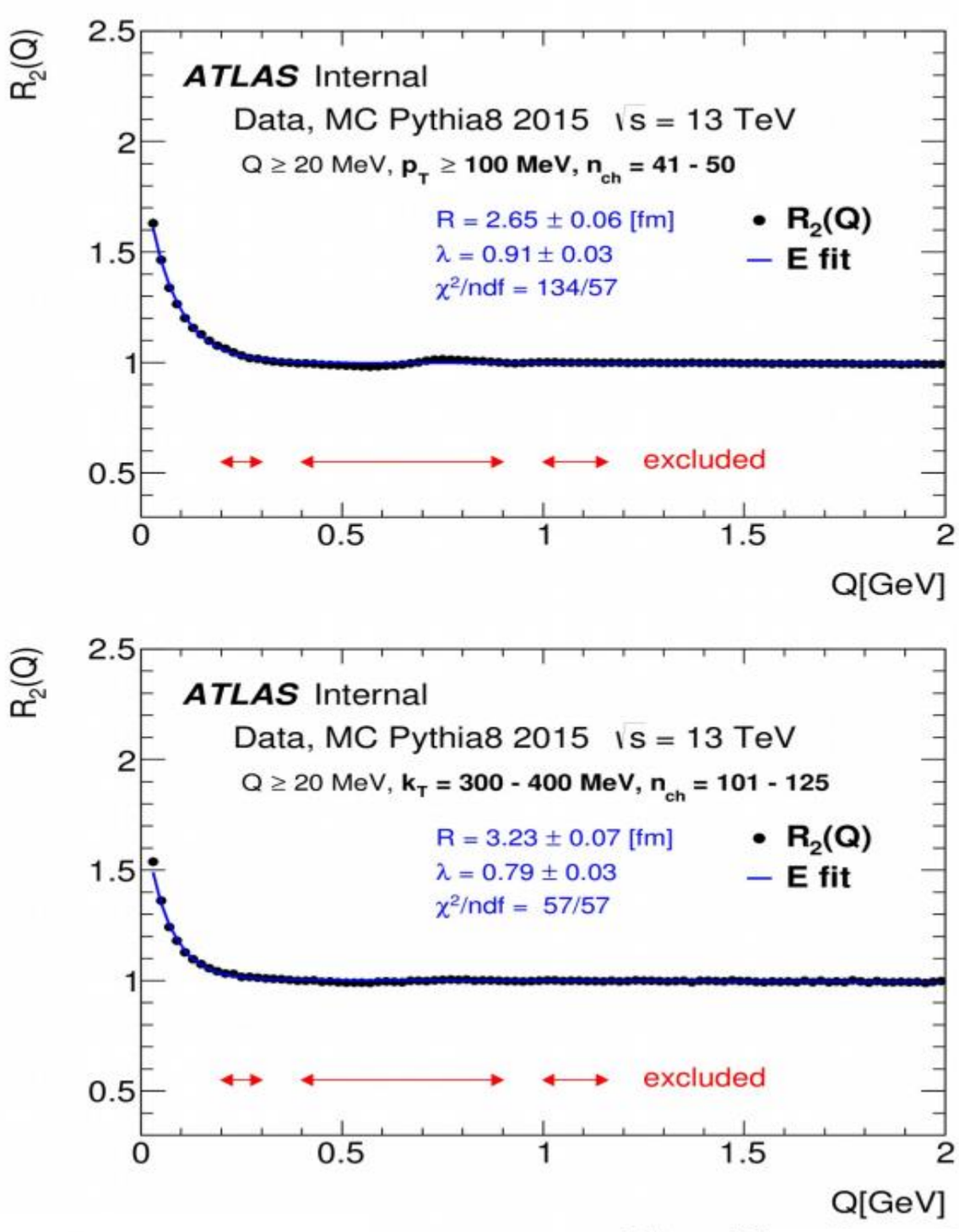

HMT

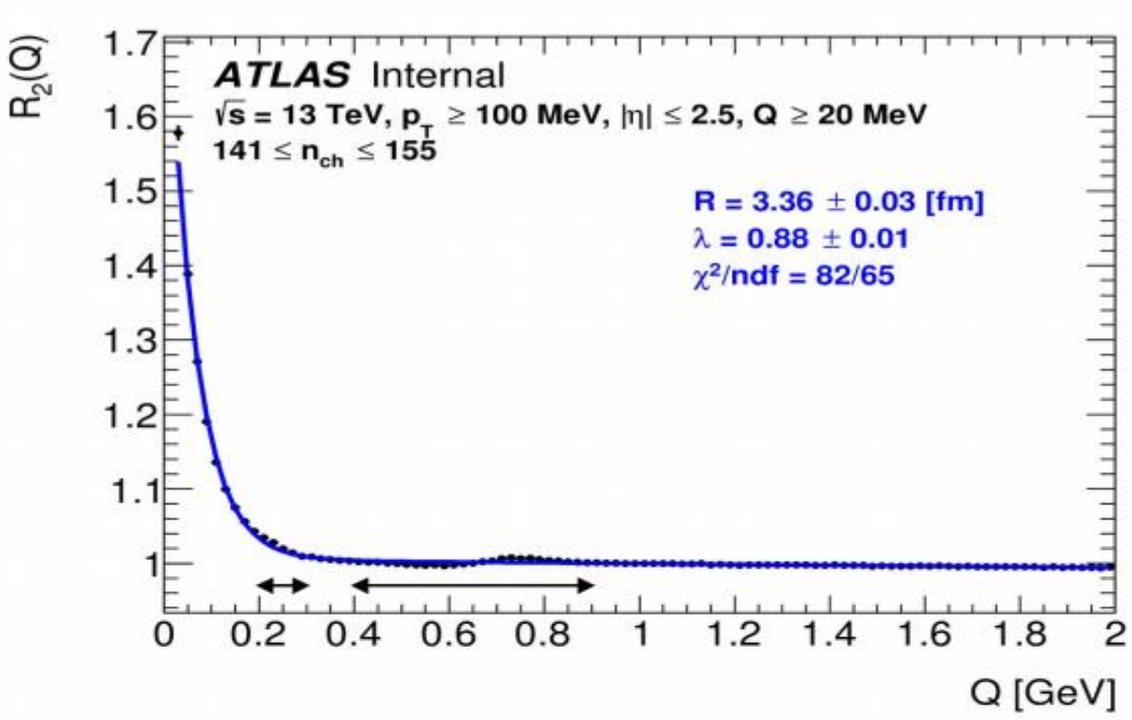

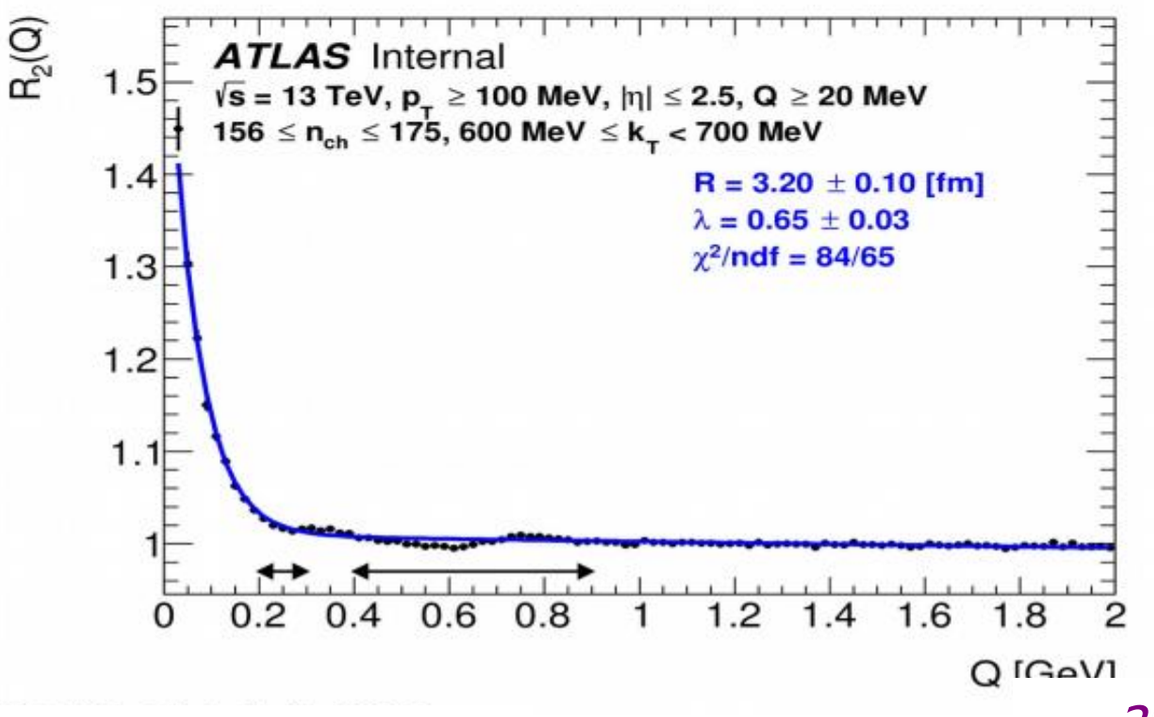

λ AND R BEC PARAMETERS FOR DIFFERENT K_T INTERVALS AT 13 TEV FOR MB EVENTS

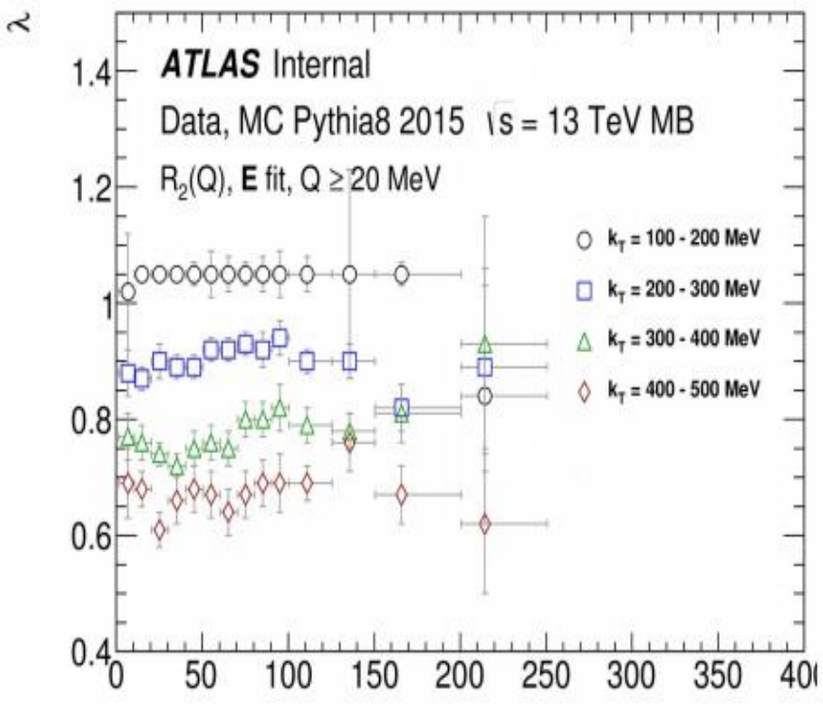

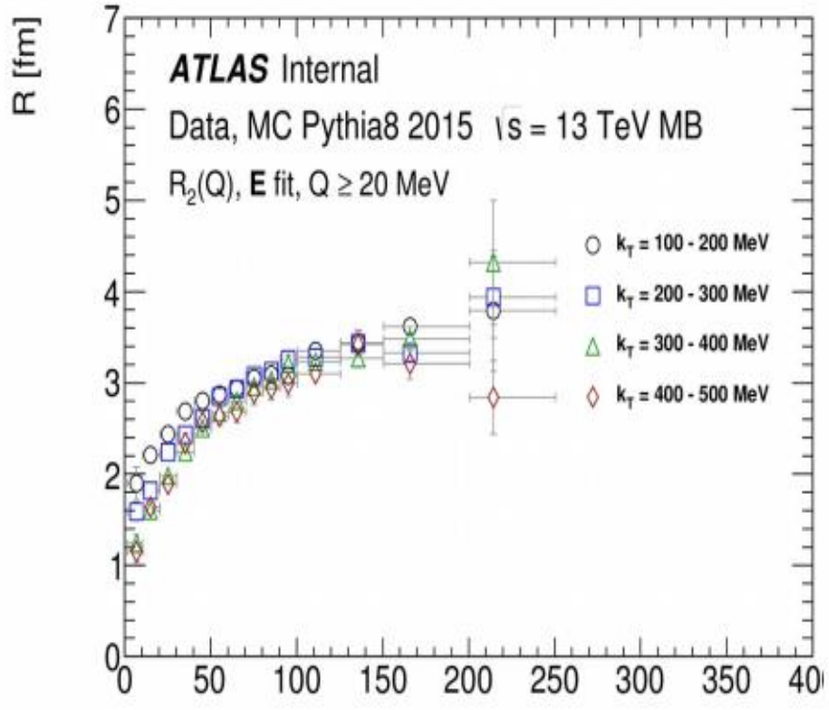

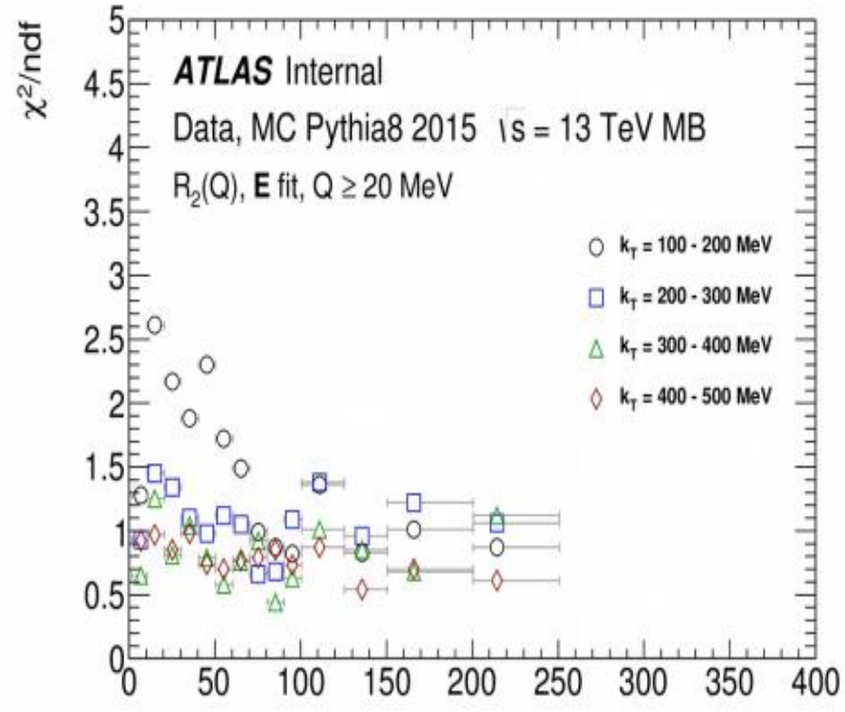

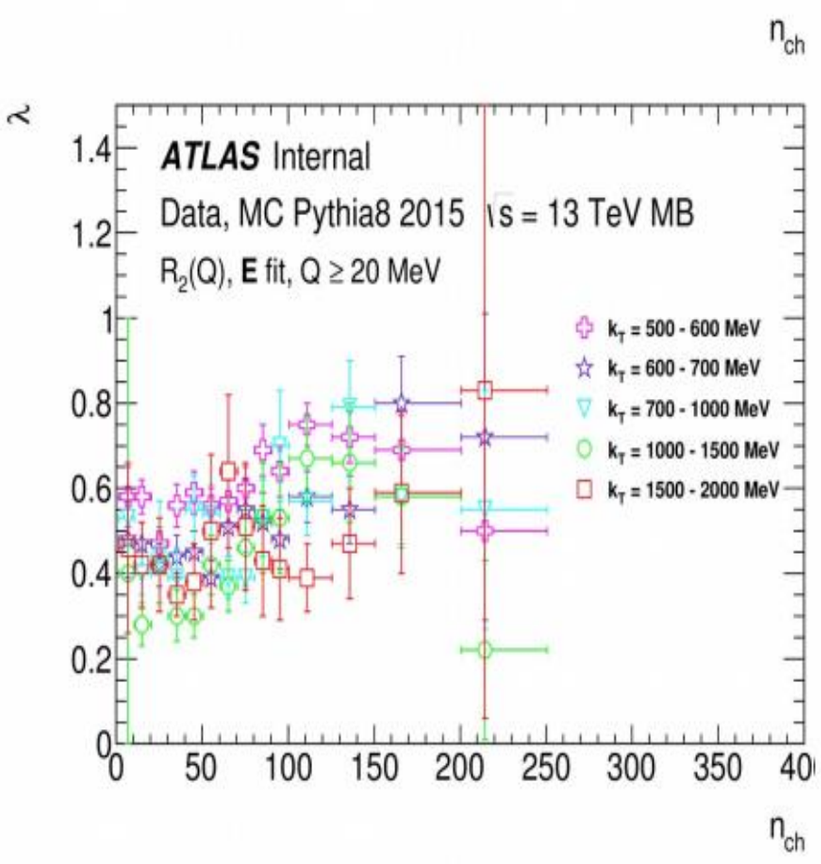

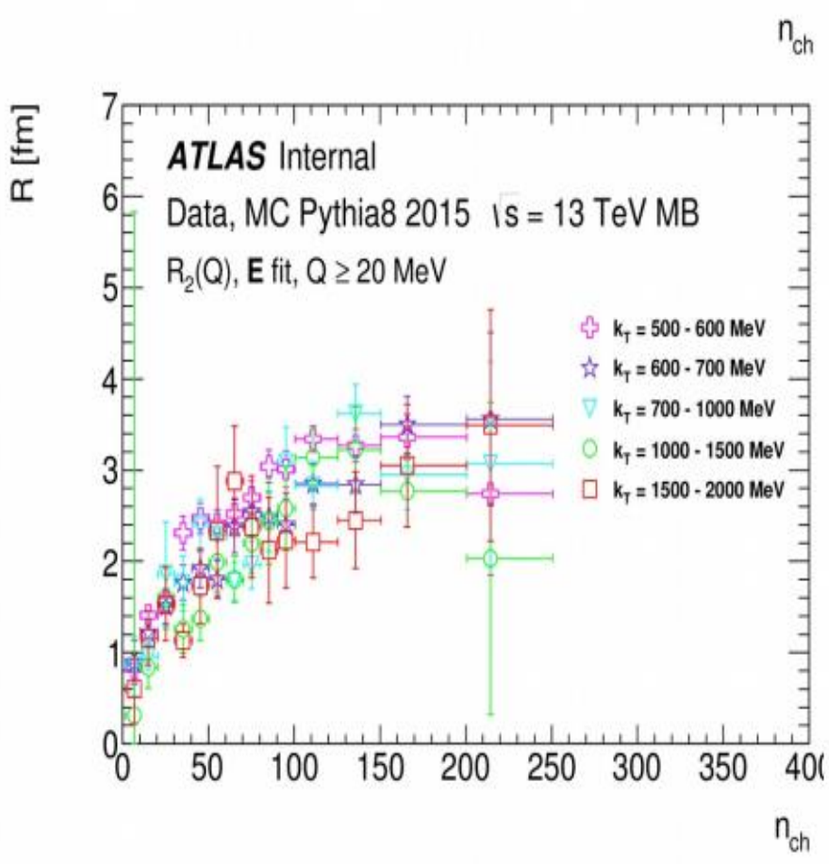

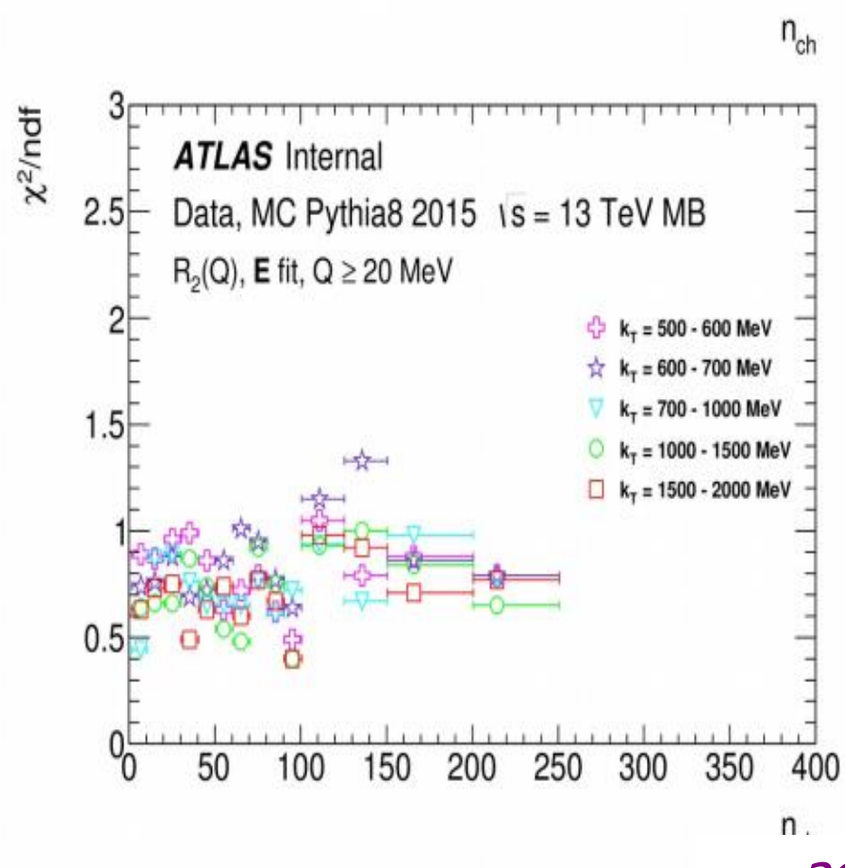

λ AND R BEC PARAMETERS FOR DIFFERENT N_{CH} INTERVALS AT 13 TEV FOR MB EVENTS

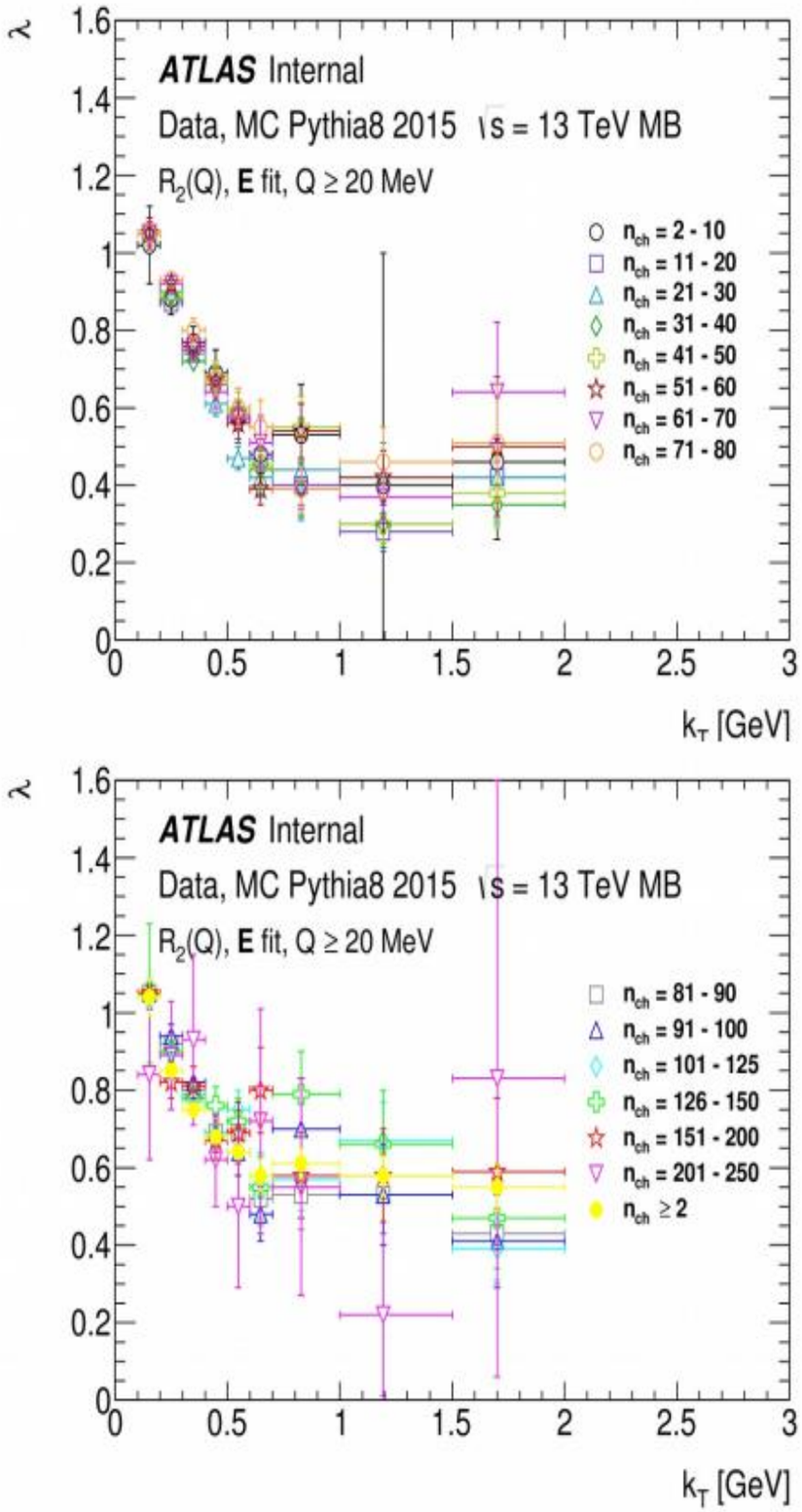

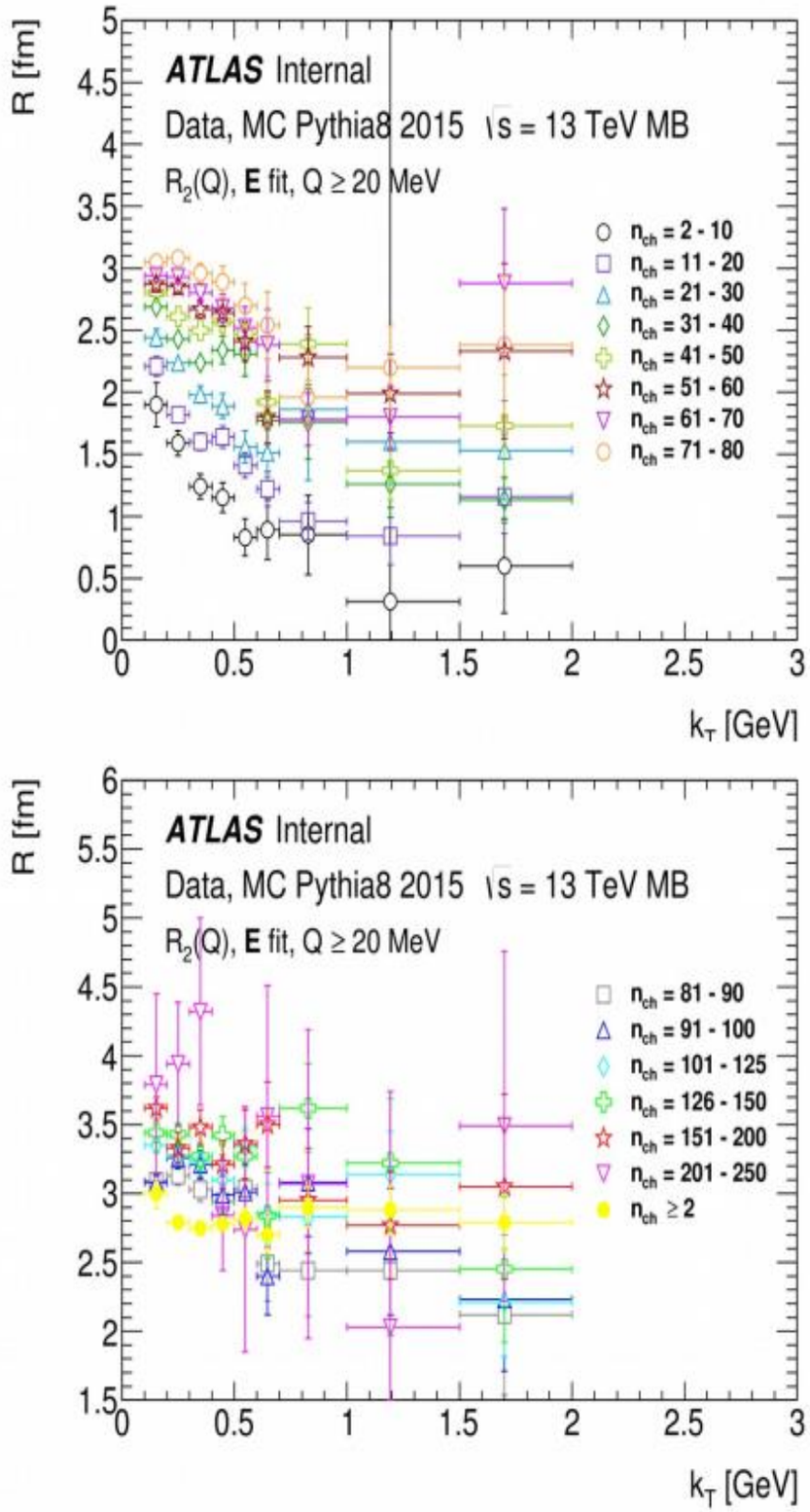

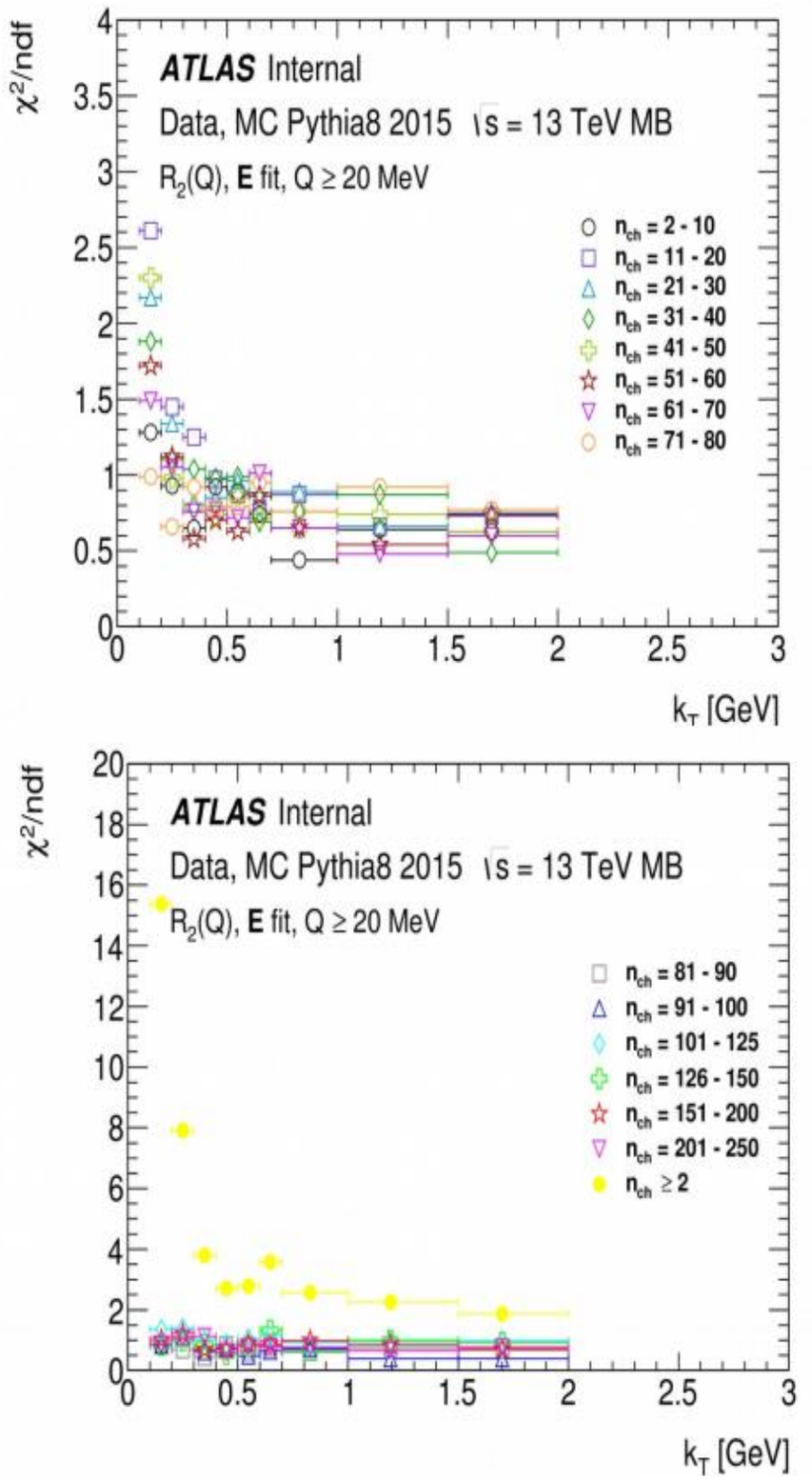

λ AND R BEC PARAMETERS FOR DIFFERENT K_T INTERVALS AT 13 TEV FOR HMT EVENTS

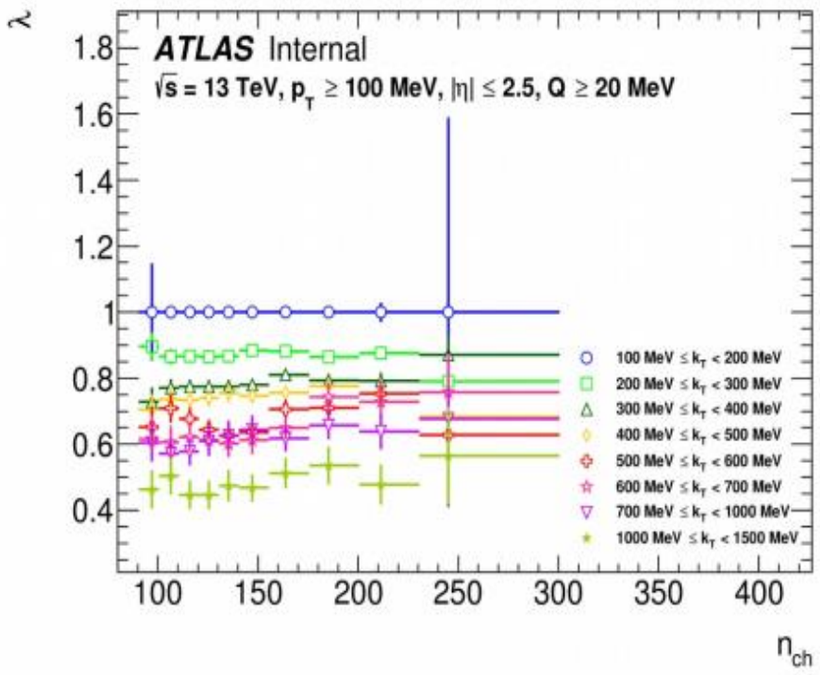

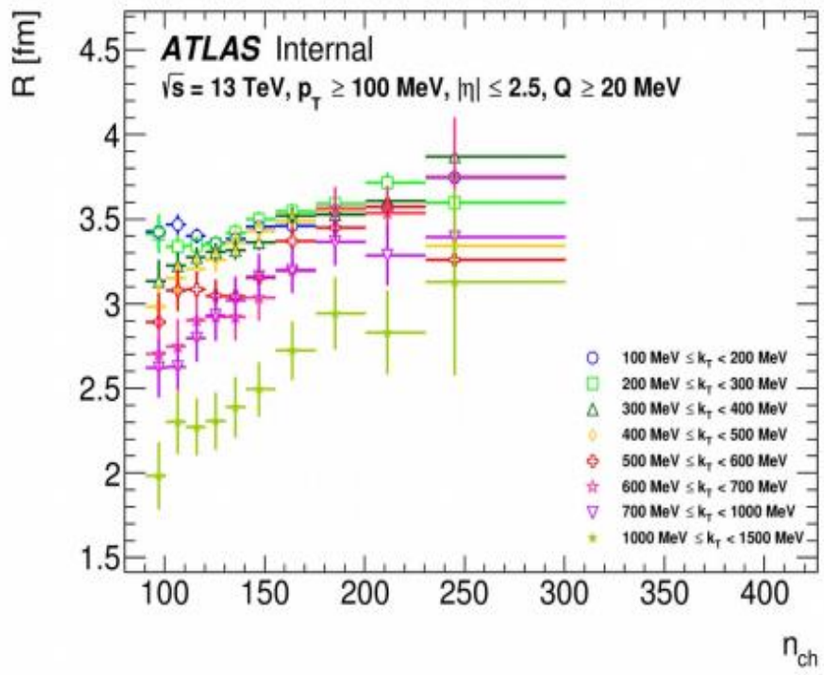

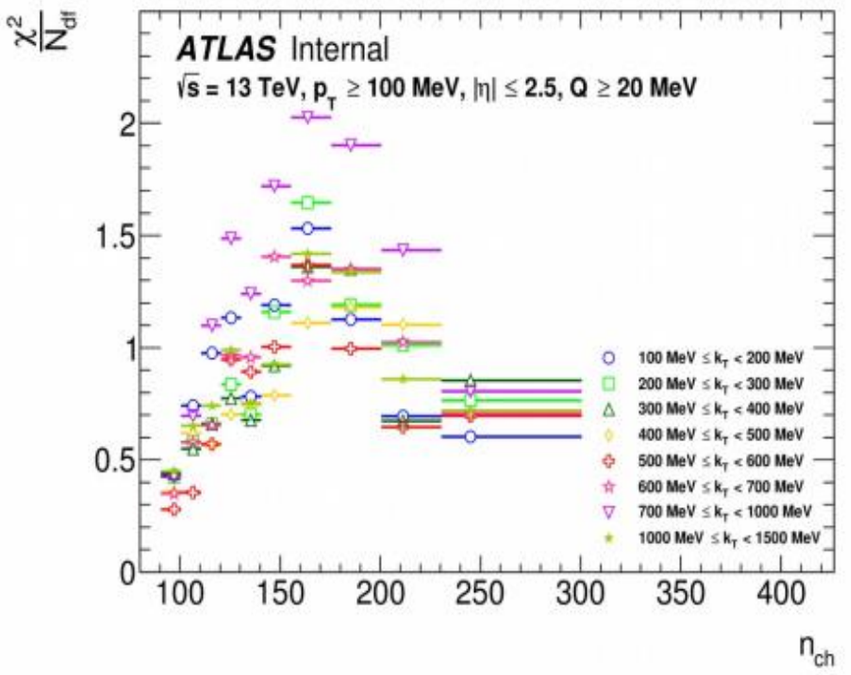

λ AND R BEC PARAMETERS FOR DIFFERENT N_{CH} INTERVALS AT 13 TEV FOR HMT EVENTS

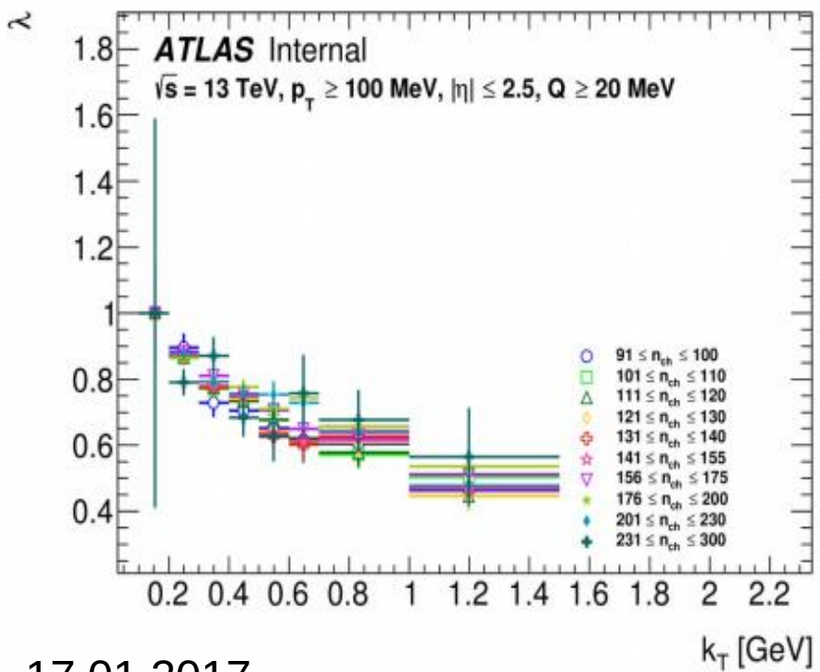

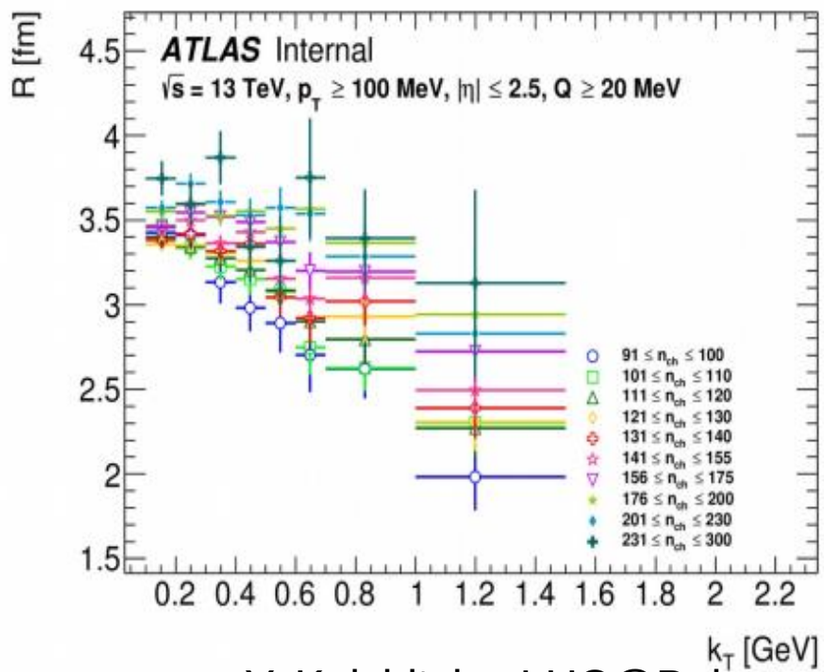

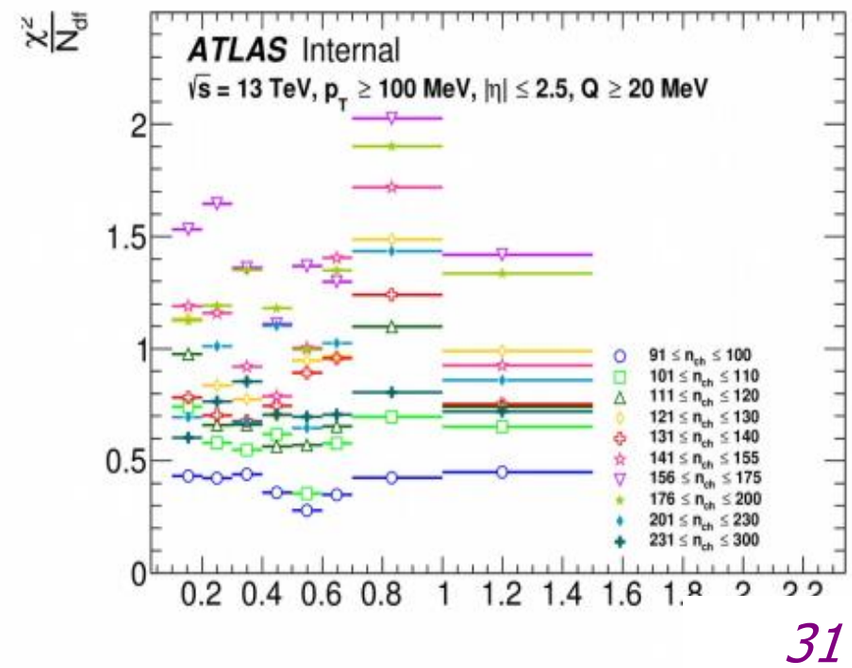

MULTIPLICITY DEPENDENCE OF λ AND R BEC PARAMETERS AT 13 TEV FOR MB AND HMT EVENTS

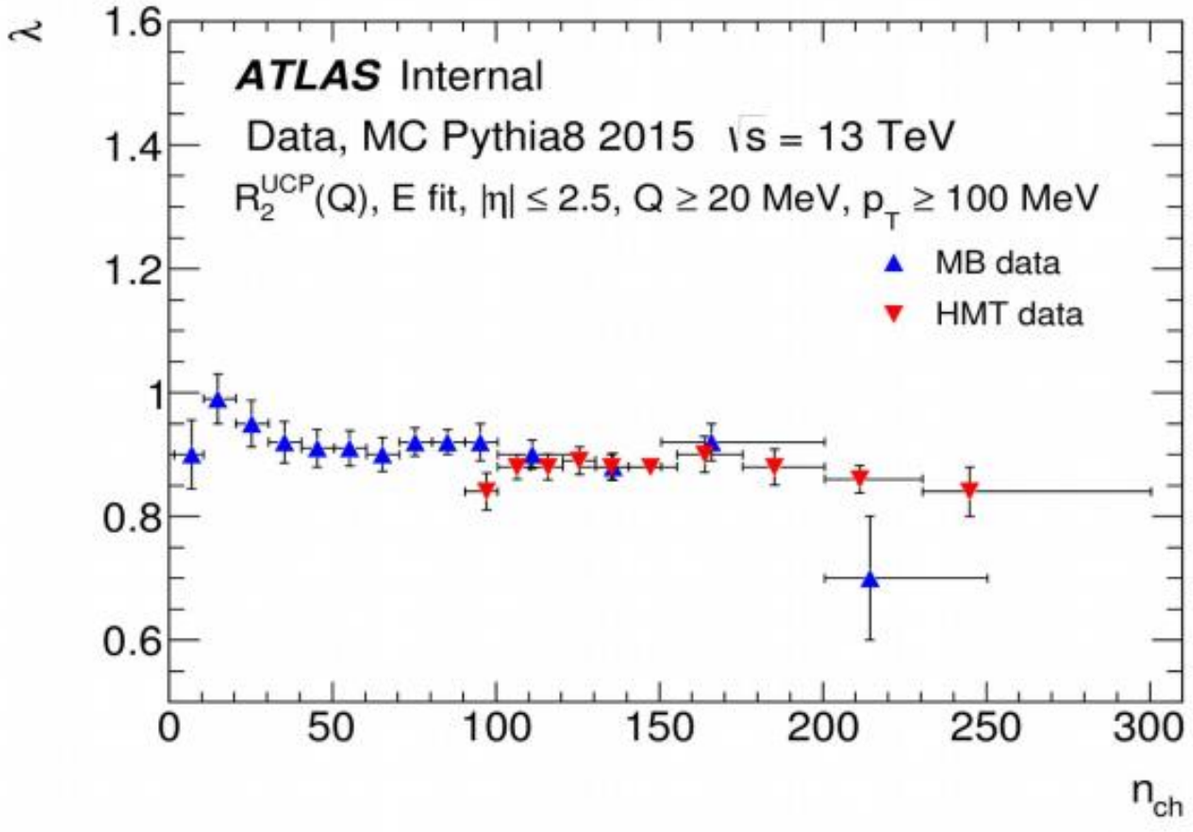

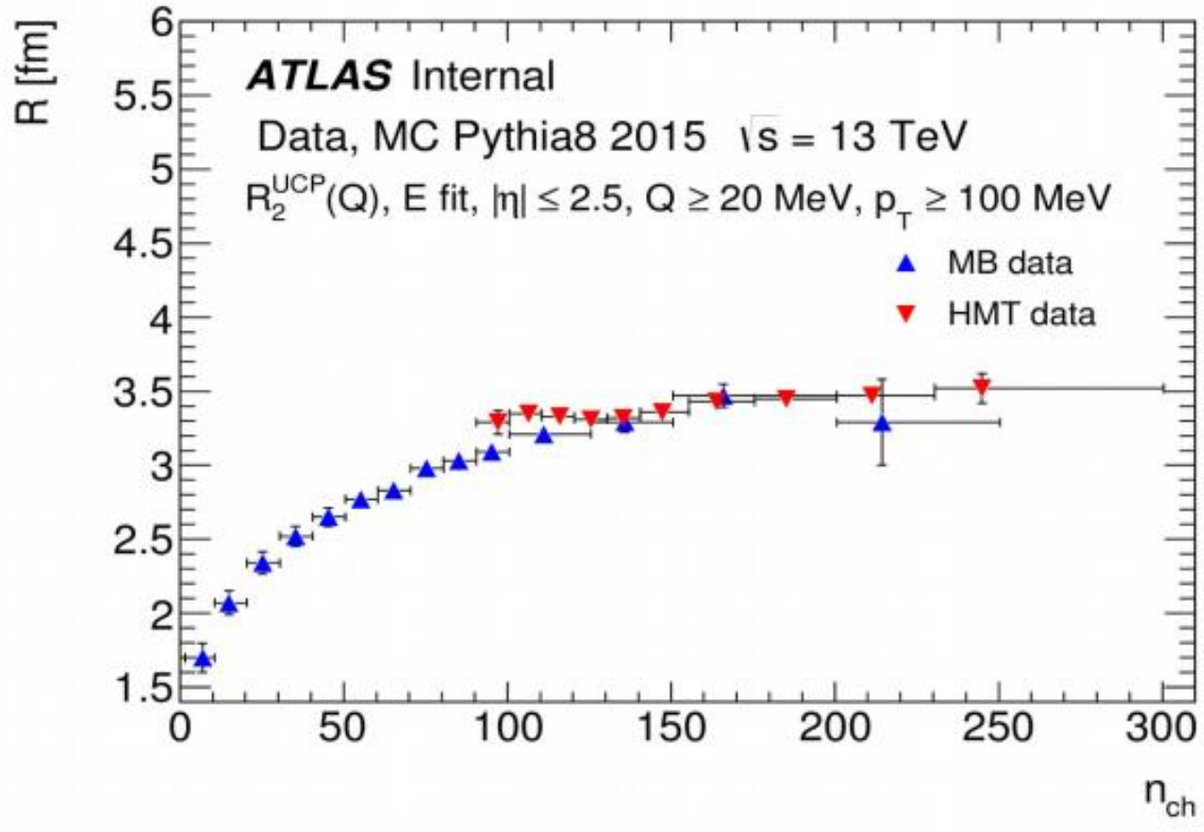

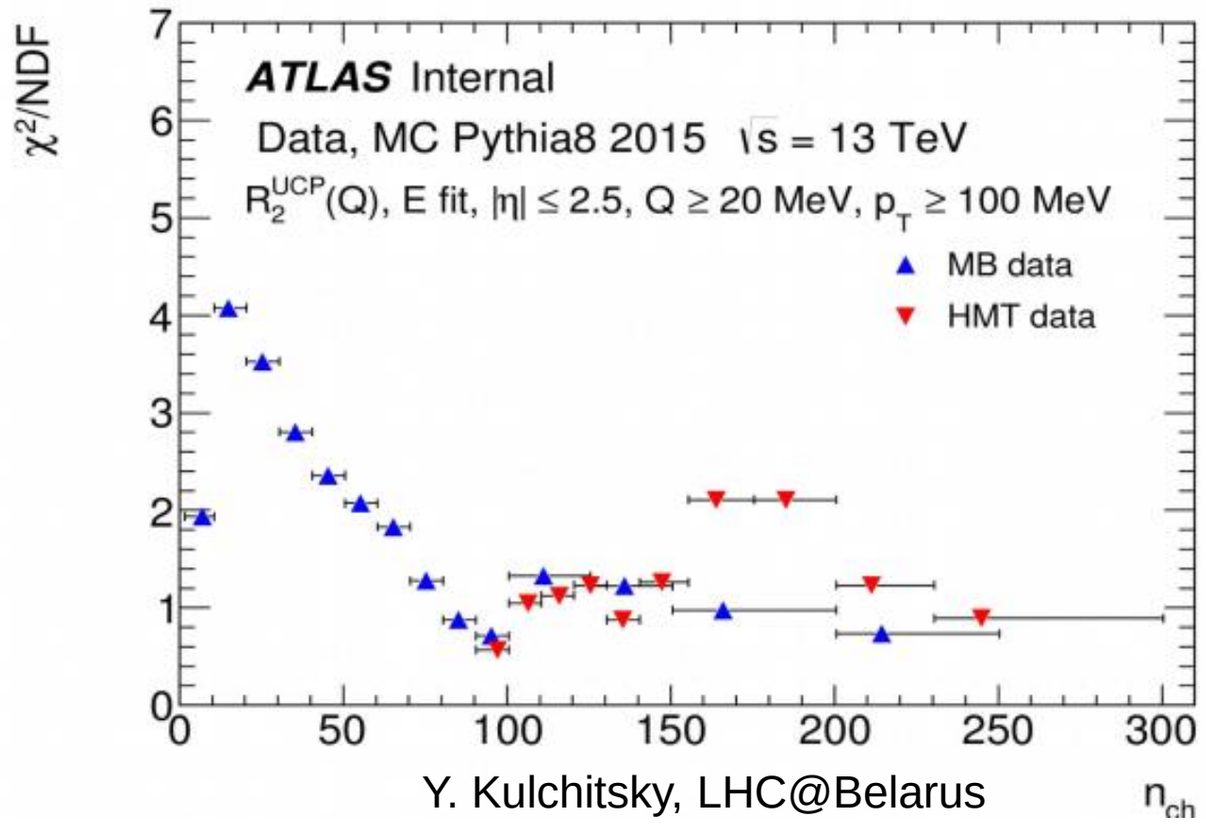

K_T DEPENDENCE OF λ AND R BEC PARAMETERS AT 13 TEV FOR MB AND HMT EVENTS

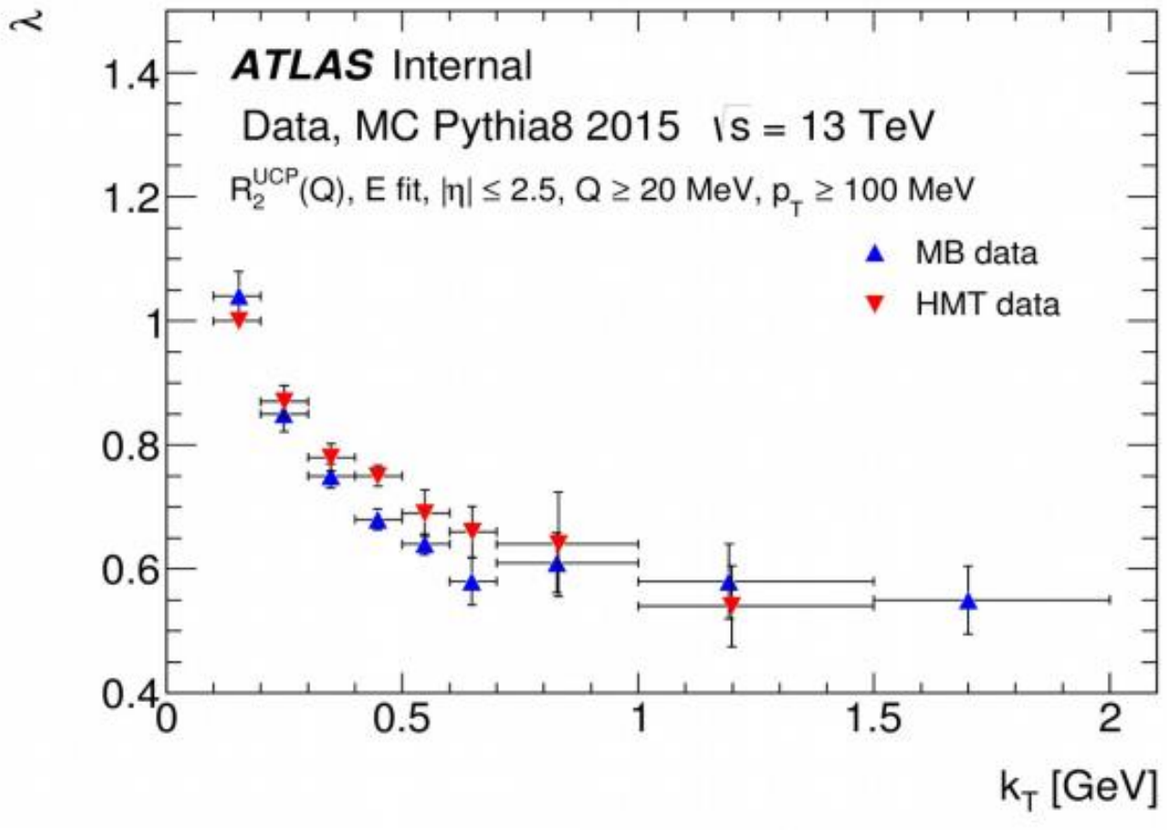

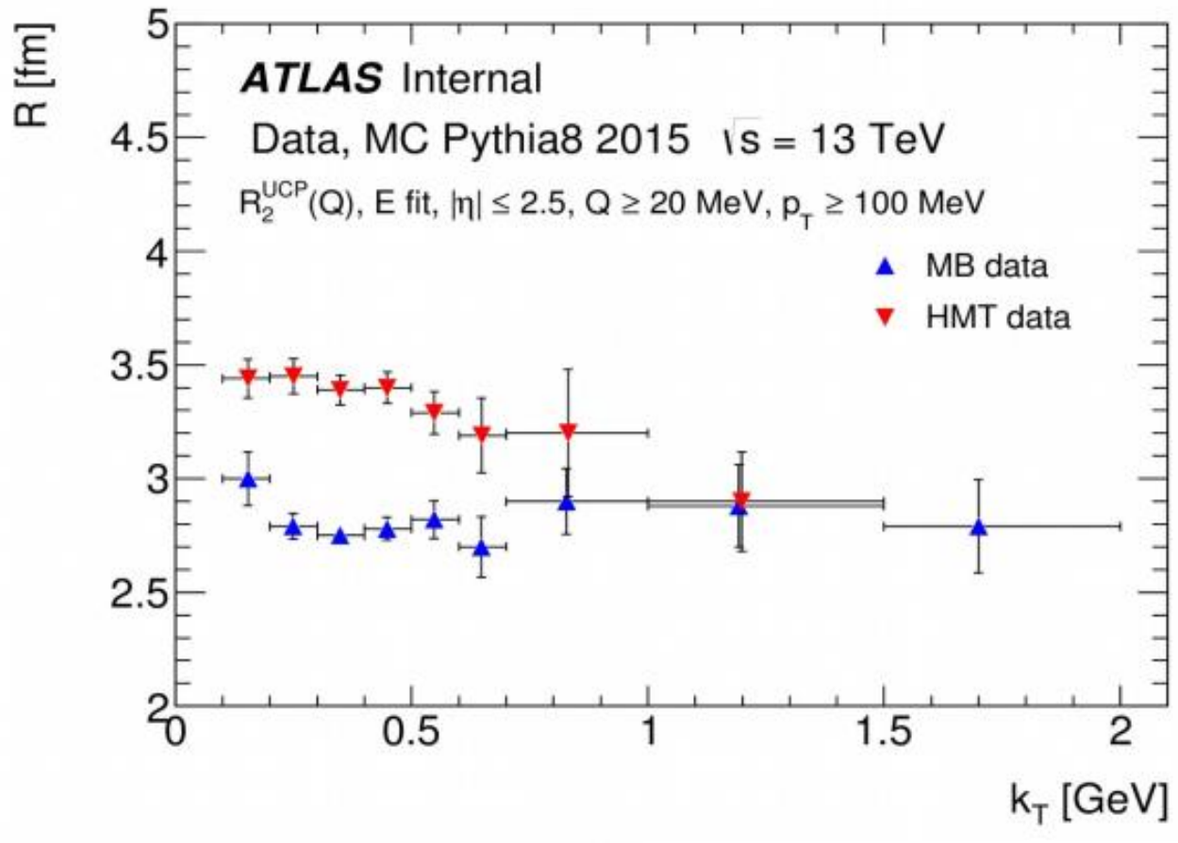

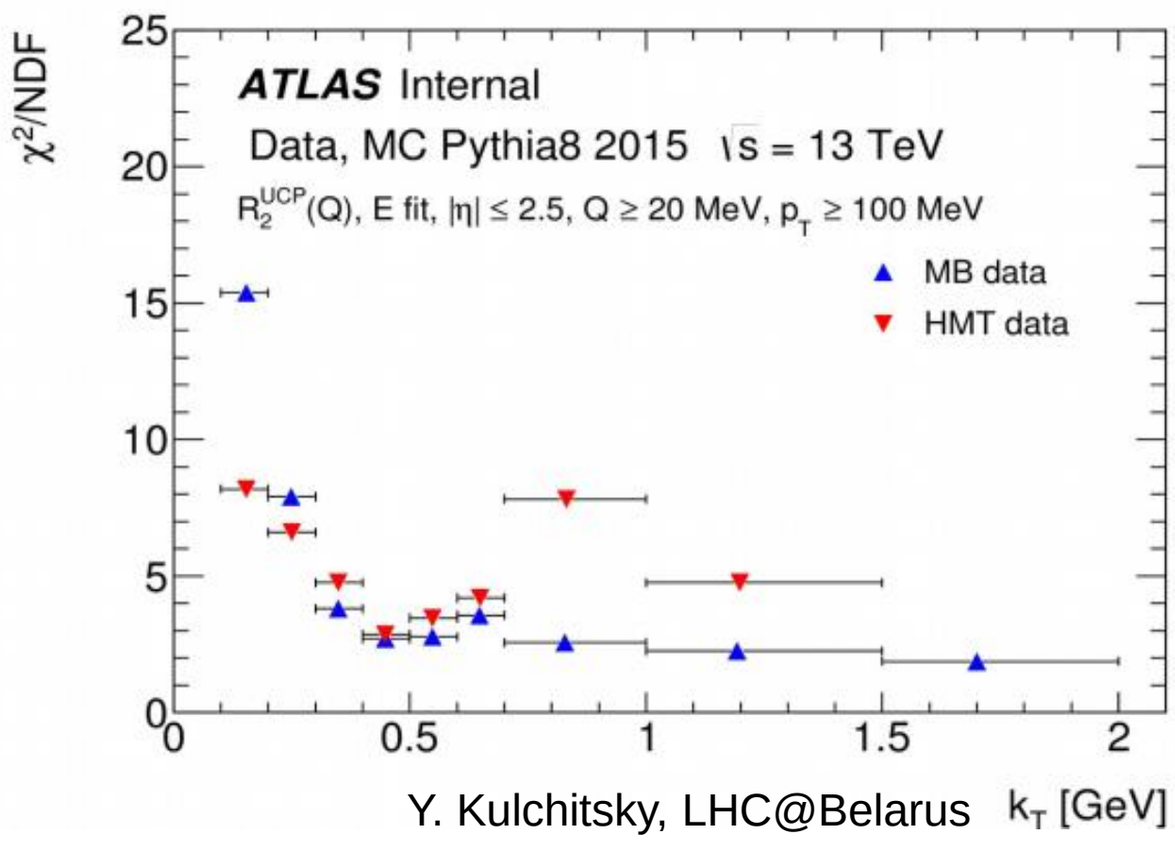

MULTIPLICITY DEPENDENCE OF R BEC PARAMETER AT 13 TEV FOR MB AND HMT EVENTS

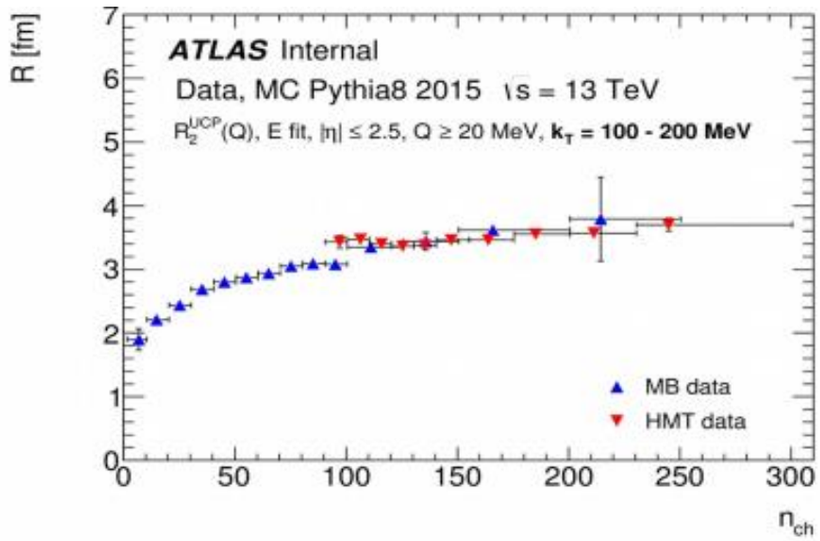

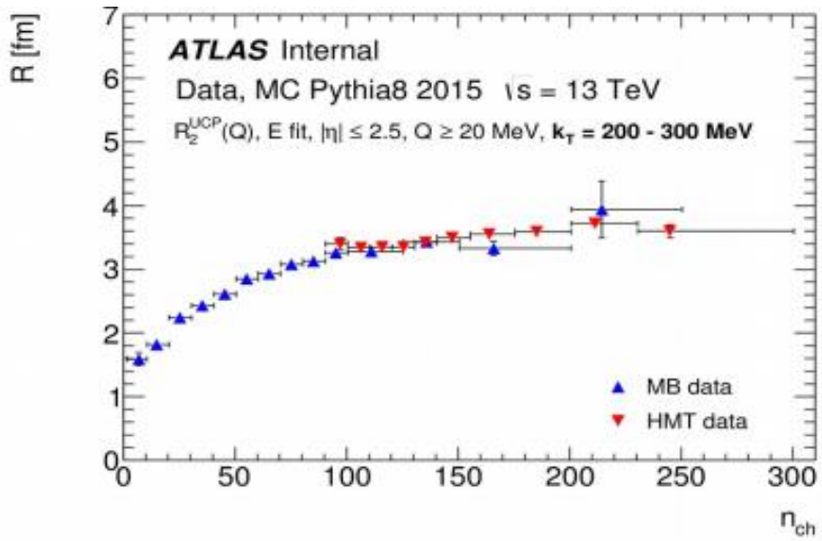

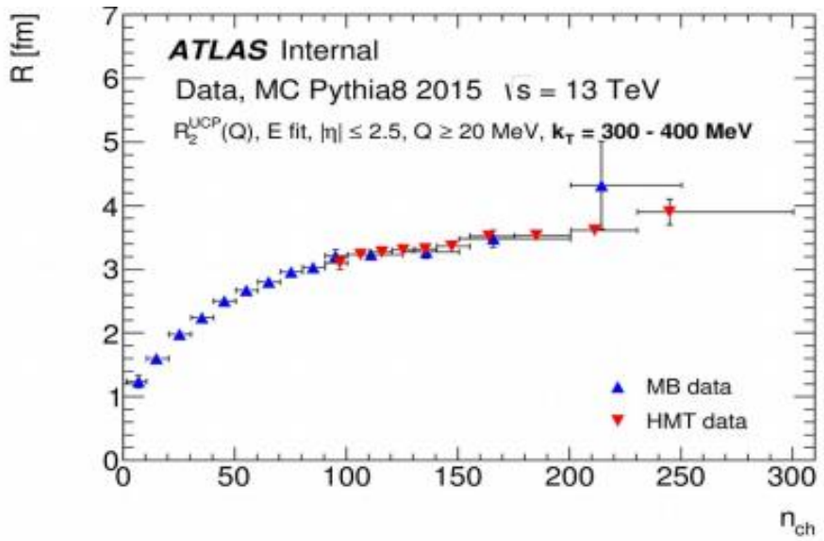

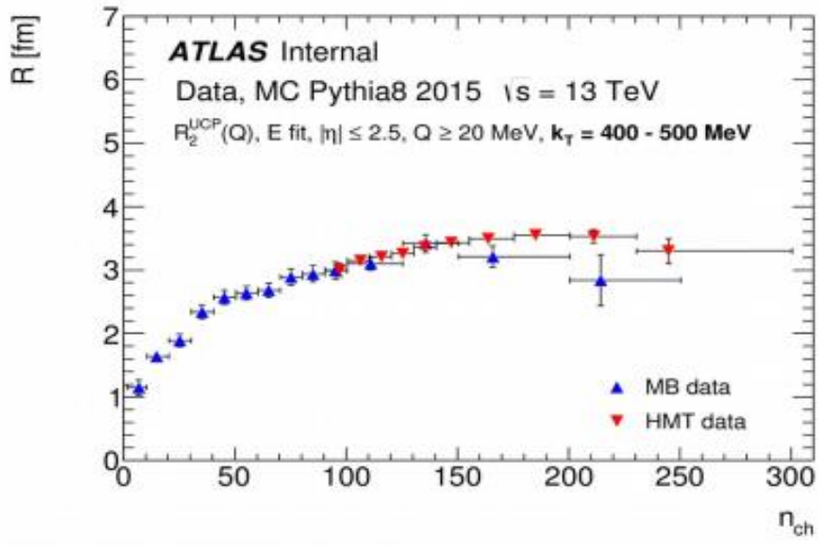

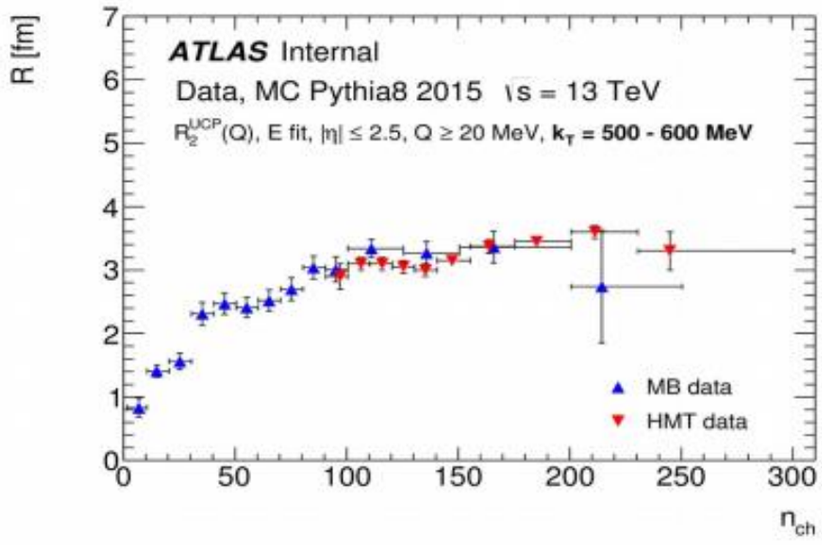

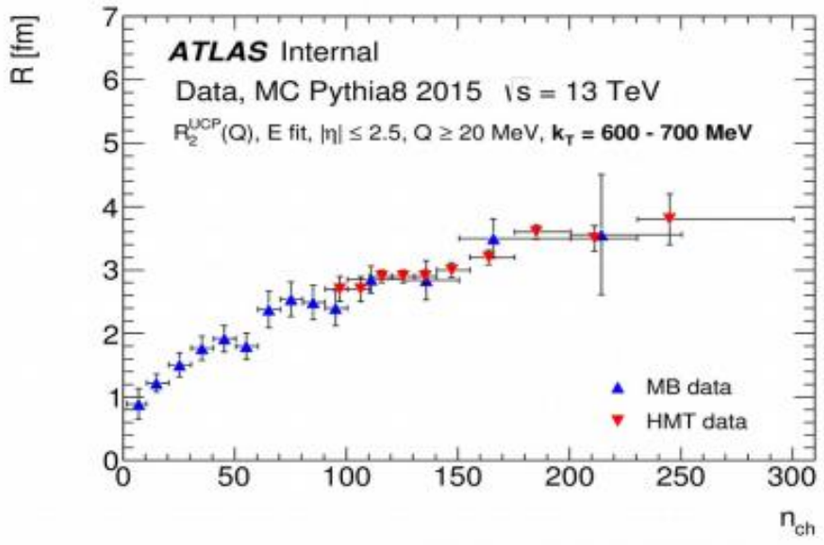

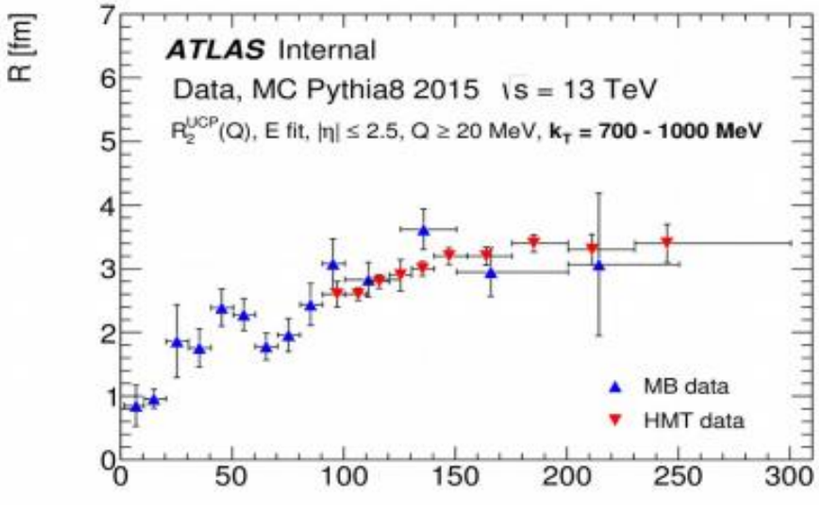

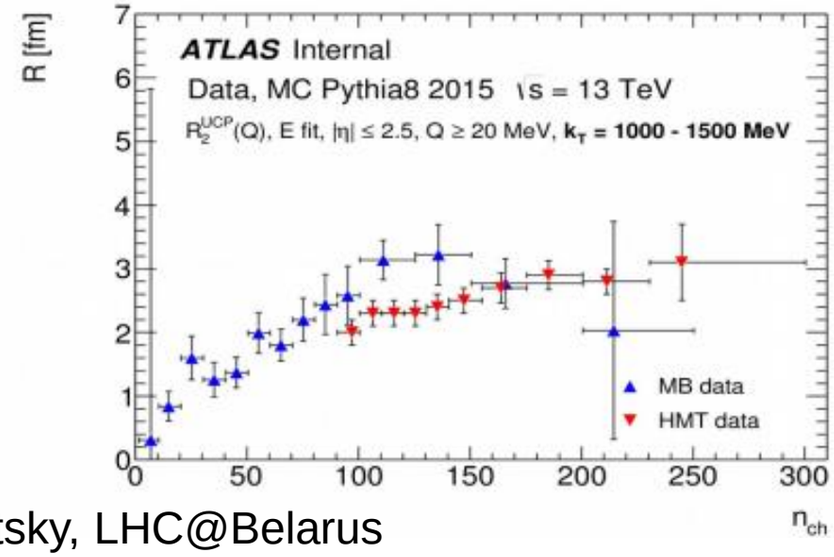

MULTIPLICITY DEPENDENCE OF λ AND R BEC PARAMETERS AT 0.9 - 13 TEV FOR MB AND HMT EVENTS

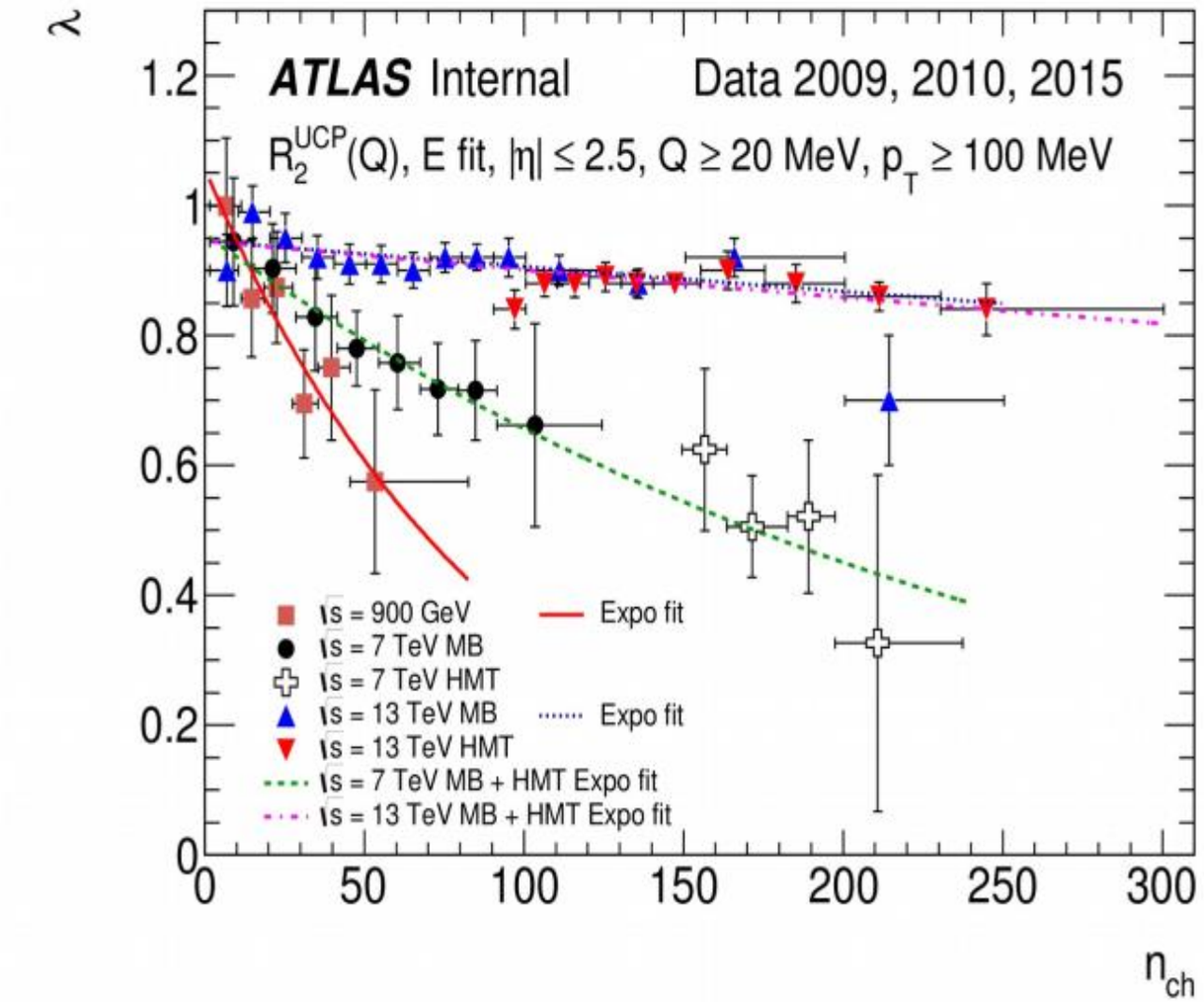

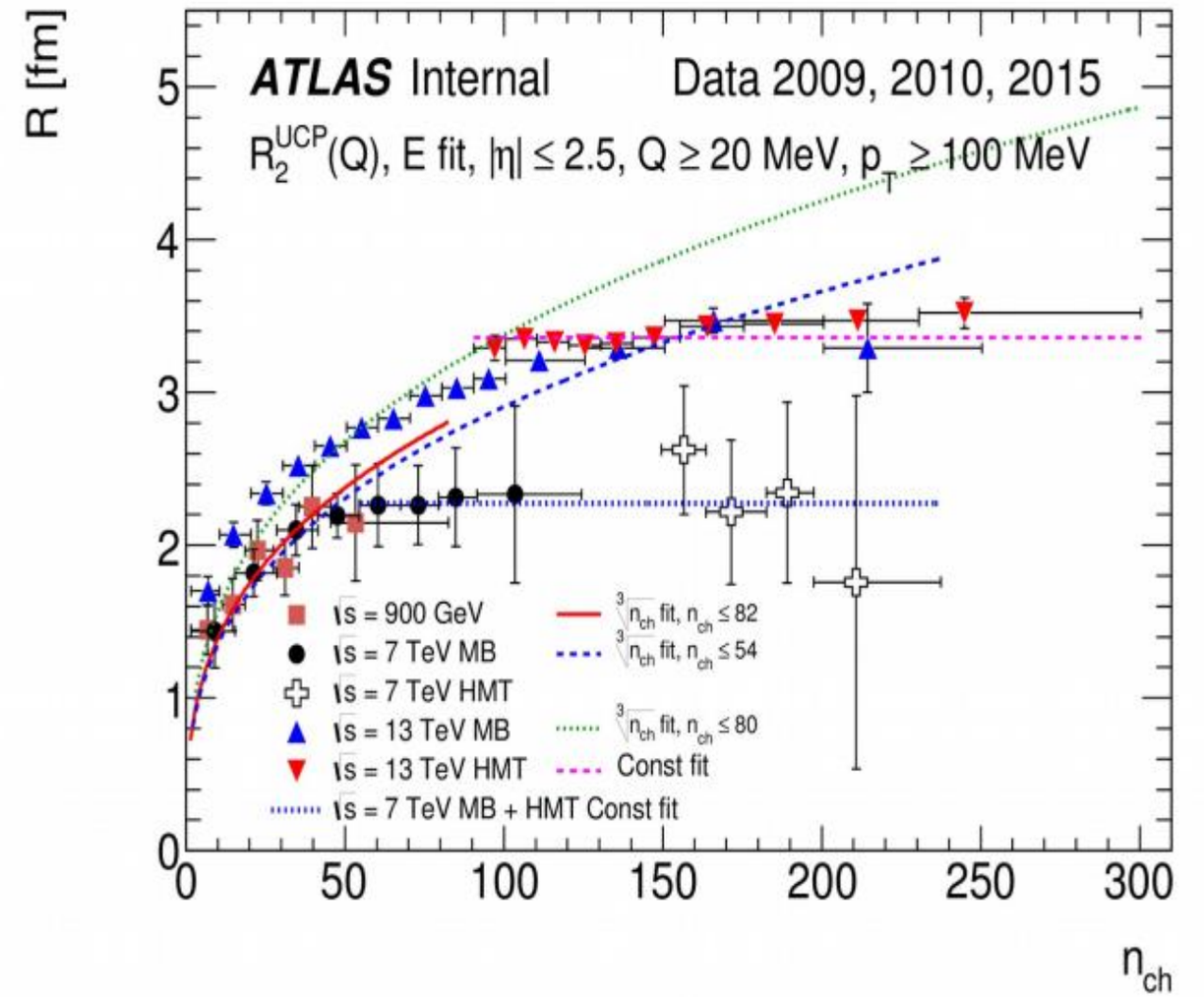

- **900 GeV**: $p_0 = 1.06 \pm 0.09 \pm 0.06$, $p_1 = 0.011 \pm 0.004 \pm 0.001$, $\chi^2/ndf = 2/4$
- **7 TeV MB + HM:** $p_0 = 0.96 \pm 0.03 \pm 0.06$, $p_1 = 0.0038 \pm 0.0004 \pm 0.0007$, $\chi^2/ndf = 4/10$
- **13 TeV MB:** $p_0 = 0.95 \pm 0.02$, $p_1 = 0.0004 \pm 0.0002$, $\chi^2/ndf = 8/12$
- **13 TeV MB + HM:** $p_0 = 0.95 \pm 0.01$, $p_1 = 0.0005 \pm 0.0001$, $\chi^2/ndf = 19/17$

- **900 GeV**: $p_0 = 0.64 \pm 0.03 \pm 0.06$[fm], $\chi^2/ndf = 3/5$
- **7 TeV MB:** $p_0 = 0.63 \pm 0.02 \pm 0.05$[fm], $\chi^2/ndf = 1/3$
- **7 TeV MB + HM:** $p_0 = 2.28 \pm 0.03 \pm 0.32$[fm], $\chi^2/ndf = 4/7$
- **13 TeV MB:** $p_0 = 0.73 \pm 0.01$[fm], $\chi^2/ndf = 8/7$
- **13 TeV HM:** $p_0 = 3.36 \pm 0.02$[fm], $\chi^2/ndf = 15/9$

K_T DEPENDENCE OF λ AND R BEC PARAMETERS AT 0.9 - 13 TEV FOR MB AND HMT EVENTS

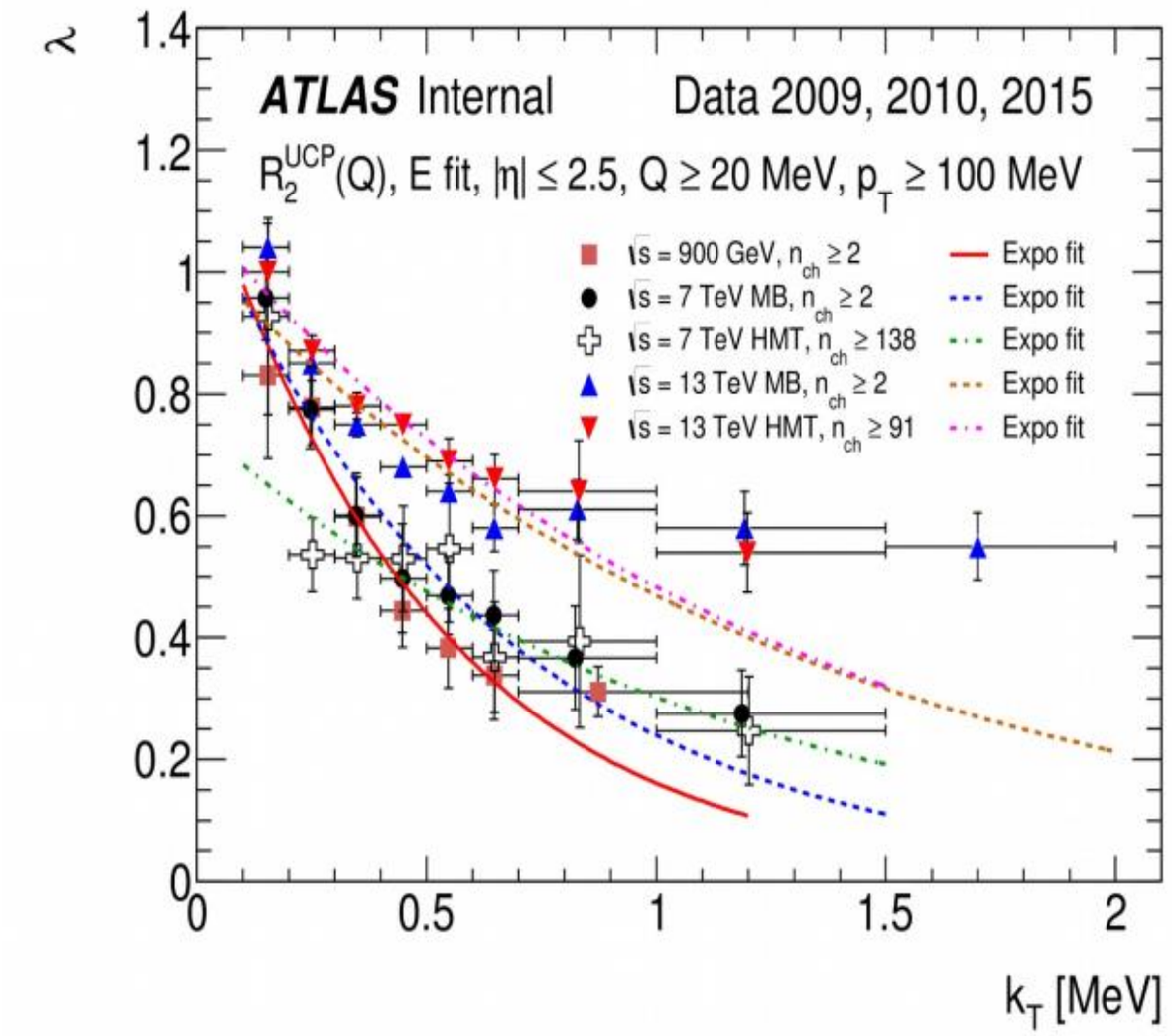

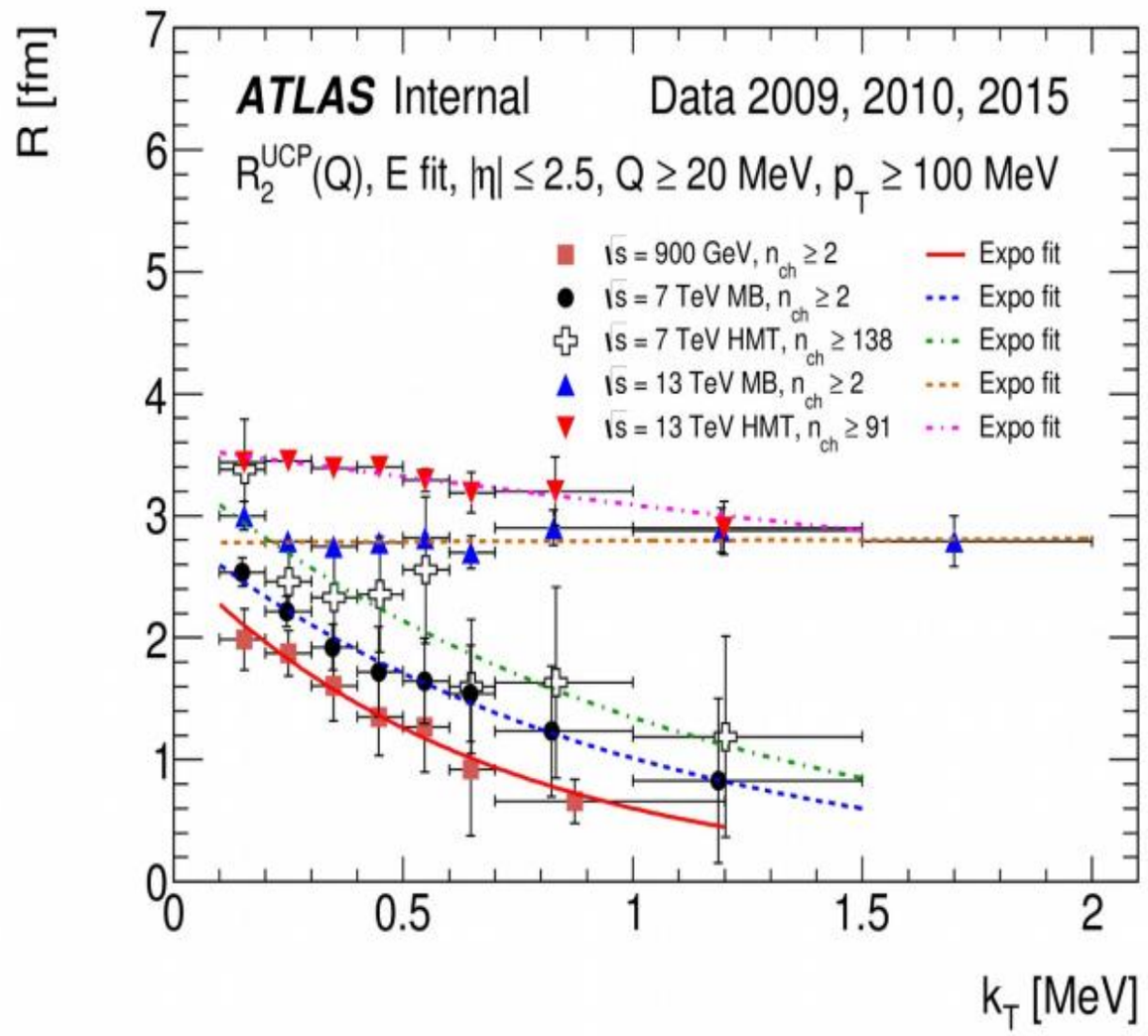

- **900 GeV**: $p_0 = 1.20 \pm 0.16 \pm 0.05$, $p_1 = 2.00 \pm 0.33 \pm 0.12$[GeV^{-1}], χ^2/ndf = 2/5
- **7 TeV MB** $p_0 = 1.12 \pm 0.09 \pm 0.04$, $p_1 = 1.54 \pm 0.17 \pm 0.21$[GeV^{-1}], χ^2/ndf = 7/6
- **7 TeV HM:** $p_0 = 0.748 \pm 0.099 \pm 0.022$, $p_1 = 0.91 \pm 0.27 \pm 0.36$[GeV^{-1}], χ^2/ndf = 7/6
- **13 TeV MB:** $p_0 = 1.03 \pm 0.09$, $p_1 = 0.79 \pm 0.18$[GeV^{-1}], χ^2/ndf = 27/7
- **13 TeV HM:** $p_0 = 1.093 \pm 0.046$, $p_1 = 0.82 \pm 0.10$[GeV^{-1}], χ^2/ndf = 4/6

- **900 GeV**: $p_0 = 2.64 \pm 0.32 \pm 0.10$[fm], $p_1 = 1.48 \pm 0.32 \pm 0.59$[GeV^{-1}], χ^2/ndf = 1/5
- **7 TeV MB:** $p_0 = 2.88 \pm 0.16 \pm 0.22$[fm], $p_1 = 1.05 \pm 0.13 \pm 0.57$[GeV^{-1}], χ^2/ndf = 2/6
- **7 TeV HM:** 3.39±0.39±0.38[fm], $p_1 = 0.92 \pm 0.24 \pm 0.69$[GeV^{-1}], χ^2/ndf = 8/6
- **13 TeV MB:** 2.78±0.05[fm], $p_1 = -0.01 \pm 0.04$[GeV^{-1}], χ^2/ndf = 6/7
- **13 TeV HM:** 3.57±0.08[fm], $p_1 = 0.14 \pm 0.06$[GeV^{-1}], χ^2/ndf

CONCLUSION

- Charged-particle multiplicity measurements at 13 TeV *using pp-collisions* are presented. Of the models considered EPOS reproduces the data the best, PYTHIA 8 A2 and MONASH give reasonable descriptions.
- The Bose-Einstein correlations results of identical charged particles pairs measured in $|\eta|<2.5$, $p_T>100$ *MeV* in pp collisions at *0.9 & 7, 13 TeV* with the ATLAS experiment are presented.
- *For the first time* the multiplicity dependence of the BEC is investigated up to *very high multiplicities* ($n_{ch} < 300$).
- *For the first time* a *saturation effect* in the multiplicity dependence of the extracted BEC radius parameter is observed for high multiplicity region.
- The dependence of the BEC parameters on k_T is investigated for different multiplicity regions up to high multiplicity.
- The k_T dependence of R is obtained to increase with increasing of the multiplicity.

BACKUP SLIDES

Systematic uncertainties

- A summary of the main systematic uncertainties affecting the η, p_T and n_{ch} distributions is given in Table

Table : Summary of systematic uncertainties on the η, p_{T} and n_{ch} distributions.

Source	Distribution	Range of values
Track reconstruction efficiency	η	$0.5\% - 1.4\%$
	p_{T}	0.7%
	n_{ch}	$0\% - {}^{+17\%}_{-14\%}$
Non-primaries	η	0.5%
	p_{T}	$0.5\% - 0.9\%$
	n_{ch}	$0\% - {}^{+10\%}_{-8\%}$
Non-closure	η	0.7%
	p_{T}	$0\% - 2\%$
	n_{ch}	$0\% - 4\%$
p_{T}-bias	p_{T}	$0\% - 5\%$
High-p_{T}	p_{T}	$0\% - 1\%$

MC models

The MC models used to correct the data for detector effects and to compare with particle-level corrected data. The **PYTHIA 8, HERWIG++, EPOS** and **QGSJET-II** generators are used.

In **PYTHIA 8** inclusive hadron–hadron interactions are described by a model that splits the total inelastic cross-section into non-diffractive (ND) processes, dominated by *t*-channel gluon exchange, and diffractive processes involving a colour-singlet exchange. The simulation of ND processes includes multiple parton-parton interactions (MPI). The diffractive processes are further divided into single-diffractive dissociation (SD), where one of the initial hadrons remains intact and the other is diffractively excited and dissociates, and double-diffractive dissociation (DD) where both hadrons dissociate.

In **HERWIG++** inclusive hadron–hadron collisions are simulated by applying an MPI model for the ND process to events with no hard scattering. It is therefore possible to generate an event with zero $2 \rightarrow 2$ partonic scatters, in which only beam remnants are produced, with nothing in between them. While **HERWIG++** has no explicit model for diffractive processes in the simulation of inclusive hadron–hadron collisions, the zero-scatter events will look similar to double-diffractive dissociation.

EPOS provides an implementation of a parton-based Gribov-Regge theory which is an effective QCD-inspired field theory describing hard and soft scattering simultaneously. **QGSJET-II** provides a phenomenological treatment of hadronic and nuclear interactions in the Reggeon field theory framework. The soft and semihard parton processes are included in the model within the “semihard Pomeron” approach.

Color Connections

Leading N_C: each parton-parton interaction scatters 'new' colors

→ incoherent addition of colors

1 or 2 strings per MPI

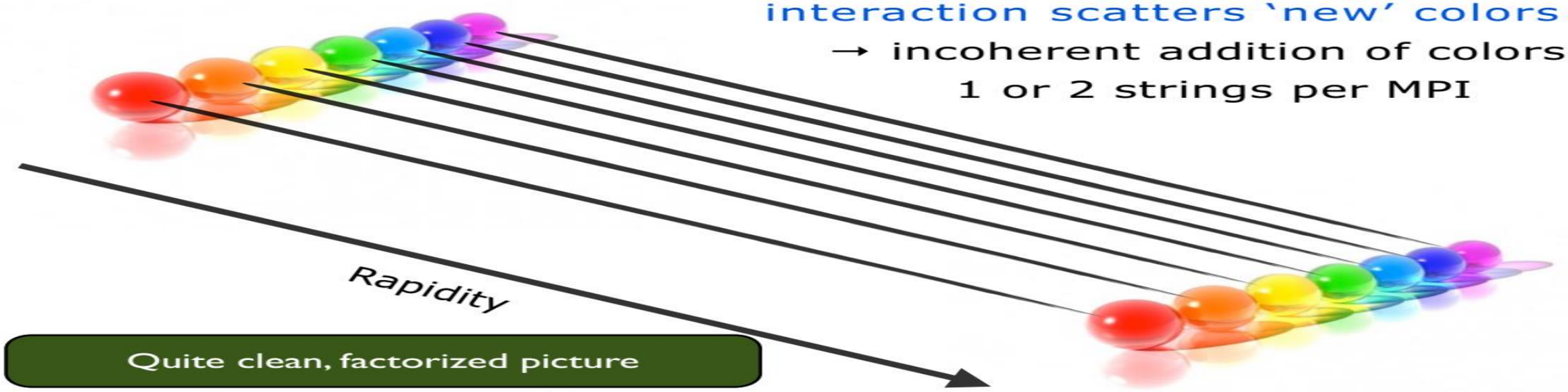

Quite clean, factorized picture

WRONG!

Multiplicity ∝ N_{MPI}

Color Reconnections?

E.g.,
Generalized Area Law (Rathsman: Phys. Lett. B452 (1999) 364)
Color Annealing (P.S., Wicke: Eur. Phys. J. C52 (2007) 133)
...

N_C=3: Colors add coherently

+ collective effects?

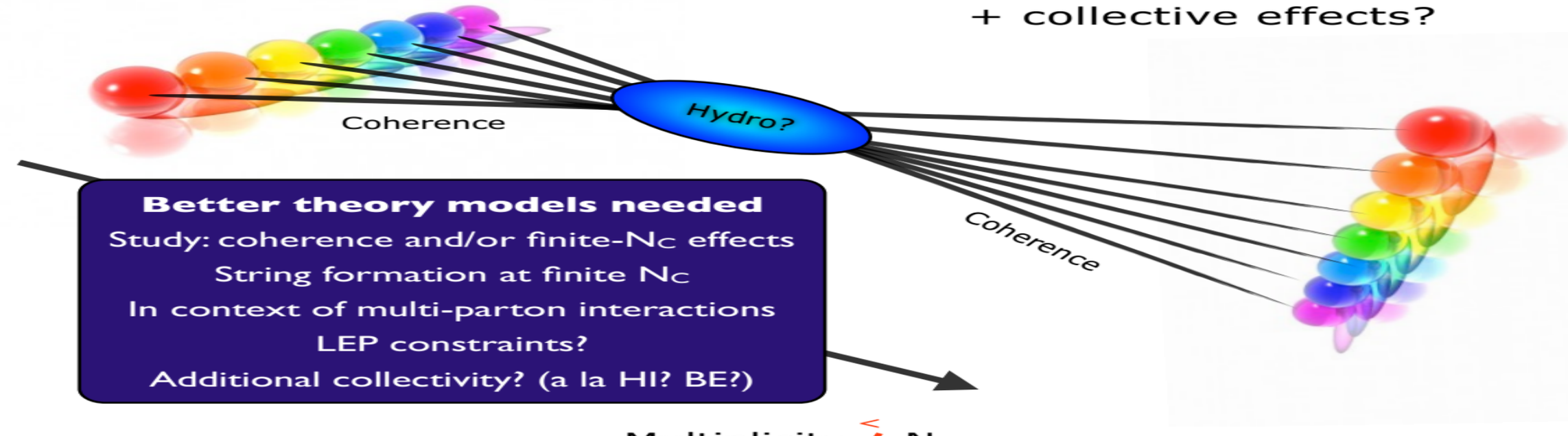

Better theory models needed

Study: coherence and/or finite-N_C effects

String formation at finite N_C

In context of multi-parton interactions

LEP constraints?

Additional collectivity? (a la HI? BE?)

Multiplicity $\not\propto$ N_{MPI}

BOSE-EINSTEIN CORRELATIONS AND HANBURY BROWN – TWISS INTERFEROMETRY

BEC are often considered to be the analogue of the Hanbury Brown and Twiss effect in astronomy, describing the interference of incoherently-emitted identical bosons.

Intensity interferometry of photons in radio-astronomy: measures angular diameter of two stars, so the physical size of the source

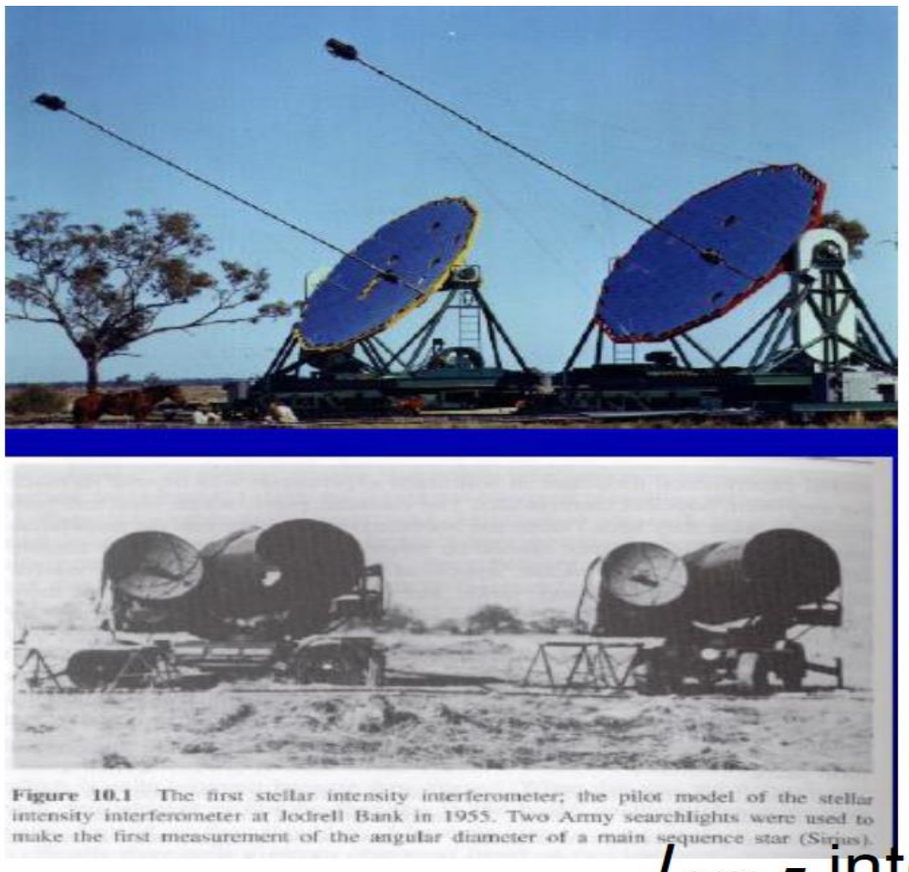

Figure 10.1 The first stellar intensity interferometer; the pilot model of the stellar intensity interferometer at Jodrell Bank in 1955. Two Army searchlights were used to make the first measurement of the angular diameter of a main sequence star (Sirius).

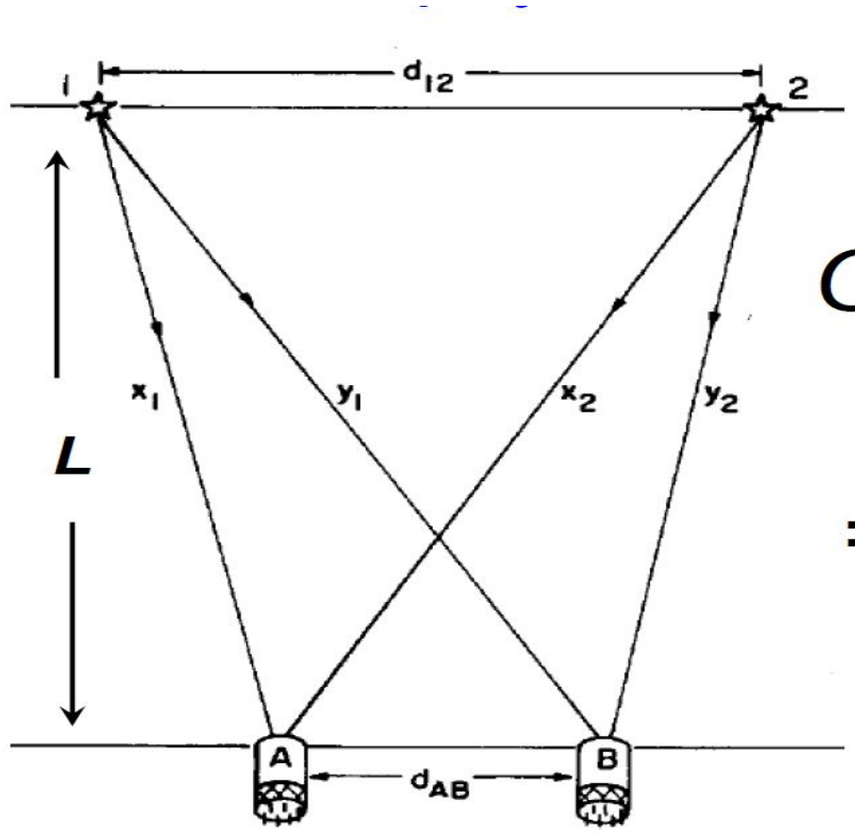

$$C(d) = \frac{\langle I_1 I_2 \rangle}{\langle I_1 \rangle \langle I_2 \rangle}$$

$$= 1 + A\cos(d_{AB})$$

$$d_{AB} = \lambda/\theta$$

$I_{1(2)}$ - intensities, $\langle x \rangle$ - averaging over random phases

λ is the wavelength of the light, $\theta = d_{12}/L$

Varying d_{AB} one learns the angle, and using the individual wave vectors, the physical size of the source

Q-RESOLUTION

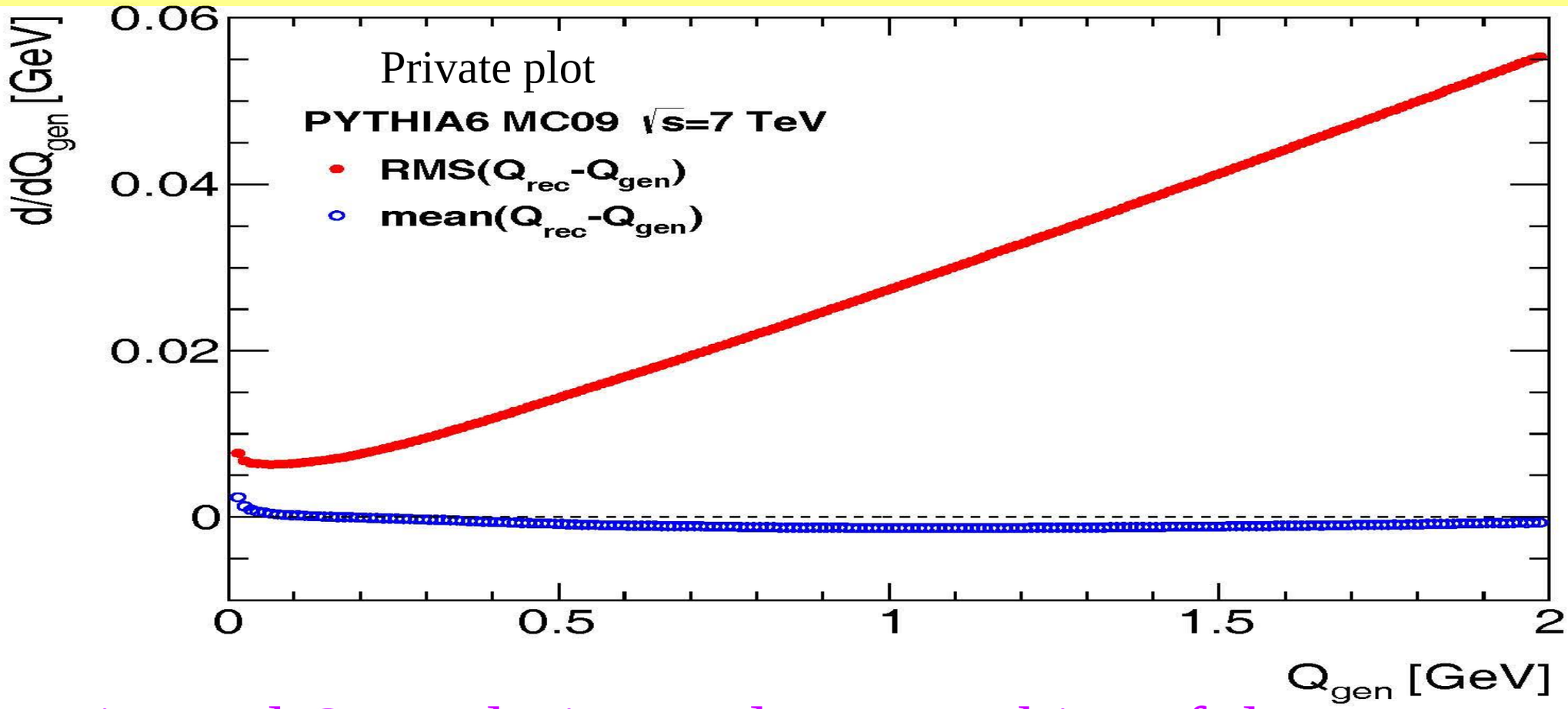

The estimated Q resolution and average bias of the reconstructed momentum difference as a function of the Q true generated value

- The basic variable in which correlation functions are expressed is the scalar momentum difference Q.
- The ATLAS detector Q resolution is found using MC.
- To exclude the region of possible two track fake reconstruction a small Q threshold was introduced, Q>20 MeV, as a minimal Q between two tracks.
- Using in fit of $R_2(Q)$ correlation functions.

$$R_2(Q) = \int_{Q_{min}}^{Q_{max}} R_2(Q') \frac{1}{\sqrt{2\pi}\sigma(Q')} e^{-\frac{(Q-Q')^2}{2\sigma(Q')^2}} dQ' ,$$

OHP(MIX) AND UCP REFERENCE SAMPLES: N_{CH}

The two-particle correlation function C_2 (Q) at 7 TeV for different n_{ch} intervals using the opposite-hemisphere reference sample for data (red) and MC (blue)

Artificial peak in C_2 in BEC region

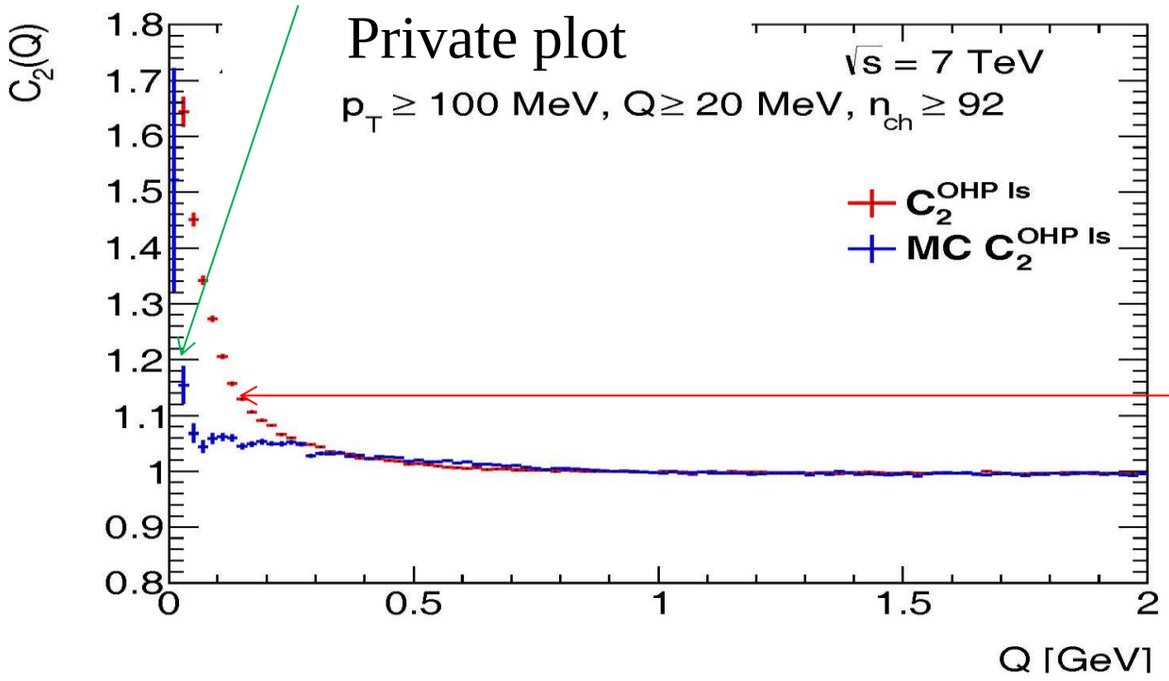

R_2 OHP & UCP

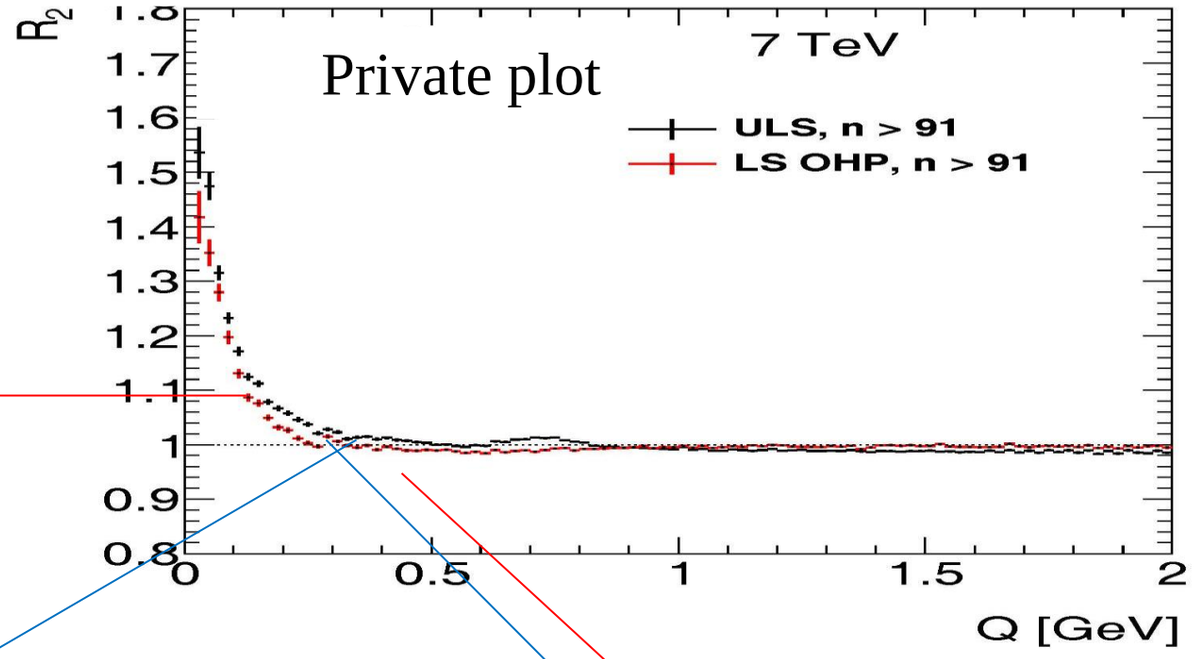

Reflection of resonances in C_2 UCP

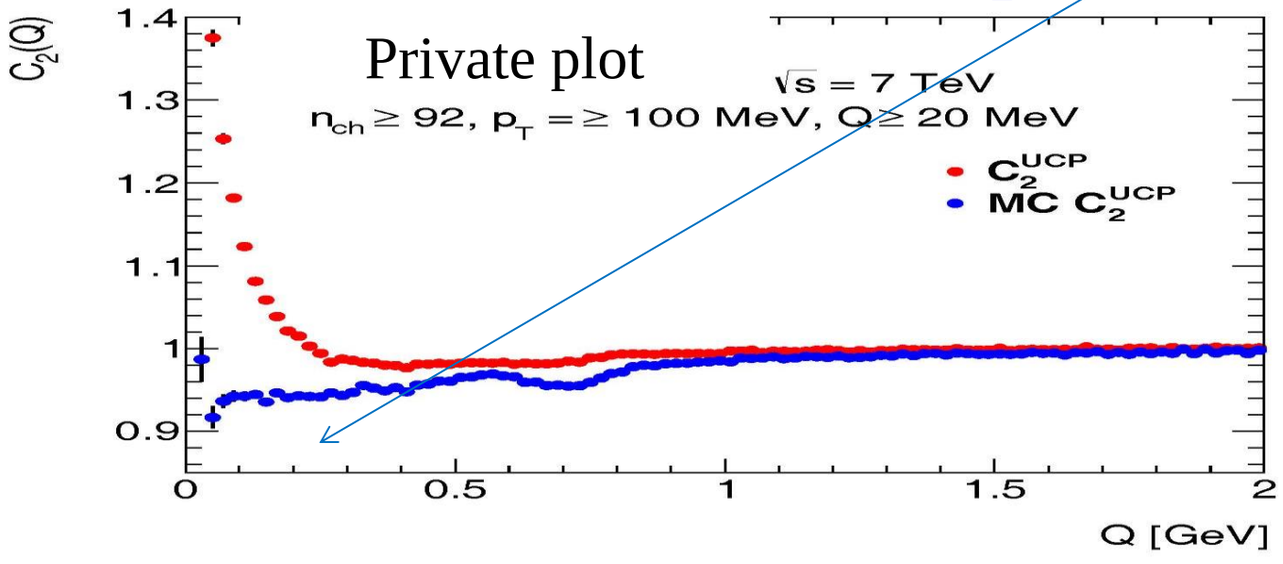

The n_{ch} dependences for parameter R for R_2 with diff reference samples

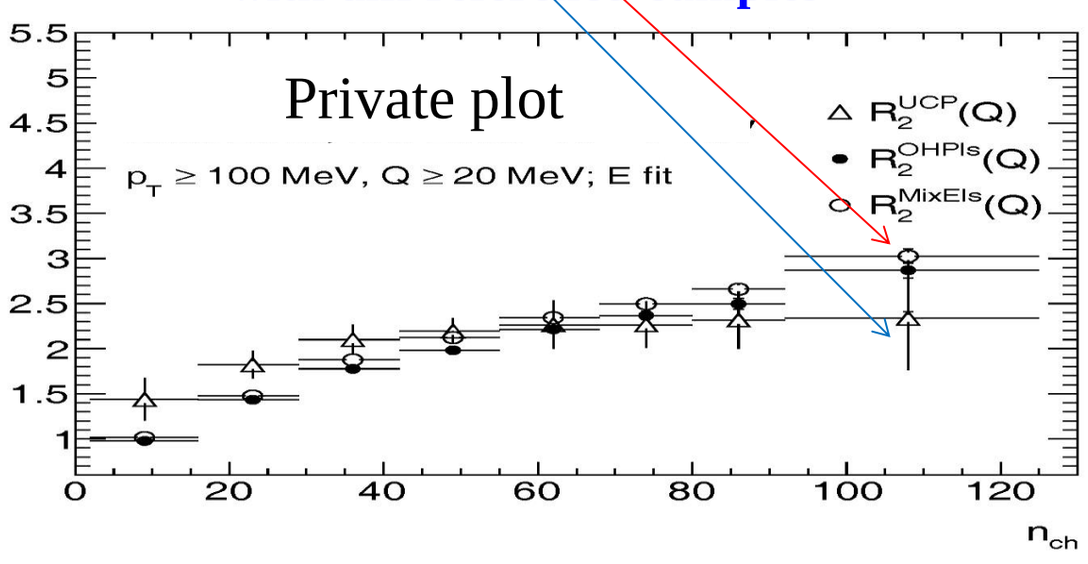

Disadvantage: violation of energy-momentum constraint, event topology, destroying other features such as non-BEC etc.

MULTIPLICITY DEPENDENCE OF λ BEC PARAMETER AT 13 TEV FOR MB AND HMT EVENTS

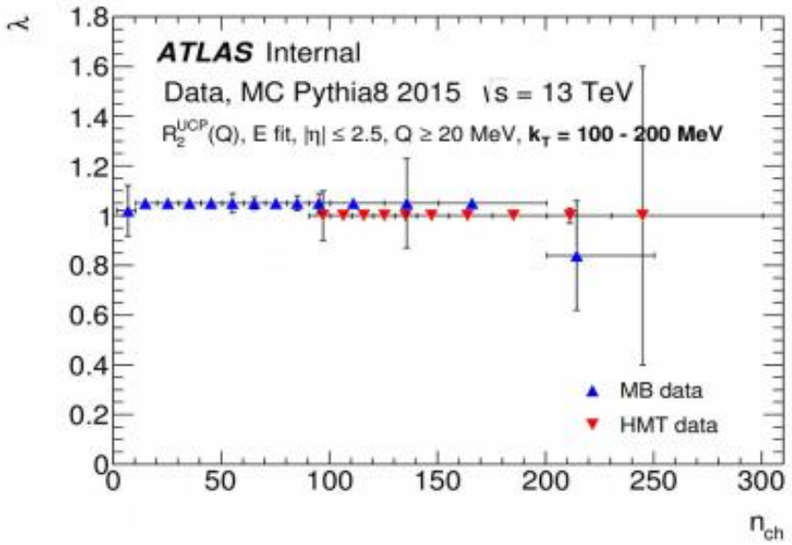

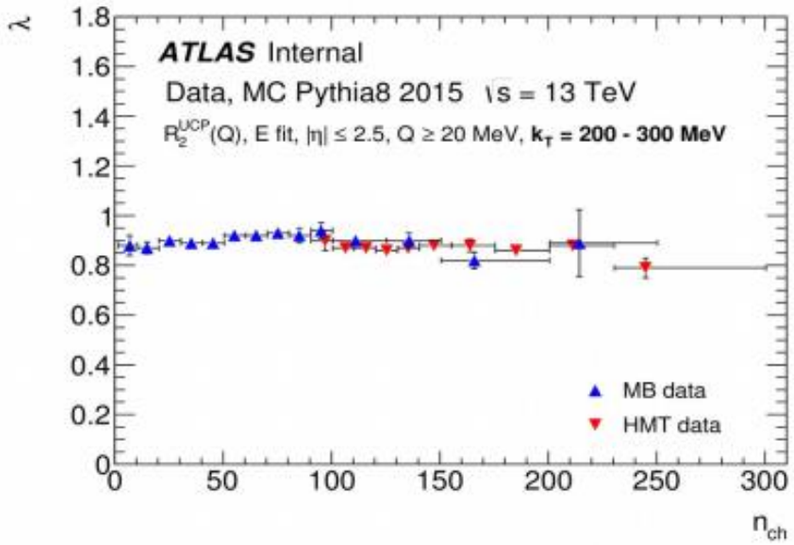

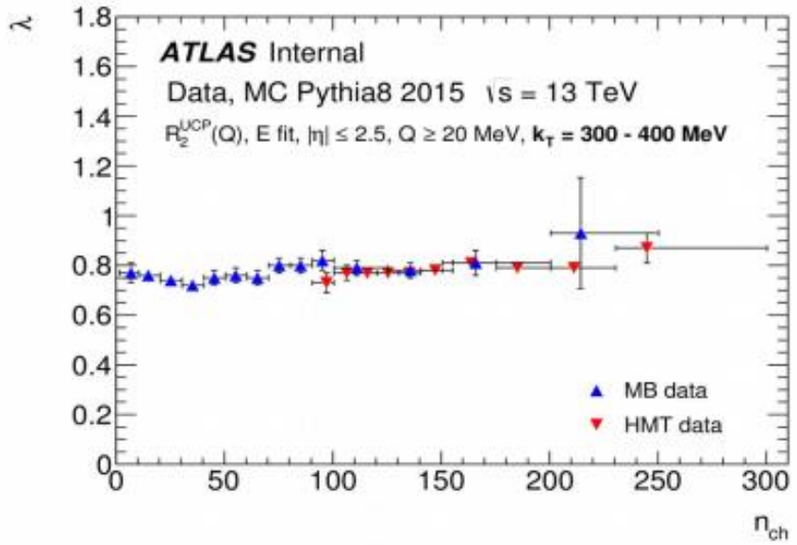

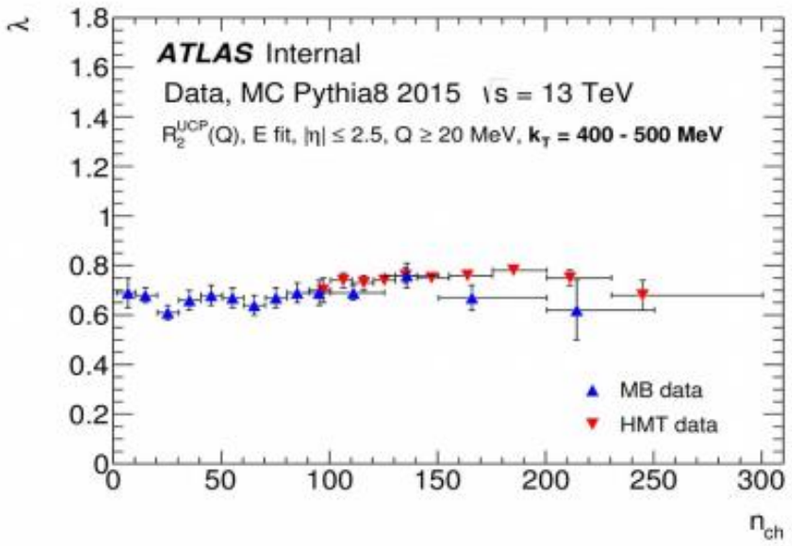

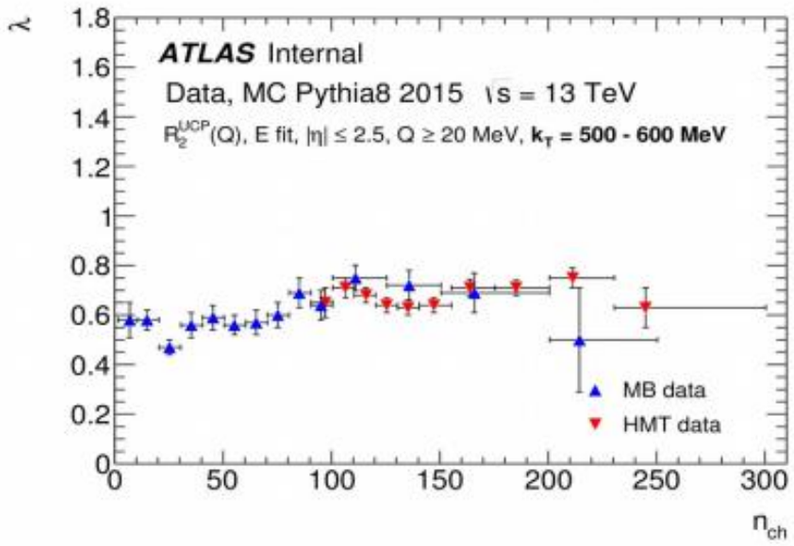

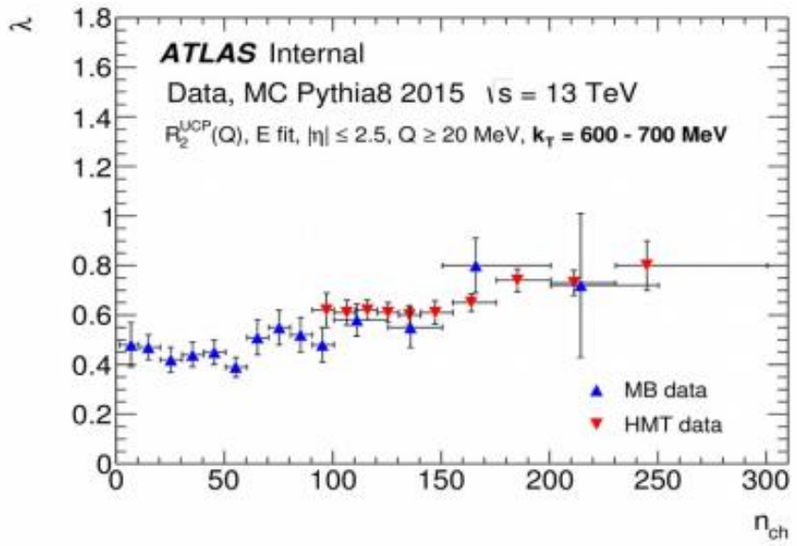

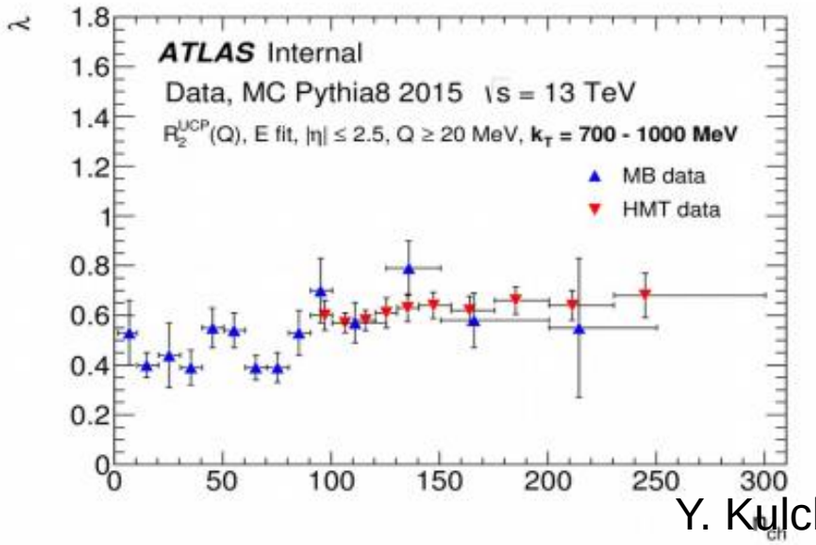

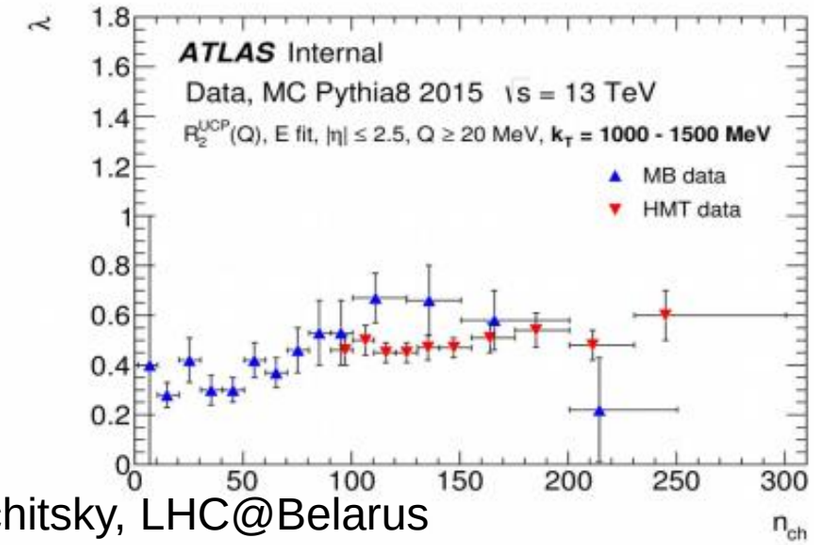

MULTIPLICITY DEPENDENCE OF χ^2/NDF PARAMETER AT 13 TEV FOR MB AND HMT EVENTS